GÖTEBORGS UNIVERSITET
GÖTEBORGS UNIVERSITETSBIBLIOTEK

84

INSTITUTE
OF
THEORETICAL PHYSICS

CHALMERS TEKNISKA HÖGSKOLA — GÖTEBORGS UNIVERSITET

GÖTEBORG — SWEDEN

84.

A STUDY OF ELECTRONS
AND PHONONS IN METALS

BY

GÖRAN GRIMVALL

A STUDY OF ELECTRONS AND PHONONS IN METALS

BY

GÖRAN GRIMVALL

GÖTEBORG 1969

A STUDY OF ELECTRONS
AND PHONONS IN METALS

BY

GÖRAN GRIMVALL
Tekn. lic.

A STUDY OF ELECTRONS
AND PHONONS IN METALS

BY

GÖRAN GRIMVALL

This thesis is based on research carried out at Chalmers University of Technology. It contains the following papers

A.   T. Claeson and G. Grimvall: The electron-phonon coupling and phonon spectra in lead-thallium alloys studied by electron tunneling. J. Phys. Chem. Solids *29*, 387 (1968).

B.   G. Grimvall: On the polarization vectors of lattice vibrations. Phys. stat. sol. *32*, 383 (1969).

C.   G. Grimvall: Numerical calculations on the electron-phonon system in sodium. Phys. kondens. Materie *6*, 15 (1967).

D.   G. Grimvall: Temperature dependent effective masses of conduction electrons. J. Phys. Chem. Solids *29*, 1221 (1968).

E.   G. Grimvall: Temperature effects in cyclotron resonance and specific heat electron masses. Solid State Comm. *7*, 213 (1969).

F.   G. Grimvall: New aspects on the electron-phonon system at finite temperatures with an application on lead and mercury. Phys. kondens. Materie (1969).

G.   G. Grimvall: Conductivities in normal metals from measurements on superconductors. Phys. kondens. Materie *8*, 202 (1968).

H.   G. Grimvall and C. Lydén: An analysis of the temperature and pressure dependence of the electrical resistivity in lead. Phys. kondens. Materie (1969).

Introduction

This summary is intended to give a background to, and an exposé of the main ideas in the thesis. The problems dealt with concern some of the most fundamental properties of metals, like the electrical conductivity and the heat capacity. Attempts [1] at a theoretical treatment date back to the beginning of this century. Drude (1900) suggested that a metal was built up of ions surrounded by a gas of conduction electrons. With this model one could explain e.g. the Wiedemann-Franz law for the ratio between the electrical and the thermal conductivities (although by a wrong argument), nevertheless it was still difficult to understand some features of conduction phenomena. One of the unsettled problems in physics at that time was the deviation of the lattice heat capacity from the classical result (Dulong-Petit's rule). Einstein (1907) used Planck's rule of quantization to describe the motion of the atoms as that of independent harmonic oscillators with discrete energy levels. Born and von Kármán (1912) by introducing force constants between nearest neighbour atoms obtained solutions to the classical equation of motion in the form of propagating waves with quantized energy. In the same year Debye published his theory for lattice vibrations viewed as elastic waves. With these rather crude concepts one could find working models to describe some metallic properties. Quite naturally, several severe discrepancies remained as the models were based on classical physics with the addition of Planck's rule of quantization.

The basis of modern solid state theory is of course quantum mechanics as it was developed around 1930. Many important qualitative results could be derived simply from the periodicity of the lattice. Nevertheless some phenomena remained unsolved. We can only think of superconductivity that was discovered in 1911 but not explained until the appearance of the BCS theory in 1957.

For some twenty years, solid state physics has been in a period of very rapid progress. Several new physical effects have been discovered and well known properties have been measured with a very high accuracy. The theory of solids has undergone a similar development. New mathematical methods are used for the description of large systems of interacting particles.

Many important qualitative results have been obtained and the computer technique has enabled calculations on real systems.

One purpose of the thesis is to show how the modern theory is used in accurate calculations of measurable properties for some metals. Before we enter into details, it can be interesting to see how well the theory can explain experimental results. We must distinguish between calculations at different levels of sophistication. In an *ab initio* calculation we start from fundamental parameters like the atomic number, the mass of the particles and the lattice spacing in equilibrium. This is, however, not the usual approach. We can often get a much better understanding of the physics if we set up a model that gives simple relations between many different properties. Experimental results for some of these properties can then be used to predict the result for others. This is the level of most of our calculations. We can also use *ad hoc* models with a few adjustable parameters, which sometimes do not have any meaningful physical interpretation.

This thesis is limited to a consideration of so called simple metals, i.e. metals with conduction electrons that can be described as an almost free electron gas. Typical examples are the alkali metals, lead and aluminium. The table below gives some idea about the accuracy one can obtain in theoretical calculations for these elements.

Calculated property	Typical deviation from experimental results
Electrical resistivity (room temperature)	20–40%
Electronic specific heat, cyclotron resonance frequency	5–15%
Phonon spectrum, elastic constants	
(*ab initio* calculation)	20–40%
(d:o *ad hoc* model)	5–10%

Lattice vibrations

Experiments

For a long time, accurate experimental values for the phonon frequencies $\omega(\mathbf{q})$ could only be obtained in the limit of long wave lengths (small $\mathbf{q}$), where the frequencies are simply related to the elastic constants. More detailed information can be obtained from diffuse scattering of X-rays and inelastic scattering of electrons or neutrons. With neutron scattering, it is often possible to determine $\omega(\mathbf{q})$ for arbitrary $\mathbf{q}$-values with a relative accuracy better than a few per cent.

4

For elements that are superconductors, there exists quite a different method to obtain information about the phonon spectrum, see paper A. The tunneling current I of electrons into a superconductor biased with a voltage U, depends on the effective interaction between electrons and phonons, i.e. on the strength of electron-phonon interaction $\alpha^2(\omega)$ times the phonon density of states $F(\omega)$. The tunneling current I, or better d^2I/dU^2, will show structure at the van Hove singularities in $F(U)$ (see fig. 1).
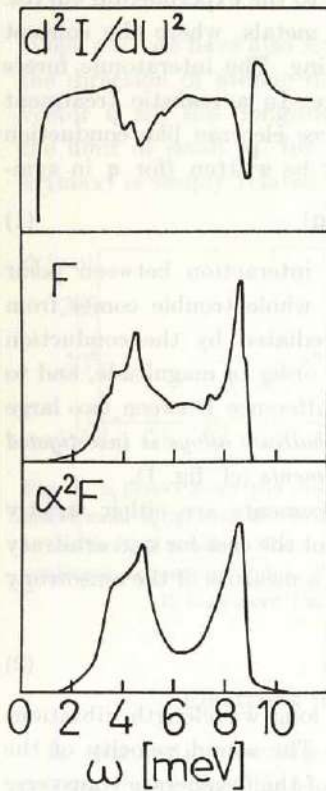
Fig. 1. The second derivative d^2I/dU^2 of the tunneling current into a superconductor biased with a voltage U shows a characteristic structure at the singularities in the phonon density of states $F(\omega)$. The energy scale in d^2I/dU^2 is given a constant shift to make the comparison easier. From measurements of the tunneling current I, one can calculate the effective electron-phonon interaction $\alpha^2(\omega)F(\omega)$ mediated by phonons of energy ω.

McMillan and Rowell have developed an ingenious method to start from measurements of $I(U)$ and its derivatives and by an iteration procedure solve a pair of coupled integral equations that describe the superconducting state. From such an analysis one obtains the effective electron-phonon interaction in the normal state $\alpha^2(\omega)F(\omega)$, mediated by phonons of energy ω. The shape of $\alpha^2(\omega)F(\omega)$ closely resembles that of the phonon density of states $F(\omega)$ as shown in fig. 1.

5

Theory

The calculation of phonon dispersion curves is one of the main problems in solid state theory. Generally the neutron scattering experiments are carried out only for **q** in symmetry directions. To find the density of states $F(\omega)$, one must have some model that is capable of reproducing the results in the symmetry directions and hopefully is good also for interpolation to an arbitrary **q**. The standard method, still in use, is that of Born and von Kármán. Force constants are introduced between a few nearest neighbour atoms and they are determined by fitting to the experimental curves. Unfortunately this method is unphysical for metals, where the concept of force constants does not have much meaning. The interatomic forces are very complicated and of quite long range. In a realistic treatment for simple metals, with small ion cores and free electron like conduction electrons, the total frequency can conveniently be written (for **q** in symmetry directions)

$$\omega^2(\mathbf{q}) = \omega_{ii}^2(\mathbf{q}) - \omega_{ie}^2(\mathbf{q}) \tag{1}$$

The term ω_{ii}^2 comes from the direct ion-ion interaction between point charges, and it can easily be calculated. The whole trouble comes from ω_{ie}^2 that describes the ion-ion interaction mediated by the conduction electrons. The two terms are often of the same order of magnitude, and to really make things worse, ω_{ie}^2 is in turn the difference between two large terms. *In paper A, the lattice dynamics of lead-thallium alloys is investigated theoretically and correlated with tunneling experiments* (cf. fig. 1).

In symmetry directions, the atomic displacements are either strictly longitudinal or transverse to **q**. This is usually not the case for **q** in arbitrary directions, not even in the sound wave limit. As a measure of the anisotropy one usually takes (for cubic structures)

$$s = (c_{11} - c_{12})/(2c_{44}) \tag{2}$$

c_{ij} are the elastic constants. If $s=1$, then the long wavelength vibrations are always strictly longitudinal or transverse. The sound velocity of the longitudinal branch is isotropic, as is also that of the degenerate transverse branches (T_1, T_2). The anisotropy index s differs widely also for simple metals. We have $s_{Na}=0.14$, $s_{Al}=0.82$ and $s_{Pb}=0.25$. This fact can be given a simple explanation. Using eqs. 1 and 2 we can alternatively write

$$s = \lim_{q \to 0} \left[\omega_{ii}^2(110;T_2) - \omega_{ie}^2(110;T_2) \right] / \left[\omega_{ii}^2(110;T_1) - \omega_{ie}^2(110;T_1) \right] \tag{3}$$

The ion-ion interaction alone would lead to a strong anisotropy, which only depends on the lattice type (fcc, bcc). For sodium, with only one

6

conduction electron per atom, ω_{ie}^2 is small and it is natural to find anisotropy. For polyvalent metals like lead and aluminium, ω_{ii}^2 and ω_{ie}^2 are of the same order of magnitude and s is therefore very sensitive to details in the electron-phonon interaction. *We therefore conclude that anisotropy is the normal behaviour and the fact aluminium is almost isotropic is only accidental.*

In paper B we show that s is in fact not a very good measure of anisotropy. Instead *we introduce a new index of anisotropy, A,* defined by

$$A = c_{11}/(c_{12} + 2c_{44}) \tag{4}$$

When s=1 we have also A=1. Let $\alpha_L(max)$ be the maximum angle between the direction of atomic displacements $\hat{e}_L(q)$ and the corresponding wave vector q for the 'longitudinal' branch. We have calculated $\alpha_L(max)$ in the limit of small $|q|$ for all cubic elements (paper B). Fig. 2 shows that $\alpha_L(max)$ is simply related to A but not to s.

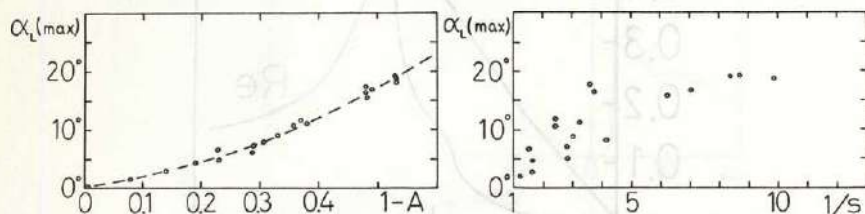Fig. 2. $\alpha_L(max)$ gives the maximum angle between the direction of the atomic displacements $\hat{e}_L(q)$ and the corresponding wave vector q for the 'longitudinal' branch in the limit of small q. The circles refer to elements with cubic structure. s is the conventional anisotropy index, $s = (c_{11} - c_{12})/2c_{44}$. A is our new index, $A = c_{11}/(c_{12} + 2c_{44})$. It is evident that A is a better measure of the anisotropy.

Electrons from a many-body point of view

In this section we discuss results for the electron self energy and the spectral function. This is the central part of the thesis, but we will here be rather brief because of the formal nature of the subject. Experimental consequencies are considered in the following sections.

The self energy M_{el-ph}

For a free particle, the total energy is just the kinetic energy $\epsilon(p) = p^2/2m$. The interaction between electrons and phonons leads to a correction, the electron self energy M_{el-ph}. The kinetic energy is a function only of the

momentum $\mathbf{p}$. The self energy M_{el-ph} on the other hand turns out to be almost independent of $\mathbf{p}$, but depends strongly on the energy and the temperature, $M_{el-ph}=M_{el-ph}(\omega; T)$. M_{el-ph} is a non-real function that depends in a complicated way on details in the electron-phonon system. It was first calculated by Engelsberg and Schrieffer for very simplified models. *In paper C we have made a very detailed calculation of the self energy M_{el-ph} for a real metal (sodium).* The result for T=0 is given in fig. 3.
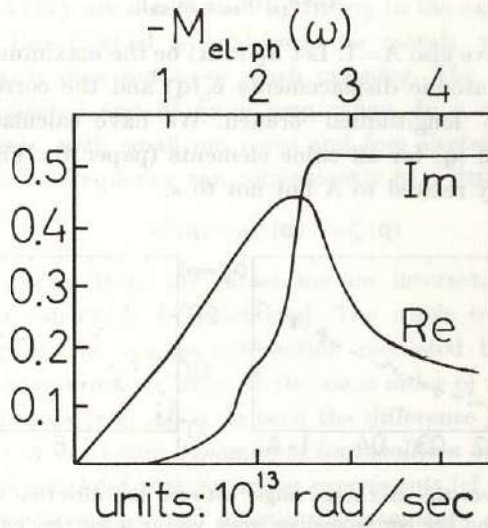
Fig. 3. The real and imaginary parts of the electron self energy $M_{el-ph}(\omega)$ caused by interactions with phonons. The curves are for sodium at $T=0°$K. $\omega_D=2.1 \times 10^{13}$ rad/sec. The frequency ω is counted from the Fermi level.

These curves are typical in shape for metals. Note that Re M_{el-ph} is different from zero only in a narrow range of a few phonon energies around the Fermi level. In the foregoing section it was mentioned that tunneling experiments in superconductors could give very accurate results for the effective electron-phonon interaction $\alpha^2(\omega)F(\omega)$ with the phonon energy as variable. This information is extremely useful in a calculation of M_{el-ph} at finite temperatures, because energy is the variable that enters the statistical Bose-Einstein and Fermi-Dirac factors. In paper F, *we have used data from tunneling experiments to calculate the self energy M_{el-ph} for lead and mercury.*

8

The spectral function $A(\mathbf{p}, \omega)$

Once we have calculated the self energy $\mathbf{M}$, we can form the spectral function $A(\mathbf{p}, \omega)$ defined by

$$A(\mathbf{p}, \omega) = \frac{1}{\pi} \frac{|\mathrm{Im} \mathbf{M}|}{[\omega - \epsilon(\mathbf{p}) - \mathrm{Re}\, \mathbf{M}]^2 + [\mathrm{Im}\, \mathbf{M}]^2} \tag{5}$$

For a non-interacting system, i.e. with $\mathbf{M}$ infinitesimal, $A(\mathbf{p}, \omega)$ simply becomes the delta function $\delta(\omega - \epsilon(\mathbf{p}))$. This corresponds to the fact that a free particle with momentum $\mathbf{p}$ is in an exact eigenstate of energy $\omega = \epsilon(\mathbf{p})$. When interactions are included, the sharp peak in $A(\mathbf{p}, \omega)$ broadens (corresponding to a decay of the eigenstate) and also shifts in energy. Typical plots of $A(\mathbf{p}, \omega)$ are given in fig. 4. The area under $A(\mathbf{p}, \omega)$ is constant
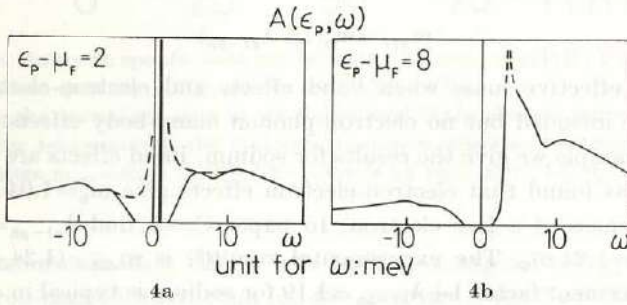
$A(\epsilon_p, \omega)$

unit for ω: meV

4a   4b

Fig. 4. The spectral function $A(p, \omega)$ for lead at two values of p (or rather two values of $\epsilon_p - \mu_F$) and at $T = 0°$K. In fig. a, there is a sharp peak at $\omega_0 = 0.8$ meV, representing a quasi particle. The area under this peak is 40% of the total area under $A(p, \omega)$. This sharp and well defined peak disappears when the temperature is raised (the dotted curve in fig. a is for $T = 11°$K) or when $\epsilon_p - \mu_F$ becomes comparable with typical phonon energies (fig. b).

$(= 1)$. At low temperatures and in the vicinity of the Fermi level μ_F, $\mathrm{Im}\, M_{el-ph}$ is small and $\mathrm{Re}\, M_{el-ph}$ depends linearly on the energy. It therefore follows that $A(\mathbf{p}, \omega)$ has a peak at an energy ω_0 given by

$$\omega_0 = [\epsilon(\mathbf{p}) - \mu_F]/(1 + \lambda_{el-ph}) \tag{6}$$

if $\epsilon(\mathbf{p}) - \mu_F$ is small compared to typical phonon energies and the temperature is much less than the Debye temperature. λ_{el-ph} is the slope of $-\mathrm{Re}\, M_{el-ph}$ at the Fermi level. It is this peak that appears as a sharp line in fig. 4 a, and it represents what we call a *quasi particle*. It is no longer well defined when the temperature is raised (fig. 4 a) or $\epsilon(\mathbf{p}) - \mu_F$

9

is comparable to typical phonon energies (fig. 4 b). It is only at low excitation energies and at low temperatures that it is meaningful to talk about a quasi particle. From eq. 6 we see that the quasi particle density of energy levels is increased by a factor $1+\lambda_{el-ph}$ over the free particle density of states.

The electronic specific heat

The low temperature electronic specific heat for a non-interacting electron gas is proportional to the density of states at the Fermi level. It takes the same form when many-body effects are included, but is then proportional to the quasi particle density of levels. The result of a specific heat measurement is often given in the form of an effective electron mass, and we have

$$m_{eff}=m_b(1+\lambda_{el-ph}) \tag{7}$$

m_b is the effective mass when band effects and electron-electron interactions are included but no electron-phonon many-body effects.

As an example we give the results for sodium. Band effects are negligible. Hedin[2] has found that electron-electron effects give $m_b=1.04\,m_0$, where m_0 is the mass of a free electron. In paper C, we find $\lambda_{el-ph}=1.19$ and thus $m_{eff}=1.24\,m_0$. The experimental result[3] is $m_{eff}=(1.24\pm0.02)\,m_0$. The enhancement factor $1+\lambda_{el-ph}=1.19$ for sodium is typical in magnitude for the alkali metals. The strong coupling superconductors lead ($\lambda_{el-ph}=1.5$) and mercury ($\lambda_{el-ph}=1.6$) have unusually large enhancement factors.

We have already mentioned that we can only talk about a constant quasi particle density of levels at very low temperatures with only low energy excitations involved. *Therefore we expect deviations from the linear behaviour of the electronic specific heat C_{el} as the temperature increases.* A formula for C_{el} valid at arbitrary temperatures has been given by Prange and Kadanoff without any really strict proof. *In paper F it is shown that their result follows rigorously from a Green function formulation of the thermodynamic potential of the coupled electron-phonon system.* Let us write

$$C_{el}=[\gamma_0+\gamma_1(T)]T \tag{8}$$

In the limit of low temperatures we have $\gamma_1(0)=\lambda_{el-ph}\gamma_0$. *In paper D, we calculate $\gamma_1(T)/\gamma_1(0)$ in an Einstein model for the phonons and in paper F we give accurate results for lead and mercury.* The result for lead is given in fig. 5. It is seen that only at very low temperatures and at $T\gtrsim\theta_E/3$ is C_{el} linear in T. At high temperatures there are, however, no electron-
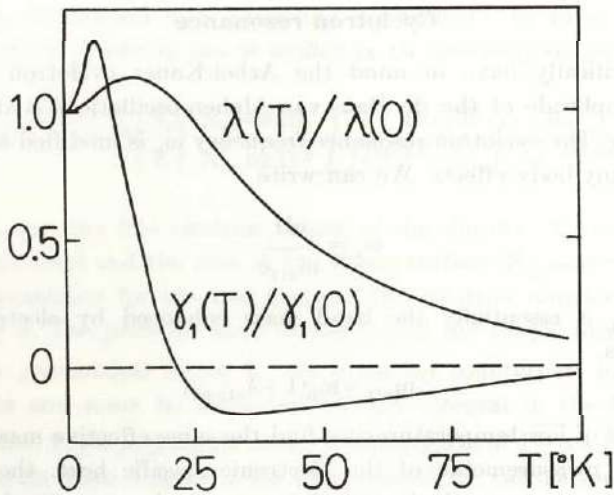
Fig. 5. The electronic specific heat can be written $C_{el}=[\gamma_0+\gamma_1(T)]T$. The figure shows the normalized quantity $\gamma_1(T)/\gamma_1(0)$ for lead. $\gamma_1(0)=1.5\gamma_0$.
$\lambda(T)/\lambda(0)$ is the normalized slope at the Fermi level of the electron self energy M_{el-ph}. At very low temperatures, the cyclotron resonance effective electron mass can be written $m_{eff}=m_b[1+\lambda(T)]$. The curve is for lead. $\lambda(0)=1.5$. $\theta_D=90°K$.

phonon renormalization effects left. $k_B\theta_E$ is a typical energy transfer in the electron-phonon interaction (cf. the quantity $\alpha^2(\omega)F(\omega)$). The temperature at which $\gamma_1(T)/\gamma_1(0)$ has its maximum is about $\theta_E/8$, no matter which metal we consider. The reason why the characteristic feature of C_{el} has not yet been verified is that it is swamped by the lattice specific heat.

In papers E and F we suggest a possible experiment to verify the non-linear temperature dependence of C_{el}. One can measure the total specific heat in the normal and in the superconducting state, i.e. with and without a magnetic field. The electronic contribution is very different in the two states, but the lattice part is practically unchanged. In this way, the electronic contribution can be isolated. Nevertheless this experiment lies at the limit of what is possible at present.

At high temperatures C_{el} has to be distinguished from effects of lattice anharmonicity. The latter contribution is also linear in T, but can be estimated from measurements of phonon frequency shifts with inelastic neutron scattering at different temperatures. Very recent high temperature specific heat measurements on lead[4] show a much better agreement with neutron scattering data if C_{el} is linear in T but with no electron-phonon renormalisation effects.

11

Cyclotron resonance

We specifically have in mind the Azbel-Kaner cyclotron resonance, but the amplitude of the de Haas-van Alphen oscillations is affected in a similar way. The cyclotron resonance frequency ω_c is modified by electron-phonon many-body effects. We can write

$$\omega_c = \frac{eH}{m_{eff}c} \qquad (9)$$

where m_{eff} is essentially the band mass enhanced by electron-phonon interactions,

$$m_{eff} = m_b(1 + \lambda_{el-ph}) \qquad (10)$$

In the limit of low temperatures we find the same effective mass enhancement from measurements of the electronic specific heat, the cyclotron resonance frequency and the de Haas-van Alphen amplitude. We are restricted to low temperatures because of the condition $\omega_c\tau \gg 1$. Therefore we consider excitations at energies where $\mathrm{Re}\,M_{el-ph}(\omega)$ is still linear in ω and $\mathrm{Im}\,M_{el-ph}$ is small. However, $\mathrm{Re}\,M_{el-ph}$ is explicitly temperature dependent. *We have shown that at finite but low temperatures, the resonance frequency is approximately given by eqs. 9 and 10 if we let λ_{el-ph} be temperature dependent. A model calculation of $\lambda(T)$ is given in paper D. Accurate calculations can be found in the papers D (Na) and E, F (Pb and Hg).* In fig. 5 we give $\lambda(T)/\lambda(0)$ for lead. The temperature dependence of the cyclotron resonance mass is a marginal effect but should be detectable with the present technique. It must be pointed out that cyclotron resonance experiments can be carried out at higher temperatures if we apply a high enough magnetic field. However, our calculations are valid only for low magnetic fields ($\omega_c \ll$ typical phonon frequencies). Cyclotron resonance in high magnetic fields is much more difficult to treat, especially if we want to go beyond simple model calculations.

Transport properties

The basic mechanism of the phonon limited electrical resistivity is thought to be fairly well understood. However, numerical calculations are very sensitive to fine details in the electron-phonon system and they often give poor results. The resistivity depends on the effective interaction between electrons and phonons but also involves a geometrical factor $1 - \cos\theta$ that makes large angle scattering most effective. Now recall that the effective electron-phonon interaction in all its details could for some

12

elements be determined from tunneling experiments. *In paper G we show that the electrical resistivity can be written in the extremely simple form*

$$S = \overline{1 - \cos\theta} \left(\frac{S_0}{S}\right)^2 \frac{N_{bs}}{N_{fe}} \frac{4\pi m\hbar}{nkTe^2} \int \frac{\alpha^2(\omega)F(\omega)\omega \, d\omega}{[e^{\hbar\omega/kT} - 1][1 - e^{-\hbar\omega/kT}]} \qquad (11)$$

N_{fe} and S_0 are the free electron values of the density of electron states at the Fermi level and the area of the Fermi surface. N_{bs} and S are corresponding quantities for the real system. The electron number density is denoted by n. The price we have to pay to get the simple form of eq. 11 is that the geometrical factor $\overline{1 - \cos\theta}$ has no counterpart in tunneling experiments and must be taken outside the integral in the form of an average value. For a polyvalent metal, a clever guess of $\overline{1 - \cos\theta}$ introduces a smaller error than that of a standard resistivity calculation. It is fascinating that *data from the superconducting state can be used to calculate the room temperature electrical resistivity.*

The validity of the Wiedemann-Franz law for the ratio between the thermal and electrical conductivities is well established at high temperatures, so the thermal conductivity need not be treated separately in this limit.

Effects of external pressure

Some experiments are very rich in information. Using cyclotron resonance, to take one example, one can map out the Fermi surface in great detail. Resistivity measurements on the other hand just give a single number. Measurements under pressure, i.e. at different lattice spacings, are important as they give an additional degree of freedom. *In paper H we consider the pressure dependence of a large variety of metallic properties. The main emphasis is on the high temperature electrical resistivity of lead.* It is shown that the volume dependence of the phonon frequencies gives the most important contribution the pressure dependence, but there are also other effects that are not negligible. The thermal expansion leads to effects similar to those of external pressure and is also considered in paper H.

Multi-phonon scattering processes and Debye-Waller factors are always neglected in standard calculations of the electrical resistivity. These two effects come in with different signs, and it is still an open question how well they cancel. A remaining net effect would give a non-linear temperature dependence in the high temperature electrical resistivity. However, the *measured temperature coefficient of the resistivity for lead is in quantitative*

agreement with the standard theory if allowance is made for the thermal expansion and purely anharmonic shifts in the phonon frequencies.

Concluding remarks on effective electron masses

We have seen that the standard formulas for the specific heat, and the cyclotron resonance frequency can be used at low temperatures if the electron mass is enhanced by the factor $1+\lambda_{\mathrm{el-ph}}$. There are other formulas, like that for the electrical resistivity, which also contain the density of electron states at the Fermi level or, equivalently, the effective electron mass. In this latter case there should be no extra factor $1+\lambda_{\mathrm{el-ph}}$ and the reason is that not only the density of states but also the wave function is renormalized and these two effects exactly cancel. Prange and Kadanoff and others have considered the effects of electron-phonon interaction in some detail. In the table we quote the results for some properties and indicate whether the effective mass that occurs in the corresponding formulas should be renormalized or not.

Effect	Mass renormalization from electron-phonon interaction
Specific heat	yes
Cyclotron resonance frequency (Azbel-Kaner)	yes
de Haas-van Alphen amplitude	yes
Thermal and d.c. electrical conductivity	no
Pauli spin paramagnetism	no

14

Acknowledgements

References

(only references not given in papers A–H)

1. The early history of lattice dynamics has been reviewed by M. Born and P. Debye in Lattice Dynamics, Edited by R. F. Wallis, Pergamon Press, Oxford (1965).
   A historical survey on the electron gas model is given in: A. H. Wilson, The theory of metals, Cambridge University Press, New York (1965).

2. Hedin, L.: Private communication.

3. Martin, D. L.: Phys. Rev. *124*, 438 (1961).

4. Leadbetter, A. J.: J. Physics C *1*, 1489 (1968).

THE ELECTRON–PHONON COUPLING AND PHONON SPECTRA IN LEAD–THALLIUM ALLOYS STUDIED BY ELECTRON TUNNELLING

T. CLAESON and G. GRIMVALL

Department of Physics and Theoretical Physics, Chalmers University of Technology, Gothenburg, Sweden

THE ELECTRON–PHONON COUPLING AND PHONON SPECTRA IN LEAD–THALLIUM ALLOYS STUDIED BY ELECTRON TUNNELLING

T. CLAESON and G. GRIMVALL

Department of Physics and Theoretical Physics, Chalmers University of Technology, Gothenburg, Sweden

Abstract – Electron tunnelling into superconducting f.c.c. lead–thallium alloys has been carried out in the homogeneity range 0–70 at.% Tl in Pb. The half energy gap, Δ_0, decreases from 1·35 meV for Pb to 0·5 meV for $Pb_{0·3}Tl_{0·7}$. The ratio $2\Delta_0/kT_c$ is reduced from the strong-coupling value of 4·4 to the weak-coupling value 3·5 at about 60 at.% Tl. The anisotropy in the energy gap remains up to about 15% Tl in Pb. A diminishing deviation of the experimental dI/dV vs. V curve from the BCS one, a lower T_c with higher Tl content, shifts in phonon frequencies, and trends in published neutron diffraction data show that the electron-phonon coupling decreases with the number of valence electrons per atom. The phonon induced structure in the tunnelling curves agrees well with phonon spectra from neutron diffraction work by Stedman *et al.* and Ng and Brockhouse. The longitudinal peak is shifted towards higher frequencies as the coupling grows weaker. The frequency band of transverse modes broadens as the number of free electrons decreases. A theoretical model was tried to account for the changes in the transverse phonon branches. It was possible to get a qualitative agreement, but the result was unreasonably sensitive to small changes in the form of the pseudopotential or the electron screening.

INTRODUCTION

AN IMAGE of the phonon spectrum of a material can often be obtained via tunnelling measurements. The method has been particularly successful for strong-coupling superconductors (i.e. where the coupling between the phonons, which are to be studied, and the electrons, the probe, is strong). Let us consider electrons injected into levels well above the gap energy in a superconductor. By the emission of a phonon, an electron can be scattered to a level close to the energy gap, where there is a high density of available states. As energy is conserved, the transition rate must depend on the number of phonon states with matching energy as well as on the strength of the electron–phonon coupling. The injected quasiparticles thus have a finite lifetime which results in an imaginary contribution to their self energy. The real part of the self energy is also changed. The gap function becomes complex and energy dependent and as the tunnelling current depends on the

gap function we will obtain structure in a recorded tunnelling characteristic. If we record not only the current vs. voltage behaviour but also its first and second derivatives with respect to voltage, the deviations from the expected BCS curves are magnified considerably.

Structure from the phonon spectrum has been seen in tunnelling characteristics for several superconducting metals[1]. Theoretically, the situation is well understood[2]. From recorded dI/dV vs. V curves it is even possible to obtain the phonon density of states (multiplied by an electron-phonon coupling strength) with respect to phonon energies[3]. Here, we report results from tunnelling into superconducting Pb–Tl alloys. Alloys have previously been investigated only to a limited extent[4, 5]. The Pb–Tl system is a very favourable one to study, since the coupling strength in Pb is particularly large, and it is possible to dissolve more than 85 at.% Tl into Pb and still maintain the f.c.c. Pb struc-

ture. Hence we can study the energy gap, the density of excited states, the electron–phonon coupling strength and the phonon spectrum and their dependence upon the electron density in the range $e/a = 3 \cdot 1 - 4$ just by tunnelling into these alloys. An introductory study of the superconducting transition temperature in the system has been published earlier[6]. Preliminary tunnelling results have also been reported briefly[7].

The phonon density of states can also be studied in other ways. Neutron diffraction gives a good and clearcut result, however a complete mapping is time consuming and costly. Although the superconducting tunnelling method does not give such a clear result as the neutron diffraction one, and the number of elements to be studied is limited, its ease of obtaining information about the phonon spectrum makes it very attractive. We shall also compare the density of phonon states obtained by neutron diffraction with our tunnelling curves.

EXPERIMENTAL TECHNIQUES

Junctions of the type $Al/Al_2O_3/Pb-Tl$ (Alloy) were evaporated at a pressure of $\lesssim 10^{-5}$ mm Hg. A thin Al strip was deposited upon a glass substrate and oxidized in dry air at normal pressure for about 15 min. Then a layer of the alloy investigated was deposited. This second film had a thickness of a few hundred Å. Three junctions, with different areas, were made upon the same glass slide. The materials used were originally supposed to be 99·999 per cent pure.

The boiling alloy could be heated resistively or by electron bombardment. Pb and Tl evaporate at similar rates, hence no large deviations in the composition of the evaporated film from the desired one are expected as long as the evaporated lump is not too big. The composition of the fabricated alloy strip could be checked by comparing its superconducting transition temperature with that of the bulk alloy. (The T_c of Pb films does not differ very much from that of bulk material.)

In this way the amount of Tl in Pb could be established within a few per cent. The composition of the strip agreed with that of the original bulk material within the accuracy of the determination.

Two of the samples (20 and 35 at. % Tl) were prepared by a flash-evaporation method. About 10–20 Å (4–8 atomic layers) were deposited at a time. In order to prevent the sample from warming up during this time-consuming procedure (and hence prevent the aluminium oxide from regrouping into islands producing short-circuit paths), it could be cooled by a heat sink at liquid nitrogen temperature. The samples were generally annealed at room temperature one day before they were investigated.

Tunnelling characteristics were recorded by employing standard techniques[8]. Current (I) and dI/dV vs. voltage (V) curves were plotted on an $x-y$ recorder when applying a constant voltage driving source. The second current derivative, d^2I/dV^2, was registered by studying the harmonic frequency of an applied sensing signal. d^2I/dV^2 and dV/dI vs. V curves were taken with a constant current bias source.

The temperature during a run was determined by measuring the vapour pressure of liquid helium. The 1958 He^4 temperature scale[9] was used for the conversion between pressure and temperature. The junctions could be investigated down to $1 \cdot 3°K$. The superconducting critical temperature of a sample was established by taking dI/dV vs. V characteristics at different temperatures. dI/dV at zero bias voltage was plotted vs. T and this curve could then be compared with corresponding theoretical BCS one[10]. $T = T_c$ at $[(dI/dV)_s/(dI/dV)_n]_{V=0} = 1$ (s and n denote superconducting and normal states respectively).

RESULTS

The superconducting energy gap could be determined by comparing a set of dI/dV vs. V curves taken at several T/T_c ratios with cor-

responding theoretical curves[10]. The error in the determination is estimated to be less than 5 per cent, except for the highest Tl concentrations, where an unfavourable (higher) T/T_c ratio gave an error of at least 10 per cent. The half energy gap at $0°K$, Δ_0; T_c; and the ratio $2\Delta_0/kT_c$ are plotted as functions of composition in Fig. 1.

directions when the electrons enjoy long-lived states (i.e. in a pure crystal). We will hence obtain our anisotropic energy gap. As impurities are added we can no longer use well-defined Bloch states but must use combinations of these with scattering taken into account. Due to this averaging one obtains isotropic properties. For low Tl concentra-
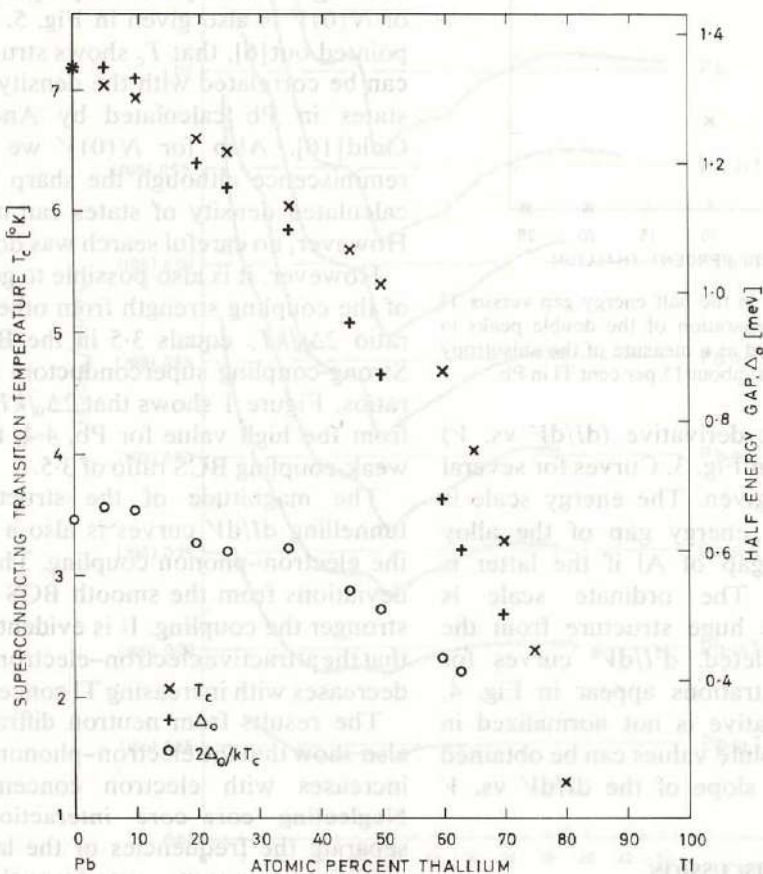
Fig. 1. The superconducting transition temperature, T_c, the half energy gap at $0°K$, Δ_0, and the ratio $2\Delta_0/kT_c$ vs. composition in Pb–Tl alloys. Δ_0 decreases faster than T_c except in the low concentration impurity range where anisotropy effects dominate. Hence $2\Delta_0/kT_c$ is reduced from the strong-coupling value of 4·4 to the weak-coupling BCS ratio of 3·5 at about 60 at.% Tl.

The anisotropy of the energy gap is rather well understood[11]. As both the phonon distribution and the Fermi surface are aniso-tropic, different electron–phonon coupling strengths will be obtained in different crystal

tions dI/dV showed no singly peaked but a doubly peaked structure in the vicinity of the gap energy ($\pm\Delta_{0\,Al}$). As a measure of the aniso-tropy we can take the difference $\delta(\Delta_0)$ obtained by determining the energy separation of the

peaks. In Fig. 2 we have plotted $\delta(\Delta_0)$ vs. at.% Tl, and we see that as scattering centres are added, the anisotropy decreases and disappears at about 15 at.% Tl in Pb.
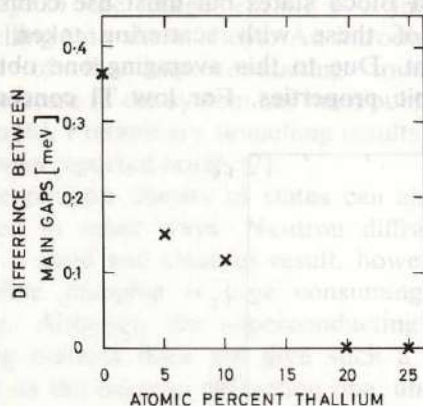

Fig. 2. The anisotropy in the half energy gap versus Tl content. The energy separation of the double peaks in dI/dV vs. V plots is used as a measure of the anisotropy which disappears at about 15 per cent Tl in Pb.

Normalized first derivative (dI/dV vs. V) curves are shown in Fig. 3. Curves for several compositions are given. The energy scale is counted from the energy gap of the alloy (plus the energy gap of Al if the latter is superconducting). The ordinate scale is magnified and the huge structure from the energy gap is deleted. d^2I/dV^2 curves for several Tl concentrations appear in Fig. 4. The second derivative is not normalized in these curves. Absolute values can be obtained by measuring the slope of the dI/dV vs. V curves.

DISCUSSION

Electron–phonon coupling strength

The superconducting transition temperature decreases in the Pb–Tl system as the number of valence electrons becomes smaller[7]. Up to about 50 at.% Tl T_c decreases slowly, but then a rapid drop is registered for an increasing Tl content. The T_c variation indicates in itself the variation of the strength of the coupling responsible for superconductivity. However we can also compute the Debye

temperature, θ_D, from ultrasonic measurements and apply the BCS formula[12] $T_c \sim \theta_D e^{-1/N(0)V}$ to get a measure of the effective electron–electron interaction $N(0)V$. In Fig. 5 we have plotted values of θ_D vs. composition taken from Alers and Karbon[13] and also values computed from measurements by Shepard and Smith[14] utilizing de Launay's tables[15]. The variation of $N(0)V$ is also given in Fig. 5. It has been pointed out[6], that T_c shows structure which can be correlated with the density of electron states in Pb calculated by Anderson and Gold[16]. Also for $N(0)V$ we notice the reminiscence although the sharp peak in the calculated density of states can not be seen. However, no careful search was done.

However, it is also possible to get estimates of the coupling strength from other data. The ratio $2\Delta_0/kT_c$ equals 3·5 in the BCS theory. Strong-coupling superconductors show larger ratios. Figure 1 shows that $2\Delta_0/kT_c$ decreases from the high value for Pb, 4·4, towards the weak-coupling BCS ratio of 3·5.

The magnitude of the structure in the tunnelling dI/dV curves is also a measure of the electron–phonon coupling. The larger the deviations from the smooth BCS curves, the stronger the coupling. It is evident from Fig. 3 that the attractive electron–electron interaction decreases with increasing Tl concentration.

The results from neutron diffraction work also show that the electron–phonon interaction increases with electron concentration[17]. Neglecting core–core interaction we can separate the frequencies of the lattice vibrations into two parts—one from the Coulomb interaction between the ions and the other from the electronic screening*

$$\omega^2 = \omega_{ii}^2 - \omega_{ie}^2 = \omega_{pl}^2(I_{ii} - I_{ie}) \qquad (1)$$

where subscripts ii and ie denote ion–ion and ion–electron interactions respectively.

---

*In the discussion of phonon properties we closely follow the presentation by Vosko, Taylor and Keech[18], and use ω_{pl} as a natural unit.
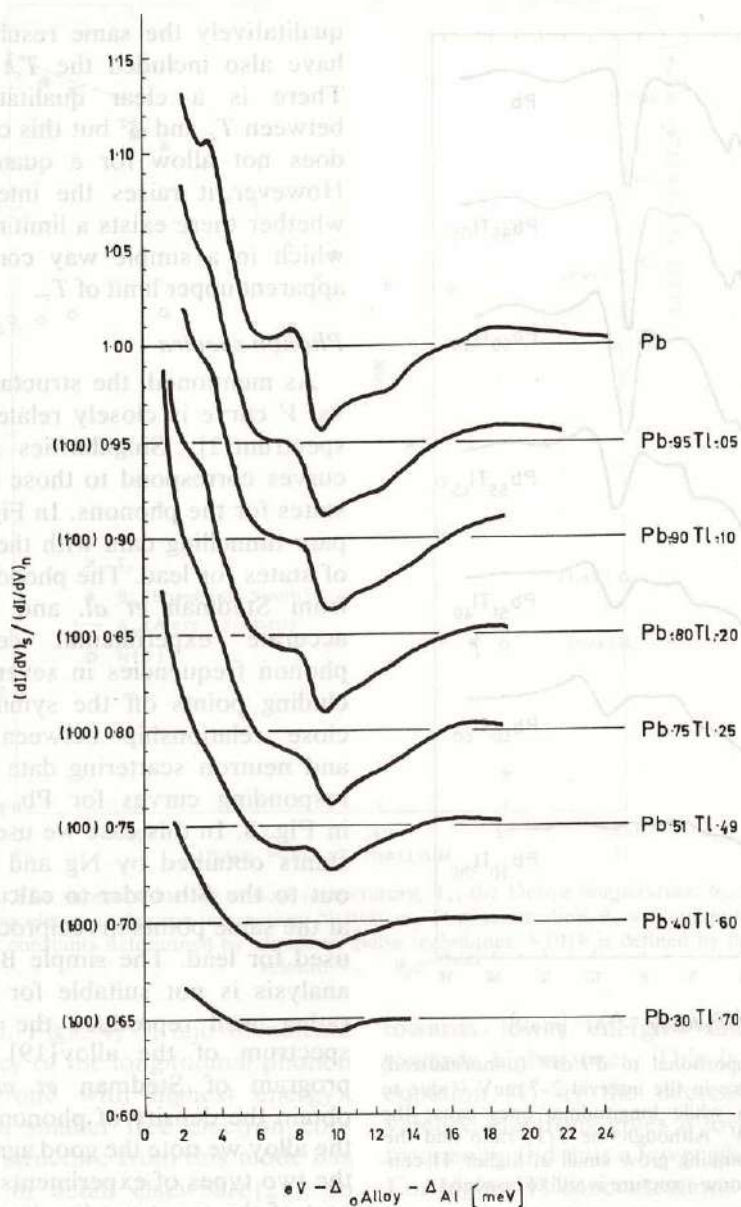
Fig. 3. Normalized dI/dV vs. energy plots for varying Tl content. The energy scale is counted from the gap of the alloy plus the one of Al if the latter is superconducting. Note that the structure grows weaker (smaller deviations from the smooth BCS curves) as the free electron concentration is reduced.

ω_{pl} is the ionic plasma frequency given by $\omega_{pl}^2 = 4\pi(Ze)^2/M\Omega_0$, where Z is the ion charge, M its mass and Ω_0 the volume of the unit cell. I_{ii} depends only on the crystal structure and I_{ie} is a measure of the strength of the electron–phonon interaction. For f.c.c. structures we can vary the number of 'free' electrons per atom e/a in the range 3(Al) to

Fig. 4. Curves proportional to d^2I/dV^2 (unnormalized) vs. eV. The structure in the interval 2–7 meV is due to transverse phonons while longitudinal ones cause the dip at about 9 meV. Although the T/T_c ratio and the electron–phonon coupling grow small at higher Tl concentrations, some structure is still to be seen.
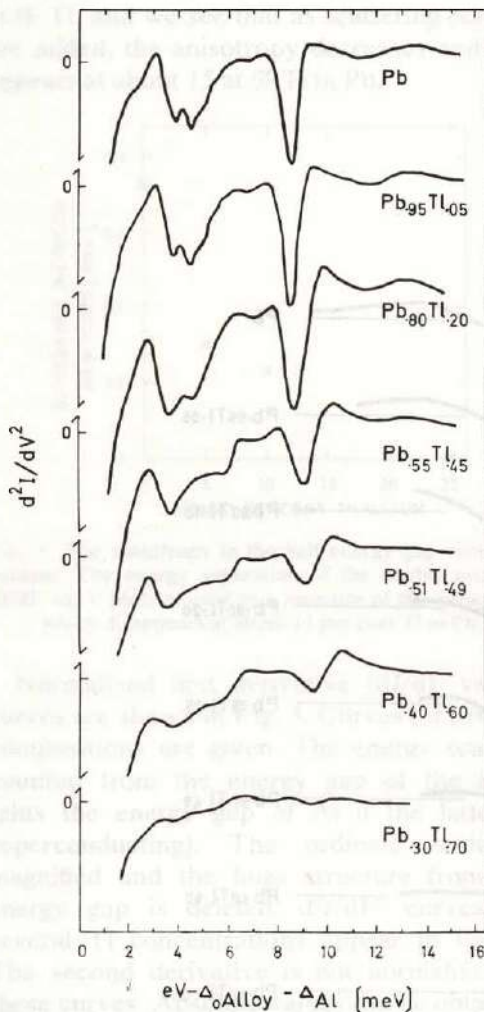
4·2 (Pb–Bi). In Fig. 6 we plot the unscreened ion–ion frequency for the transverse mode in the [100]–direction and experimental dispersion curves with $e/a = 3$ (Al)[19], 3·4 ($Pb_{0.4}Tl_{0.6}$)[17], and 4 (Pb)[17]. A theoretical curve for Na ($e/a = 1$) in a hypothetical f.c.c. structure[20] is also included. For the alloy we used an average ion mass and charge to define ω_{pl}. Other transverse modes give

qualitatively the same results. In Fig. 6 we have also included the $T_c:s$ of the metals. There is a clear qualitative relationship between T_c and ω^2 but this crude comparison does not allow for a quantitative relation. However it raises the interesting question whether there exists a limiting property of ω^2 which in a simple way corresponds to the apparent upper limit of T_c.

Phonon spectra

As mentioned, the structure in the d^2I/dV^2 vs. V curve is closely related to the phonon spectrum[2]. Singularities in the d^2I/dV^2 curves correspond to those in the density of states for the phonons. In Fig. 7 we can compare tunnelling data with the phonon density of states for lead. The phonon curve is taken from Stedman *et al.* and is based on an accurate experimental determination of phonon frequencies in several directions including points off the symmetry axes. The close relationship between the tunnelling and neutron scattering data is evident. Corresponding curves for $Pb_{0.4}Tl_{0.6}$ are shown in Fig. 8. In this case we used the force constants obtained by Ng and Brockhouse[17] out to the 8th order to calculate frequencies at the same points in reciprocal space as those used for lead. The simple Born–vonKármán analysis is not suitable for lead but should rather well reproduce the smooth phonon spectrum of the alloy[19]. The computer program of Stedman *et al.* was used to obtain the density of phonon states. Also for the alloy we note the good agreement between the two types of experiments. The transverse part of the spectrum has lost the rich details of the Pb density of states, and a larger energy spread is also registered.

If one is only interested in the location of the singularities in the phonon spectrum, tunnelling experiments have clear advantages compared to the conventional neutron scattering technique. We will devote the rest of this section to an analysis of the location of singularities.
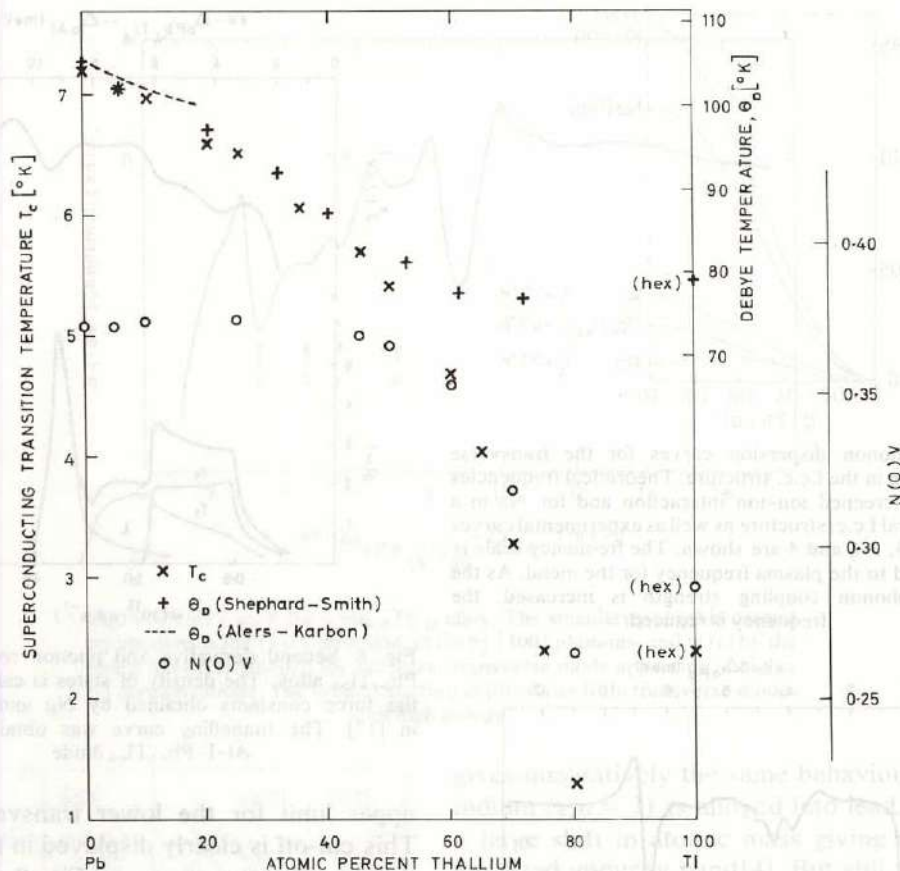
Fig. 5. The superconducting critical temperature, T_c, the Debye temperature, θ_D, and the effective electron–electron interaction, $N(0)V$, vs. Tl concentration. θ_D was computed from elastic constants determined by ultrasonic pulse techniques. $N(0)V$ is defined by the BCS relation $T_c \sim \theta_D e^{-1/N(0)V}$.

As mentioned, Figs. 4, 7, and 8 indicate that the frequency of the longitudinal phonon mode (i.e. the one with highest energy), increases with a smaller free electron concentration. The structure from this mode has been discussed in detail elsewhere[21], so we concentrate on the structure caused by the transverse modes. The singularity (a) in Fig. 9 stems from phonons near the zone boundary in the [111]-direction. Phonon dispersion curves for Pb and $Pb_{0.4}Tl_{0.6}$ are given for comparison in Fig. 10. These curves are taken from measurements by Stedman *et al.*[19] and by Ng and Brockhouse[17]. As thallium is alloyed into lead (a) first moves

towards lower energies and then slightly towards higher ones. This is consistent with equation (1) as the decreasing number of valence electrons gives a lower ionic plasma frequency and thus a lower phonon frequency. For higher Tl concentrations this tendency is counteracted by the rapidly decreasing electron–phonon coupling. The structure at (b) in Fig. 9 is caused by the maximum in the transverse mode in the [100]-direction. This structure gradually disappears with a smaller e/a, an effect which is clearly displayed in both the tunnelling and the diffraction curves. A new structure appears at (c) when the dispersion curves for the alloy indicate a sharp
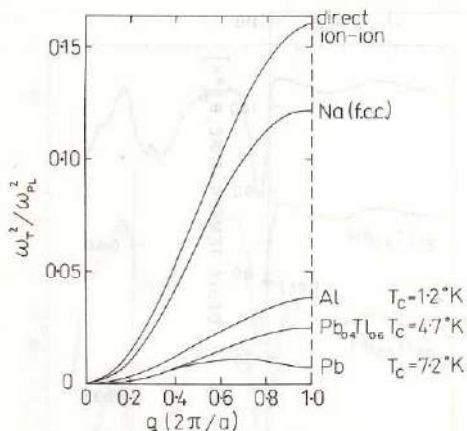
Fig. 6. Phonon dispersion curves for the transverse [100]-mode in the f.c.c. structure. Theoretical frequencies for an unscreened ion–ion interaction and for Na in a hypothetical f.c.c. structure as well as experimental curves for $e/a = 3$, 3·4, and 4 are shown. The frequency scale is normalized to the plasma frequency for the metal. As the electron–phonon coupling strength is increased, the frequency is reduced.
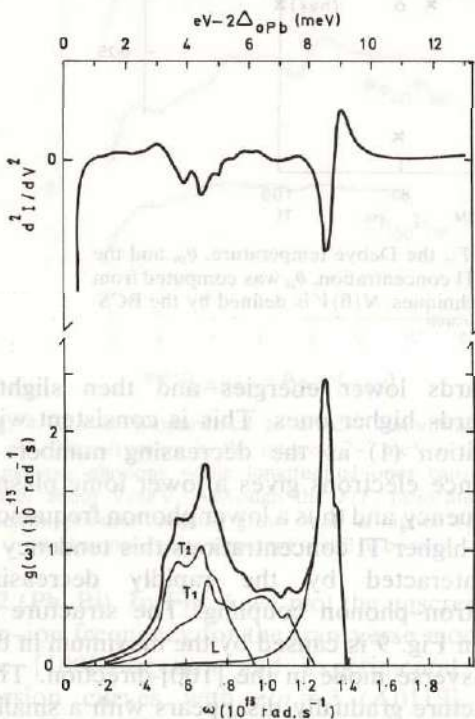

Fig. 7. d^2I/dV^2 vs. energy for a Pb–I–Pb junction compared with the phonon density of states vs. energy curve computed by Stedman et al.[19] from neutron diffraction data. The energy scales in the two curves are adjusted to coincide.
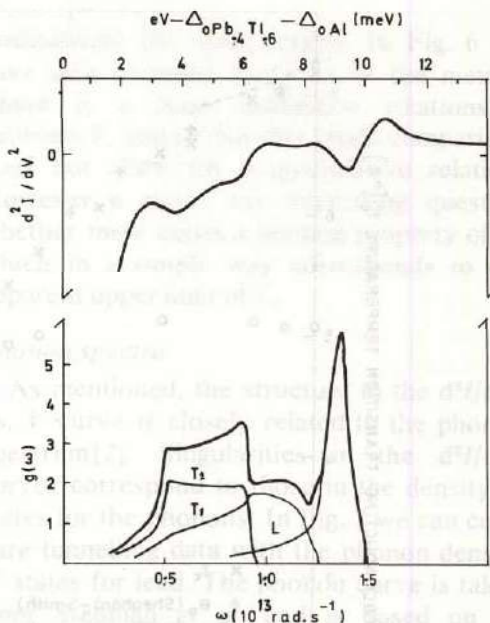
Fig. 8. Second derivative and phonon spectrum for a $Pb_{0.4}Tl_{0.6}$ alloy. The density of states is calculated using the force constants obtained by Ng and Brockhouse in [17]. The tunnelling curve was obtained from an Al–I–$Pb_{0.4}Tl_{0.6}$ diode.

upper limit for the lower transverse mode. This cut-off is clearly displayed in the phonon density of states curve of Fig. 8. The broad structure at (d) comes from the high energy part of the T_1-mode. These phonon frequencies correspond to points in reciprocal space which lie off the symmetry axes[19], a fact which makes an analysis difficult and uncertain.

An interesting composition is $Pb_{0.65}Tl_{0.35}$ (the d^2I/dV^2 vs. V curve is shown in Fig. 9). Neutron diffraction data[17] indicates that around this composition we should be in an intermediate region, where the dispersion curves are expected to have flat regions (i.e. peaks in the density of states). The tunnelling curve also displays sharper structure than corresponding curves for alloys with somewhat higher and lower Tl concentrations. Unfortunately no neutron diffraction data are available for the transverse mode at this composition.

Fig. 9. d^2I/dV^2 vs. V for a $Pb_{0.65}Tl_{0.35}$ alloy. The singularity at (a) is caused by phonons is the [111]-direction, at (b) by [100] phonons, and at (c) by the sharp cut-off frequency for the lower transverse mode appearing at higher Tl concentrations. The broad structure at (d) comes from transverse modes of high energy.
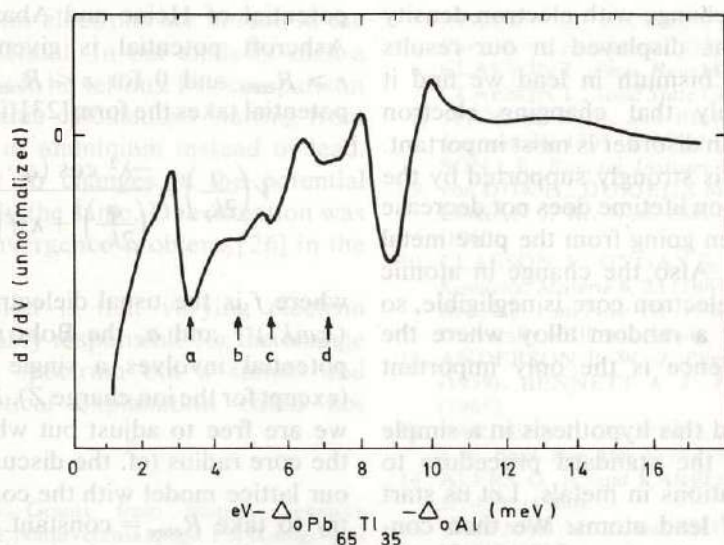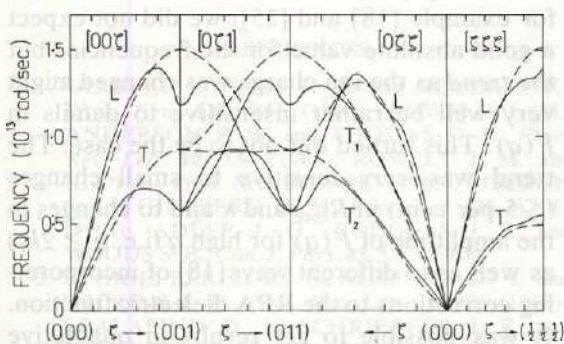
Fig. 10. Phonon dispersion curves for Pb and $Pb_{0.4}Tl_{0.6}$ measured by Stedman et al. (full line) and Ng and Brockhouse (dashed line) respectively.

The tunnelling result for a Pb + 10 at.% Bi alloy[5] $(e/a = 4.1)$ gives a good 'extrapolation' of our Pb–Tl data. The structures at (a) and (b) coincide and form a broadened dip, which indicates a coincidence between the transverse phonon peaks in the [111]- and [100]-directions. A preliminary result from a $Pb_{0.7}Tl_{0.15}Bi_{0.15}$ alloy $(e/a = 4)$, where the coupling strength has increased,

gives qualitatively the same behaviour. When indium $(e/a = 3)$ is alloyed into lead, there is a large shift in atomic mass giving rise to a localized impurity band[4]. But still there are qualitative similarities in the structure from the transverse modes compared to the case of Pb–Tl. Tunnelling data by Adler et al.[5] show the same behaviour as our curves. The four elements In, Tl, Pb and Bi are close together in the periodic table and thus well suited for investigations on the effects of changing ion mass or charge.

It remains to give a theoretical explanation of the behaviour of the transverse modes when lead is alloyed. We will concentrate upon the degenerate branches in the [100]- and [111]-directions, where we noted that the phonon peaks in these branches come closer as e/a grows. In the Tl–Pb–Bi system the crystal structure remains f.c.c. from approximately $e/a = 3.1$ to 4.2, and the interatomic distance is practically constant[22]. If disorder effects are important we face a theoretical problem which is extremely complicated. Considering

the monotonous change with electron density around $e/a = 4$ as displayed in our results and in those for bismuth in lead we find it much more likely that changing electron density rather than disorder is most important. This assumption is strongly supported by the fact that the phonon lifetime does not decrease considerably when going from the pure metal to the alloy[17]. Also the change in atomic mass and in the electron core is negligible, so we can consider a random alloy where the difference in valence is the only important feature.

We have tested this hypothesis in a simple model following the standard procedure to treat lattice vibrations in metals. Let us start with a lattice of lead atoms. We then continuously change the ion charge and the number of valence electrons, at the same time keeping mass and interatomic distance constant. The contributions to the phonon frequencies are separated into an ion–ion and an ion–electron part as was done in (1). As the core–core overlap is small and in our model practically constant, we neglect it. $I_{ii}(q)$ depends only on structure and is thus unchanged. For strictly transverse modes I_{ie} takes the form[18]

$$I_{ie}(q) = \sum_{G \neq 0} (\hat{e}_T \cdot \mathbf{G})^2 \left\{ \frac{F(\mathbf{G}+\mathbf{q})}{(\mathbf{G}+\mathbf{q})^2} - \frac{F(\mathbf{G})}{\mathbf{G}^2} \right\} \quad (2)$$

where F is the so called form factor and G is a reciprocal lattice vector. The form factor F contains the electron–phonon interaction in the form of a screened pseudopotential. The choice of a pseudopotential is not simple. Most of the potentials are either very complicated or fitted just to one of the phonon branches we want to consider. For reasons to be seen later we do not want to use potentials fitted to experiments where one determines not the pseudopotential but a combination of pseudopotential and screening functions. Recently, Ashcroft[23] has proposed a potential which in spite of its very simple form shows good agreement with the

potential of Heine and Abarenkov[24]. The Ashcroft potential is given by $-Ze^2/r$ for $r \geq R_{core}$ and 0 for $r < R_{core}$. The screened potential takes the form[23] (in units of $2 E_F/3$)

$$V\left(\frac{q}{2k_F}\right) = \frac{-\lambda^2 \cos(q \cdot R_{core})}{\left(\frac{q}{2k_F}\right)^2 + \lambda^2 f\left(\frac{q}{2k_F}\right)} \quad (3)$$

where f is the usual dielectric function, $\lambda^2 = (\pi a_0 k_F)^{-1}$ and a_0 the Bohr radius. Thus the potential involves a single parameter R_{core} (except for the ion charge Z). R_{core} is a quantity we are free to adjust but which is related to the core radius (cf. the discussion in [23]). In our lattice model with the core unchanged we try to take $R_{core} = $ constant. The continuous change in the ion charge Z means that we change the plasma frequency, the Fermi level and the parameters in the dielectric function for a free electron gas. Considering the great difficulties other authors have met when calculating phonon frequencies in lead (cf. for example [18] and [25]) we did not expect a good absolute value for the frequencies but the *trend* as the ion charge was changed might very well be rather insensitive to details in $F(q)$. This turned out not to be the case. The trend was *very* sensitive to small changes ($\lesssim 5$ per cent) in R_{core} and λ and to changes in the amplitude of $F(q)$ for high q (i.e. $q \gtrsim 2k_F$) as well as to different ways[18] of incorporating corrections to the RPA dielectric function. It was possible to get results in qualitative agreement with the experimental data but small and reasonable changes gave completely different results. It was also noted that the sensitivity to changes could be very different for different electron densities. This was unexpected and gives another warning against an uncritical use of the pseudopotential concept. A usual approach when keeping to one special element is to start with a simple form of the electron screening function and then solve for a 'good' bare pseudopotential by a fit to some experimental data, e.g. phonon curves. In this way deficiencies in the handling

of the conduction electrons are hidden in the bare pseudopotential. In our analysis such a procedure seems to be serious. For comparison we made the same calculations starting from the properties of aluminium instead of lead. The sensitivity to changes in the potential was qualitatively the same. Due attention was paid to the convergence problems [26] in the sum (2).

Our conclusion is that varying electron density is probably responsible for the change in the phonon spectrum but a simple and reliable theoretical explanation could not be established.

REFERENCES

1. GIAEVER I., HART H. R. and MEGERLE K., *Phys. Rev.* **126**, 941 (1962); ROWELL J. M., ANDERSON P. W. and THOMAS D. E., *Phys. Rev. Lett.* **10**, 334 (1963); ROWELL J. M. and KOPF L., *Phys. Rev.* **137**, A907 (1965); BERMON S. and GINSBERG D. M., *Phys. Rev.* **135**, A306, (1964); ADLER J. G., RODGERS J. S. and WOODS S. B., *Can. J. Phys.* **43**, 557 (1965).
2. SCHRIEFFER J. R., SCALAPINO D. J. and WILKINS J. W., *Phys. Rev. Lett.* **10**, 336 (1963); SCALAPINO D. J., SCHRIEFFER J. R. and WILKINS J. W., *Phys. Rev.* **148**, 263 (1966).
3. McMILLAN W. L. and ROWELL J. M., *Phys. Rev. Lett.* **14**, 108 (1965).
4. ADLER J. G., JACKSON J. E. and CHANDRA-SEKHAR B. S., *Phys. Rev. Lett.* **16**, 53 (1966); ROWELL J. M., McMILLAN W. L. and ANDERSON P. W., *Phys. Rev. Lett.* **14**, 633 (1965).
5. ADLER J. G., JACKSON J. E. and WILL T. A., *Phys. Rev. Lett.* **24A**, 407 (1967).
6. CLAESON T., *Phys. Rev.* **147**, 340 (1966).
7. CLAESON T., *Solid State Commun.* **5**, 119 (1967).
8. THOMAS D. E. and ROWELL J. M., *Rev. sci. Instrum.* **36**, 1301 (1965); ADLER J. G. and JACKSON J. E., *Rev. sci. Instrum.* **37**, 1049 (1966).
9. von DIJK H., DURIEUX M., CLEMENT J. R. and LOGAN J. K., *Natl. Bur. Stand. Monogr.* **10**, 12 (1960).
10. CLAESON T., GYGAX S. and MAKI K., *Physik Kondens. Materie* **6**, 23 (1967); BERMON S., *Tech. Rep.* No. 1 on NSF-GP 1100, Physics Department, University of Illinois (1964).
11. ANDERSON P. W., *J. Phys. Chem. Solids* **11**, 26 (1959); BENNETT A. J., *Phys. Rev.* **140**, A1902 (1965).
12. BARDEEN J., COOPER L. N. and SCHRIEFFER J. R., *Phys. Rev.* **108**, 1175 (1957).
13. ALERS G. A. and KARBON J. A., *J. appl. Phys.* **37**, 4252 (1966).
14. SHEPARD M. L. and SMITH J. F., *Acta Metall.* **15**, 357 (1967).
15. de LAUNAY J., *J. chem. Phys.* **22**, 1676 (1954).
16. ANDERSON J. R. and GOLD A. V., *Phys. Rev.* **139**, A1459 (1965).
17. NG S. C. and BROCKHOUSE B. N., *Solid State Commun.* **5**, 79 (1967).
18. VOSKO S. H. TAYLOR R. and KEECH G. H., *Can. J. Phys.* **43**, 1187 (1965).
19. STEDMAN R., and NILSSON G., *Phys. Rev.* **145**, 492 (1966); STEDMAN R., ALMQVIST L., NILSSON G. and RAUNIO G., *Phys. Rev.* **162**, 545 (1967); STEDMAN R., ALMQVIST L. and NILSSON G., *Phys. Rev.* **162**, 549 (1967).
20. TOYA T., *Inelastic Scattering of Neutrons*, Vol. I p. 39. IAEA, Vienna (1965).
21. ROWELL J. M. and KOPF L., *Phys. Rev.* **137**, A907 (1965); SCALAPINO D. J. and ANDERSON P. W., *Phys. Rev.* **133**, A921 (1965).
22. TANG Y.-C. and PAULING L., *Acta crystallogr.* **5**, 44 (1952); ÖLANDER A., *Z. phys. Chem.* **168**, 274 (1934).
23. ASHCROFT N. W., *Phys. Rev. Lett.* **23**, 48 (1966); ASHCROFT N. W., To be published.
24. HEINE V. and ABARENKOV I., *Phil. Mag.* **9**, 451 (1964); ANIMALU A. D. E. and HEINE V., *Phil. Mag.* **12**, 1249 (1965).
25. HARRISON W. A., *Pseudopotentials in the Theory of Metals* Benjamin, New York (1966).
26. WESTIN A., Unpublished report, Institute of Theoretical Physics, Univ. of Upsala, Sweden.

Institute of Theoretical Physics, Fack, Göteborg

On the Polarization Vectors of Lattice Vibrations

By

G. Grimvall

The polarization vectors of lattice vibrations in anisotropic crystals of cubic structure are considered from a quantitative point of view. A new anisotropy index $A = c_{11}/(c_{12} + 2 c_{44})$ is shown to be more adequate as a measure of anisotropy than the conventional $s = (c_{11} - c_{12})/2 c_{44}$. The reason for anisotropy is discussed briefly, with special emphasis on simple metals. The approximation of assuming the lattice vibrations to be strictly longitudinal or transverse is discussed for several properties of metals, with sodium taken as an example.

Die Polarisationsvektoren für Gitterschwingungen werden in anisotropen Kristallen mit kubischer Symmetrie numerisch untersucht. Es wird gezeigt, daß ein neuer Index der Anisotropie $A = c_{11}/(c_{11} + 2 c_{44})$ besser als $s = (c_{11} - c_{12})/2 c_{44}$ die Anisotropie charakterisiert. Die Ursache der Anisotropie in Metallen wird kurz behandelt. Als Beispiel wird die theoretische Approximation mit der Annahme genau longitudinaler und transversaler Gitterschwingungen an Natrium untersucht.

1. Introduction

A knowledge of the eigenvalues of lattice vibrations in solids is of considerable importance and this field has attracted much interest. The purpose of this paper is to consider, mainly from a quantitative point of view, the eigenvectors which generally do not receive much attention. We also consider in some detail various applications where a detailed knowledge of the eigenvectors is essential. Qualitative aspects based on group theoretical considerations can be found in two comprehensive articles by Maradudin and Vosko [1] and Warren [2].

Phonon frequencies can now be measured with a high degree of accuracy and can be calculated theoretically from some specific model. The theoretical approach in general involves much labour if accurate results are desired. The eigenvectors (or polarization vectors) on the other hand are difficult to measure with precision [3], but instead symmetry requirements are of dominant importance. We will mainly consider monoatomic cubic crystals. For lattice vibration with small q-vectors, the dynamical matrix is then obtained from the three elastic constants, so in this limit we can easily solve for the eigenvalues and eigenvectors.

As the eigenvectors are to great extent determined by symmetry conditions at the zone faces and in general can be expected to vary slowly with $|q|$ at fixed direction $\hat{q}$, an overall knowledge can be inferred from a solution in the limit of small $|q|$.

2. The Long Wave Limit

2.1 General theory

We consider monoatomic crystals with cubic symmetry. Eigenvectors $\hat{e} = (e_1, e_2, e_3)$ and eigenvalues $\omega = 2\,\pi\,\nu$ are then obtained from the set of equations [4]

$$[(c_{11} - c_{44})\,q_1^2 + c_{44}\,q^2 - \varrho\,\nu^2]\,e_1 + (c_{12} + c_{44})\,q_1\,q_2\,e_2 + (c_{12} + c_{44})\,q_1\,q_2\,e_3 = 0, \quad (1a)$$

$$(c_{12} + c_{44})\,q_1\,q_2\,e_1 + [(c_{11} - c_{44})\,q_2^2 + c_{44}\,q^2 - \varrho\,\nu^2]\,e_2 + (c_{12} + c_{44})\,q_2\,q_3\,e_3 = 0, \quad (1b)$$

$$(c_{12} + c_{44})\,q_1\,q_3\,e_1 + (c_{12} + c_{44})\,q_2\,q_3\,e_2 + [(c_{11} - c_{44})\,q_3^2 + c_{44}\,q^2 - \varrho\,\nu^2]\,e_3 = 0. \quad (1c)$$

Here the wave vector q is denoted by $q = (q_1, q_2, q_3)$, ϱ is the mass density.

For non-degenerate eigenvalues the eigenvectors are orthogonal and fulfil a relation for scalar products with an arbitrary unit vector $\hat{a}$.

$$\hat{e}_{\lambda_1} \cdot \hat{e}_{\lambda_2} = \delta_{\lambda_1 \lambda_2}, \quad (2)$$

$$\sum_{\lambda} (\hat{e}_{\lambda} \cdot \hat{a})^2 = 1 . \quad (3)$$

It is convenient to introduce the dimensionless quantity s,

$$s = \frac{c_{11} - c_{12}}{2\,c_{44}} \quad (4)$$

which is in general called the anisotropy index. From equations (1) one finds that there is a simple relation between s and the velocities of transverse sound waves in the [100]-direction. We therefore write

$$s = \lim_{q \to 0} \frac{\omega_{T_2}^2(110)}{\omega_{T_1}^2(110)}, \quad (5)$$

where T_1 is the transverse mode with $\hat{e}_{T_1}$ parallel to the [001]-axes.

It is easy to find that a necessary and sufficient condition for the eigenvectors to be strictly longitudinal and transverse is that $s = 1$. A simple proof has been given by de Launey [4]. The branch that has the highest frequency will be called "longitudinal" even when $s \neq 1$, for it can be shown that the eigenvector of this mode forms the smallest angle with $\hat{q}$. From the proof of de Launey just mentioned, it is easy to see that approximate isotropy holds if $|c_{11} - c_{12} - 2\,c_{44}| \ll c_{12} + 2\,c_{44}$. We therefore introduce a new dimensionless index of anisotropy, A, defined by

$$A = \frac{c_{11}}{c_{12} + 2\,c_{44}} . \quad (6)$$

$A = 1$ when $s = 1$. From the numerical calculations in the next section it will be clear that A and not s gives a good measure of the anisotropy for the eigenvectors. However the form $s = \lim_{q \to 0} [\omega_{T_2}^2(110)/\omega_{T_1}^2(110)]$ makes s a convenient measure of the splitting of the lowest eigenvalues. Note that $s = 1$ only gives degenerate eigenvalues for transverse branches ($\omega_T^2 \propto c_{44}$). The longitudinal branch has $\omega_L^2 \propto c_{11}$ for $s = 1$. Not even if the Cauchy relation $c_{12} = c_{44}$ holds, will the three branches have the same frequency when $s = 1$.

2.2 Numerical examples

We will solve equations (1) numerically and calculate some quantities of interest in applications to be discussed later. First we consider the average value $\overline{(\hat{e}_L \cdot \hat{q})^2}$ for the longitudinal branch over all directions $\hat{q}$. Of interest are also the dimensionless averages $\overline{I_i}$

$$\overline{I_i} = \int \frac{\sum_\lambda \frac{(\hat{e}_\lambda \cdot \hat{q})^2}{(\omega_\lambda)^i}}{\left(\frac{1}{\omega_L}\right)^i} \frac{d\Omega}{4\pi} \qquad (7)$$

for $i = 1, 2, 4,$ and 6. For isotropic materials, all $\overline{I_i} = 1$. In the evaluations of these averages for cubic elements it is sufficient to consider only 1/48 of the first Brillouin zone. To form the averages we have used a modification of Houston's method [5] and solved the secular equation for 15 different directions and then used proper weighting factors. In Table 1 we give values of the parameters used, and the corresponding averages $\overline{(\hat{e}_L \cdot \hat{q})^2}$ for some elements of cubic structure. We also include some two-atomic cubic crystals which are exceptional in their values of s or A. For comparison we have also calculated $\overline{(\hat{e}_L \cdot \hat{q})^2}$ for q ranging over the surface of the first Brillouin zone, using the fact that $\hat{e}_L$ is then determined entirely by symmetry. We find for an f.c.c. structure $\overline{(\hat{e}_L \cdot \hat{q})^2} = 0.81$ and for a b.c.c. structure $\overline{(\hat{e}_L \cdot \hat{q})^2} = 0.82$. In Table 2 we give the averages $\overline{I_1}, \overline{I_2}, \overline{I_4}$, and $\overline{I_6}$ for some metals. For extremely anisotropic elements even the 15 term Houston method may be inaccurate, but still the values can be made a basis for the discussion on applications later. It could also be interesting to see, how the angle between the eigenvector e_λ and the unit vector $\hat{q}$ changes with s and A. The notation α_L, $(\alpha_{T_1}, \alpha_{T_2})$, will be used for the angle between $\hat{e}_\lambda$ and the direc-
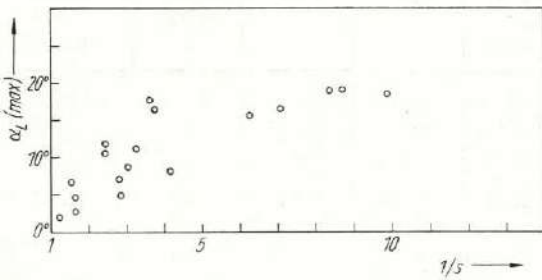
Fig. 1. The anisotropy index $s = (c_{11} - c_{12})/(2\,c_{44})$ is not a good measure of the maximum angle of deviation $\alpha_L(\max)$ between a wave vector $\hat{q}$ and the corresponding eigenvector $\hat{e}_L$ for the "longitudinal" mode. The points are for elements with $A < 1$. Tl In has $\alpha_L(\max) \approx 6°$ and $1/s = 29$ so this point falls outside the range of the plot

Fig. 2. The anisotropy index $A = c_{11}/(c_{12} + 2\,c_{44})$ gives a quantitative measure of the angle $\alpha_L(\max)$ (cf. Fig. 1). The dashed curve is only a rough fit to the points. Note that TlIn falls nicely on the curve
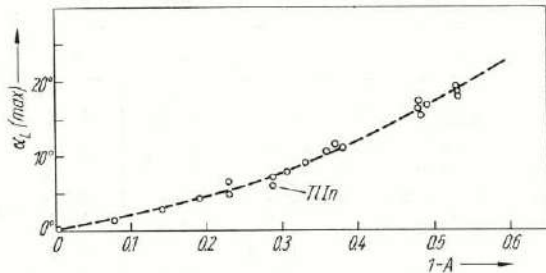
Table 1

Elastic constants are taken from [17] except for Rb [18] and Pt and Ir [19]. The values refer to room temperatures except for Rb (80 °K)

	c_{11}	c_{12}	c_{44}	A	s	$\overline{(\hat{e}_L \cdot \hat{q})^2}$
		$(10^{11}$ dyn/cm$^2)$				
b.c.c.						
chromium	35.0	6.8	10.1	1.29	1.35	0.994
niobium	24.6	13.4	2.87	1.28	1.95	0.997
molybdenum	47.0	16.8	10.7	1.23	1.41	0.997
vanadium	22.8	11.9	4.26	1.11	1.28	0.999
tungsten	51.5	20.4	15.6	1.00	1.00	1.000
tantalum	26.1	15.7	8.18	0.81	0.64	0.997
iron (α)	23.0	13.5	11.4	0.63	0.42	0.983
rubidium	0.296	0.244	0.160	0.52	0.16	0.970
potassium	0.457	0.374	0.263	0.52	0.17	0.968
sodium	0.739	0.622	0.419	0.51	0.14	0.967
lithium	1.35	1.14	0.88	0.47	0.11	0.957
coulomb lattice					0.13	
zone faces						0.82
f.c.c.						
aluminum	10.9	6.3	2.80	0.92	0.82	0.999
platinum	34.7	25.1	7.65	0.86	0.63	0.999
gold	18.9	15.9	4.26	0.77	0.35	0.996
iridium	58.0	24.2	25.6	0.77	0.66	0.994
palladium	22.7	17.6	7.17	0.71	0.36	0.993
lead	4.81	4.08	1.46	0.69	0.25	0.992
silver	12.2	9.2	4.46	0.67	0.34	0.990
nickel	24.8	15.3	11.6	0.64	0.41	0.985
copper	16.9	12.2	7.54	0.62	0.31	0.983
thorium	7.53	4.89	4.78	0.52	0.28	0.964
coulomb lattice					0.11	
zone faces						0.81
PbTe	10.7	1.30	0.77	3.8	6.1	0.881
RbI	2.56	0.36	0.28	2.8	3.9	0.930
Tl–In (28% Tl)	4.007	4.949	0.833	0.71	0.03	0.994
β-brass (48% Zn)	12.66	11.05	7.97	0.47	0.10	0.959
Li–Mg (4.3% Mg)	1.429	1.217	0.924	0.47	0.12	0.957

Table 2

Some important averages for metals, defined by equation (7)

Element	s	A	$\overline{I_1}$	$\overline{I_2}$	$\overline{I_4}$	$\overline{I_6}$
aluminum	0.82	0.92	1.00	1.00	1.01	1.04
lead	0.25	0.69	1.01	1.05	1.43	4.63
copper	0.31	0.62	1.02	1.06	1.37	3.02
rubidium	0.16	0.52	1.04	1.13	1.91	7.10
potassium	0.17	0.52	1.04	1.13	1.88	6.56
sodium	0.14	0.51	1.04	1.14	2.05	8.10
lithium	0.11	0.47	1.05	1.18	2.30	9.31

tion the considered mode would have in an isotropic medium. We have plotted the maximum angular deviation $\alpha_L(\max)$ as a function of the standard anisotropy index s and as a function of A (Figs. 1 and 2). The region $s > 1$ has been left out because of the small number of elements with such s-values. It is immediately clear from the figures that A and not s is a relevant measure of anisotropy for the polarization vectors. Note especially the properties of TlIn. What has now been said about $\alpha_L(\max)$ also holds for the related quantity $(\hat{e}_L \cdot \hat{q})^2$. See Table 1 for comparison. Typical plots of the directional dependence of α_L, α_{T_1}, and α_{T_2} can be found in a previous paper [6] dealing with sodium. There a specific model was also used to solve for the eigenvectors at points throughout the whole first Brillouin zone.

3. Reasons for Anisotropy

This section will be devoted to a discussion of why in general elements are anisotropic. For mathematical convenience we consider the index s and use relation (4). From the discreteness of the lattice, it follows that in a force constant model with only very short range forces, we should have a high degree of anisotropy. As an example we can consider forces between nearest and next nearest neighbours with a force ratio β (β = force from next nearest neighbour/force from nearest neighbour). Then from the dynamical matrix [4] it is easy to show that for a f.c.c. structure $s = \beta + 0.5$ and for a b.c.c. structure $s = 3\beta$. If the forces are of long range, this does not imply that the substance is elastically fairly isotropic, as can be seen in a simple example. Let us consider the coulomb ion–ion interaction between atoms for example in a metal. The forces are of very long range but still $s = 0.13$ for a b.c.c. structure and $s = 0.11$ for a f.c.c. structure. These values are obtained from a calculation by Jones [7] using Ewald's method of summation.

A comparison between the three metals Na, Al, and Pb gives reason for a more detailed investigation. The anisotropy index s differs widely ($s_{\mathrm{Na}} = 0.14$, $s_{\mathrm{Al}} = 0.82$. and $s_{\mathrm{Pb}} = 0.25$). Sodium is b.c.c. and the other two metals are f.c.c. To circumvent the influence of crystal structure we can compare with results from a theoretical calculation [8] of the lattice vibrations in sodium in a hypothetical f.c.c. structure. This calculation gives an anisotropy for sodium which is of the same order of magnitude as that of lead. For all three elements the lattice vibrations can be reasonably treated by considering only the direct ion–ion interaction and the interaction between the atoms mediated by the conduction electrons, thus neglecting other contributions such as core overlap. Also the free electron approximation for the conduction electrons is good for these metals. Still the s-values differ very much. We will start from the relation (4) to discuss this fact. The eigenvalues of mode (q, λ) can be written [9]

$$\omega^2(q, \lambda) = \omega_{ii}^2(q, \lambda) - \omega_{ie}^2(q, \lambda) \,, \tag{8}$$

where ω_{ii}^2 is the contribution from direct ion–ion interaction (Coulomb interaction) and ω_{ie}^2 comes from the interaction via the conduction electrons. This latter term can in some cases be negative [9]. For the index s we now have

$$s = \lim_{q \to 0} \frac{\omega_{ii}^2(110; T_2) - \omega_{ie}^2(110; T_2)}{\omega_{ii}^2(110; T_1) - \omega_{ie}^2(110; T_1)}. \tag{9}$$

The terms ω_{ii}^2 only depend on structure (i.e. are different for f.c.c. and b.c.c.) (9). We recall, that considering only the terms ω_{ii}^2 gives a high anisotropy. For

25*

elements with comparatively weak electron–phonon interaction, s is essentially determined by the anisotropic coulomb part. For elements with stronger electron–phonon interaction the terms ω_{ii}^2 and ω_{ie}^2 can be of the same order of magnitude. The value of s is therefore very sensitive to details in the electron–phonon interaction. This is the case for aluminium and lead. It is clear that anisotropy is the normal behaviour and that isotropy is only accidental. A more accurate determination of s would be equivalent to the calculation of the low energy phonon frequencies, a problem which is known to be very difficult even for simple metals.

4. An Application on Sodium

We will now demonstrate how the results obtained can be used in simple estimates. As an example we will investigate some properties of sodium. Our main interest will be an estimate of what error is introduced in calculations when the phonons are assumed to be strictly longitudinal and transverse (SLT). Let us start with consideration of the electron effective mass enhancement factor $1 + \lambda_{\text{el-ph}}$ due to electron–phonon interaction. We have [10]

$$\lambda_{\text{el-ph}} \propto \sum_\lambda \int_{S_F} \frac{[\hat{e} \cdot (K + q)]^2 \, (K + q) \, h^2(K + q)}{\omega^2(q)} \, \mathrm{d}(K + q), \tag{10}$$

where phonon frequencies of mode λ and wave vector q are denoted by $\omega_\lambda(q)$, the reciprocal wave vectors by K and the electron–phonon interaction by $h(K + q)$. $K + q$ connects two points on the Fermi surface. For sodium $2\,k_F = 1.24 \times \times (2\,\pi/a)$ in standard notation. We consider contributions to the integral from three regions in q-space: Normal processes ($K = 0$) for small q-values and q-values close to the boundary of the first Brillouin zone, and Umklapp processes, where most of the values of $q + K$ lie rather close to the faces of the first Brillouin zone. The two last regions can be treated together. From Table 1 we have $\overline{(\hat{e}_L \cdot \hat{q})^2} = 0.82$ at the zone faces and thus $\overline{(\hat{e}_{T_1} \cdot \hat{q})^2 + (\hat{e}_{T_2} \cdot \hat{q})^2} = 0.18$. From phonon dispersion curves we can estimate the relative difference between frequencies of the longitudinal and transverse branches close to the zone boundary. The low lying transverse modes around the [110]-direction are rather unimportant because q is normal to the zone face in this direction. As a result one finds that SLT underestimates the contribution from q-values close to the zone face by 10 to 15%. (Note that there is some ambiguity in SLT for Umklapp processes, as the eigenvectors of the transverse modes can be rotated in their plane.) From the value of $\overline{I_2} = 1.14$, that gives information about the small q-region, we conclude that the relative underestimation is roughly the same for all regions in the integrand of (10) in the case of sodium and amounts to 10 to 15%.

Next we turn to some low energy phenomena. Let τ_{el} denote the average life time of an electron at the Fermi level at finite temperatures. The inverse life time is proportional to the imaginary part of the electron self energy and one has for the contribution from electron–phonon interaction [10]

$$\frac{1}{\tau_{\text{el}}} \propto T^3 \sum_\lambda \int \frac{(\hat{e}_\lambda \cdot \hat{q})^2}{c^4(\theta, \varphi)} \, \mathrm{d}\Omega, \tag{11}$$

where $c(\theta, \varphi)$ is a directional dependent sound velocity. At low temperatures no Umklapp processes can occur as they involve energy losses $\gg kT$ (recall that $2\,k_F = 1.24\,(2\,\pi/a)$). It is therefore sufficient to consider $\overline{I_4}$ and we see that

SLT gives a lifetime which is a factor 2 too long. To this lifetime should of course then be added the effect of impurity scattering.

The very low temperature electrical resistivity ϱ is closely related to the life time τ_{el}. Again almost no Umklapp processes enter, but the integral in q-space for ϱ will contain an extra geometrical factor leading to the form [11] (for normal processes)

$$\varrho \propto T^5 \sum_\lambda \int \frac{(\hat{e} \cdot \hat{q})^2}{c^6(\theta, \varphi)} \, \mathrm{d}\Omega \ . \tag{12}$$

As we have $\overline{I_6} = 8.10$ for sodium, SLT will give almost an order of magnitude too low value. In the treatment above we have assumed the validity of the standard resistivity formula [12] for simple metals and neglected the possible influence of phonon drag. It is however important to note, that although Umklapp scattering is rare at low temperatures, it is weighted so strongly that it in fact dominates the resistivity down to very low temperatures [13]. In Umklapp processes there is always coupling to transverse modes (also with SLT) so the discussion above based on $\overline{I_6}$ exaggerates the failure of SLT.

Finally we consider the average lifetime τ_{ph} of phonons as limited by electron–phonon interaction. For a phonon (λ, q) we have [15]

$$\frac{1}{\tau_{\mathrm{ph}}} \propto \sum_K{}' \frac{[\hat{e}_\lambda \cdot (K + q)]^2}{(K + q)^2} G \left(K + q\right), \tag{13}$$

where G includes the electron–phonon interaction and the sum goes over all $|K| < 2 k_{\mathrm{F}}$. For sodium only $K = 0$ enters. From Fig. 2 we find that the lowest value of $\overline{(\hat{e}_L \cdot \hat{q})^2} \approx 0.92$ and consequently $\overline{(\hat{e}_T \cdot \hat{q})^2}$ never exceeds 0.08. Except for damping due to electron–phonon interaction there is of course also damping due to anharmonic effects. Experimental [16] and theoretical [15] investigations of the damping of phonons in metals are not very accurate, so it is not feasible at present to see any anisotropy in the damping of phonons due to electron–phonon interaction.

5. Conclusions

We have first demonstrated that the quantity $A = c_{11}/(c_{12} + 2 c_{44})$ is a better measure of anisotropy of the polarization vectors than the standard anisotropy index $s = (c_{11} - c_{12})/2 c_{44}$. In a short digression on the reasons of anisotropy a simple argument was given to show that anisotropy and not isotropy is the "normal" behaviour of metals. After numerical calculations on most of the cubic elements we finally discussed the approximation of assuming the phonons to be strictly longitudinal or transverse (SLT), taking sodium as an example. It was found that for example the low temperature electrical conductivity is considerably underestimated in SLT while on the other hand the effective mass enhancement from electron–phonon interaction is underestimated by only 10 to 15% (in Na).

References

[1] A. A. MARADUDIN and S. H. VOSKO, Rev. mod. Phys. **40**, 1 (1968).

[2] J. L. WARREN, Rev. mod. Phys. **40**, 38 (1968).

[3] B. N. BROCKHOUSE, L. N. BECKA, K. R. RAO, and A. D. B. WOODS, Inelastic Scattering of Neutrons in Solids and Liquids II, IAEA, Vienna 1963.

[4] J. DE LAUNAY, Solid State Phys. **2**, 219 (1956).

[5] D. D. BETTS, Canad. J. Phys. **39**, 233 (1961).

[6] G. BJÖRKMAN and G. GRIMVALL, phys. stat. sol. **19**, 863 (1967).

[7] H. JONES, Physica **15**, 13 (1949).

[8] T. TOYA, Inelastic Scattering of Neutrons I, IAEA, Vienna 1965.

[9] S. H. VOSKO, R. TAYLOR, and G. H. KEECH, Canad. J. Phys. **43**, 1187 (1965).

[10] G. GRIMVALL, Phys. kondens. Materie **6**, 15 (1967).

[11] H. BROSS, G. BOHN, and H. STÖHR, Z. Phys. **194**, 101 (1966).

[12] J. M. ZIMAN, Electrons and Phonons, Clarendon Press, Oxford 1960.

[13] M. BAILYN, Phys. Rev. **120**, 381 (1960).

[14] K. C. SHARMA and S. K. JOSHI, Phys. Rev. **140**, A1799 (1965).

[15] G. BJÖRKMAN, B. I. LUNDQVIST, and A. SJÖLANDER, Phys. Rev. **159**, 551 (1967).

[16] R. STEDMAN and G. NILSSON, Phys. Rev. **145**, 492 (1966).

[17] R. F. S. HEARMON, in: LANDOLT-BÖRNSTEIN, Numerical Data and Functional Relations, Vol. 1 (group III), Springer-Verlag, 1966.

[18] C. A. ROBERTS and R. MEISTER, J. Phys. Chem. Solids **27**, 1401 (1966).

[19] R. E. MAC FARLANE, J. A. RAYNE, and C. K. JONES, Phys. Letters (Netherlands) **20**, 234 (1966).

Numerical Calculations on the Electron-Phonon System in Sodium

Göran Grimvall

Institute of Theoretical Physics*, Sven Hultins gata, Göteborg, Sweden

Numerical results are given for the phonon contribution to the electron self-energy in sodium. The importance of including in detail the phonon properties is stressed. Anisotropy in the effective mass and in the damping of an electron is investigated. Most of the calculations are at zero temperature, but the imaginary part of the self energy is calculated for several values of the temperature.

On présente des calculs numériques de la contribution des phonons á la selfenergie des électrons pour le sodium. C'est important de rendre compte des propriétés des phonons en detail. L'anisotropie de la masse effective et de l'amortissement d'un électron ont été étudié. La plupart des calculs a été faite pour la temperature zéro, mais la partie imaginaire de l'énergie a été calculée pour plusieurs valeurs de la temperature.

Numerische Resultate werden für den Phononenbeitrag zur Elektronen-Eigenenergie in Natrium angegeben. Die Wichtigkeit, Einzelheiten des Phononenspektrums einzuschließen, wird hervorgehoben. Anisotropie der effektiven Masse und der Elektronendämpfung wird untersucht. Die meisten Berechnungen werden für 0° K ausgeführt, der imaginäre Teil der Elektronenenergie wird jedoch für verschiedene Temperaturen berechnet.

1. Introduction

In recent years there has been much interest in electron-phonon interaction. Engelsberg and Schrieffer [1, 2], Migdal [3] and Abrikosov et al. [4] have treated the self-energy of electrons due to interaction with phonons in a Green's function formalism. Many authors have also taken up the problem of the effective mass of an electron on the Fermi surface [5—9]. The purpose of this paper is not to give a very accurate numerical result but to investigate numerically in more detail the structure of the electron self-energy due to interaction with lattice vibrations. Therefore we do not hesitate to be inconsistent in that we use one model (Sham's [10]) for the electron-phonon interaction matrix element and another model (Krebs's [12]) for the phonon properties.

The Green's function treatment of the problem is dealt with in detail in a book by Schrieffer [2], so we only give the main formulas. At zero temperature the electron self-energy due to interaction with phonons can be written

$$M_{el-ph}(\boldsymbol{p}, p_0) = \frac{i}{(2\pi)^4} \int g^2(p-k) G(k) D(p-k) d^4k. \tag{1}$$

Non-diagonal terms in wavevector space have been completely neglected. The three terms in the integrand mean the electron-phonon coupling function, the electron Green's function and the phonon Green's function. Here we have

---

* The institute serves both Chalmers Institute of Technology and Göteborg University.

taken the vertex function equal to unity according to the wellknown argument of MIGDAL [3]. The frequencies occuring in the coupling function g are of the order of the Debye frequency so it is a good approximation to take a static g.

Using the fact that the self-energy M_{el-ph} depends slowly on the wavevector in the vicinity of the Fermi surface and integrating twice we get for M_{el-ph} the following two integrals which are equal to those given by SCHRIEFFER [2] apart from the angular integration and the sum over the phonon branches.

$$\mathrm{Re}\, M_{el-ph}(p, \omega) = - \frac{m}{16\, p\, \pi^3} \sum_\lambda \int_0^{2\pi} d\varphi \int_0^{2k_F} \frac{q(\hat{e}_{\lambda,q} \cdot q)^2 h^2(q)}{\omega_\lambda(q)} \ln \left| \frac{\omega + \omega_\lambda(q)}{\omega - \omega_\lambda(q)} \right| dq, \quad (2a)$$

$$\mathrm{Im}\, M_{el-ph}(p, \omega) = - \frac{m}{16\, p\, \pi^2} \sum_\lambda \int_0^{2\pi} d\varphi \int_0^{|\omega_\lambda(q)| < \infty} \frac{q(\hat{e}_{\lambda,q} \cdot q)^2 h^2(q)}{\omega_\lambda(q)} dq. \quad (2b)$$

Here we have

$\omega_\lambda(q)$ the phonon frequency of branch λ and properly reduced wavevector,

$(\hat{e}_{\lambda,q} \cdot q)\, h(q)$ the screened matrix element between an ion and an electron,

φ the angle of rotation round the axis p,

q the total momentum transfer. In the integration q is always taken between p and another point on the Fermi surface,

m electron mass,

$\hbar = 1$.

We have assumed that the Fermi surface is spherical but we have retained in full the non-isotropic properties of the phonons. From now on we take the zero point of the electron energy at the Fermi surface.

2. Numerical Results

Previous calculations [1—4] of M_{el-ph} have used simple models, e.g. a Debye model for the phonons. We here want to make a more realistic calculation and especially see the relative importance of umklapp processes and the effect of not assuming the lattice vibrations to be purely longitudinal and transverse.

To investigate the relative importance of umklapp processes it is essential to have a good approximation for the matrix element of the electron-phonon interaction at large momentum transfers. We are not going to dwell upon this difficult point but instead take the result from the so-called non-local model by SHAM [10], being one of the most detailed recent calculations. The numerical difficulties are considerable when the lattice vibrations are not assumed to be purely longitudinal and transverse. In a previous work [11] the properties of the lattice vibrations have been calculated with KREBS [12] model in a network corresponding to 1000 points in the first Brillouin zone. These results have been directly used here. In this connection we should mention that the usual method of expanding the phonon properties in cubic harmonics by fitting to symmetry directions is not good as the effect of the lattice vibrations being non-longitudinal and non-transverse then disappears. The direction of the wavevector p in $M(p, \omega)$ was taken along the [100]-axis.
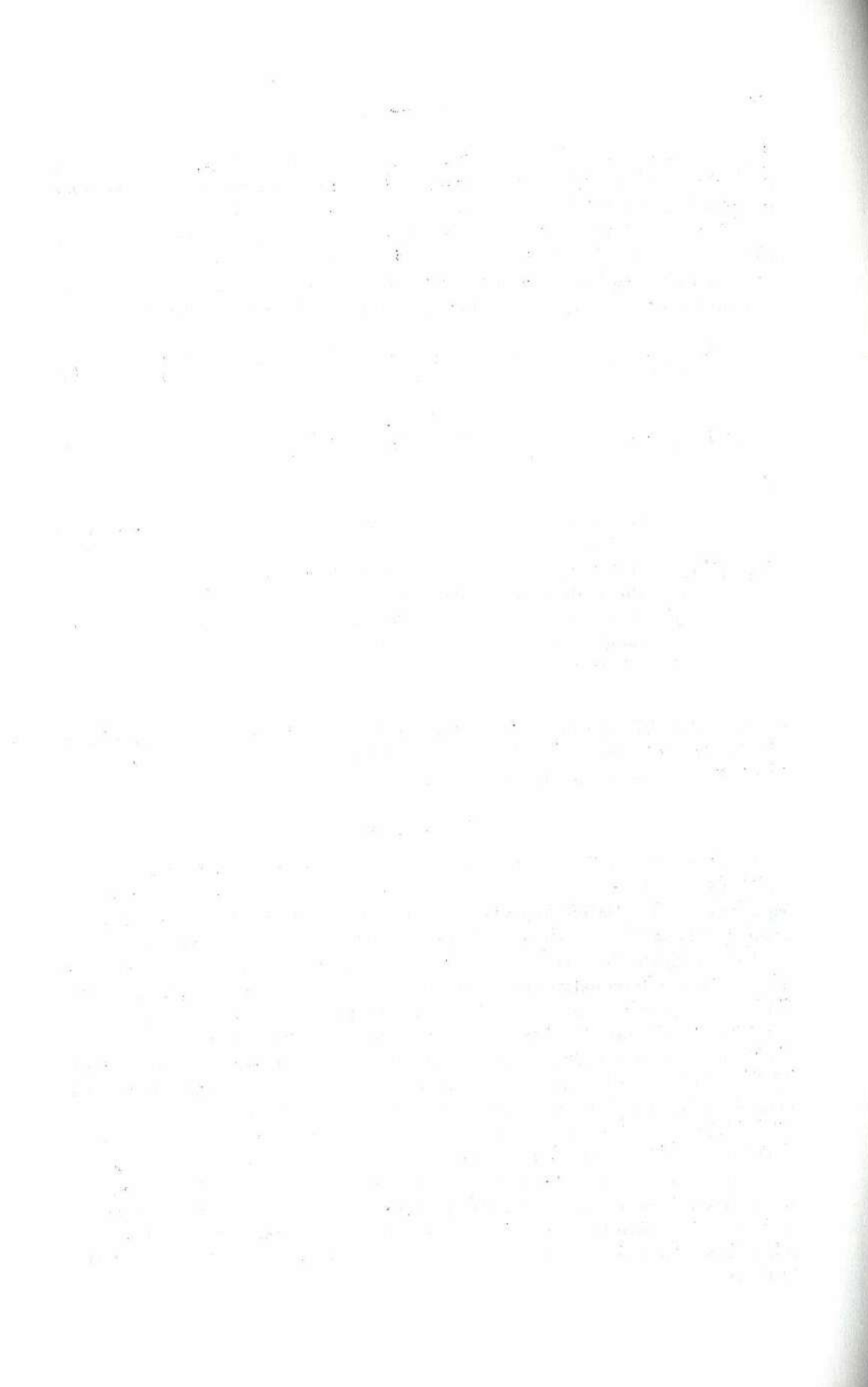
In Fig. 1 we give $\text{Re}\,M_{\text{el-ph}}$ resolved into four contributing parts: normal processes with "longitudinal" and "transverse" phonons and umklapp processes with "longitudinal" and "transverse" phonons. From the derivative of $\text{Re}\,M_{\text{el-ph}}$
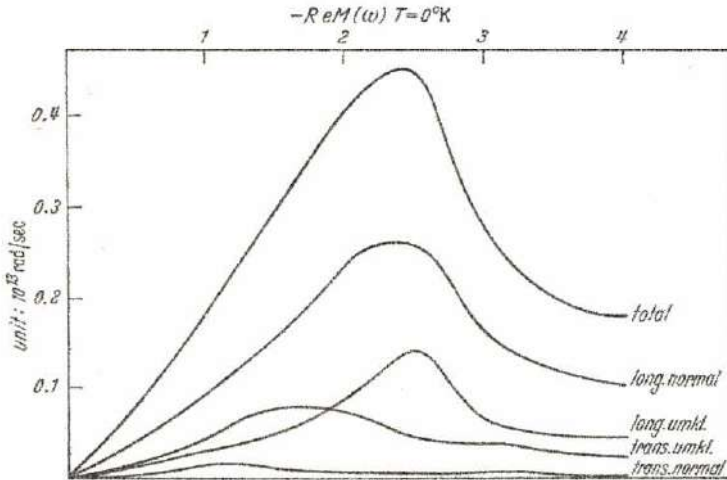

Fig. 1. Contributions to the real part of the self-energy at $T = 0°K$. ($k\theta_D = 2.1 \times 10^{13}$ rad/sec)

at the Fermi surface we can obtain the increase of the electron effective mass related to the density of states. We get for this increase

$$\left(\frac{\delta m}{m}\right)_{\text{el-ph}} = 0.19\,.$$

This value includes a small correction due to the discrepancy between the phonon frequencies used and the experimental values given by Woods et al. [13]. This correction is not made in the curves given. Our value for the increase of the effective mass is in good agreement with recent calculations. In the Table we give $\left(\frac{\delta m}{m}\right)_{\text{el-ph}}$ from some theoretical works.

Table. *Theoretical Calculations of the Contribution to the Effective Mass*

author	FERRELL [5] 1958	QUINN [6] 1960	NAKAJIMA [7] et al. 1963	DARBY [8] 1965	ANIMALU [9] et al. 1966	this work 1966
$\left(\dfrac{\delta m}{m}\right)_{\text{el-ph}}$	0.20	0.45	0.32	0.18	0.15	0.19

The agreement with experiment is satifactory considering the present uncertainty in the experimental data and in the electron-electron contribution.

As for the real part of the self-energy we get no greater changes compared to earlier results. When we consider the damping of the electron the effect of the Pauli principle can however give essential changes. Let us consider an electron close to the Fermi surface at zero temperature. This electron can be damped by exciting a phonon. According to the "golden rule" of transition probabilities the damping rate depends in an essential way on the number of available final states. When

there are "transverse" phonon branches with frequencies much less than those of the "longitudinal" branch we can thus have a large damping due to "transverse" phonons in spite of their relatively weak coupling to the electron. In the case of electron energies very close to the Fermi surface we get a very simple result, namely the third-power law, that ENGELSBERG and SCHRIEFFER [1] got for all electron
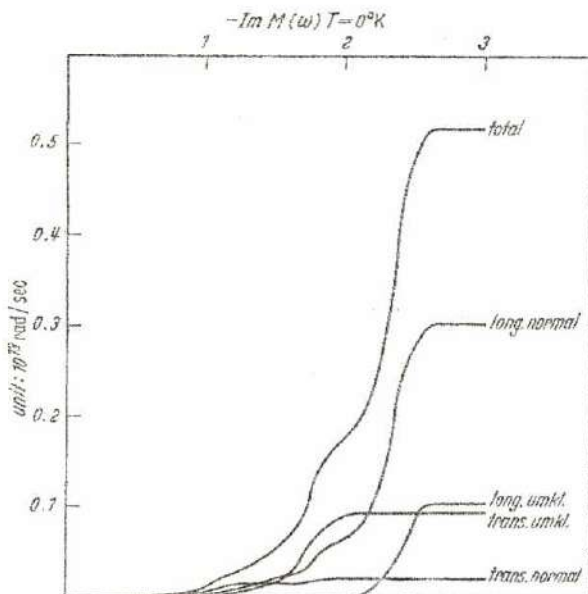

Fig. 2. Contributions to the imaginary part of the self-energy at $T = 0\,^\circ$K

energies up to the Debye energy. In the limit of small ω no umklapp process can occur. The matrix element is practically constant and only wavevectors smaller than ω/c are involved. c is a directional dependent sound velocity. Then we have from (2b)

$$\mathrm{Im}\, M_{el-ph}(\boldsymbol{p}, \omega) = A \int d\varphi \int_0^{\omega/c} \frac{(\hat{e}_{\lambda,q} \cdot \hat{q})^2 q^2}{c}\, dq = \frac{A\,\omega^3}{3} \int \frac{(\hat{e}_{\lambda,q} \cdot \hat{q})^2}{c^4}\, d\varphi = B_\lambda \omega^3, \quad (3)$$

where A and B are constants. Our calculations give for the "longitudinal" part $B_l = 9.1 \cdot 10^{-3}$ and for the "transverse" part $B_t = 8.0 \cdot 10^{-3}$ (unit 10^{13} rad/sec). In Fig. 2 we give $\mathrm{Im}\, M_{el-ph}$ for the more complicated region where a third-power law is not valid.

We should mention that because of the normalization condition

$$\sum_\lambda (\hat{e}_{\lambda,q} \cdot \hat{q})^2 = 1 \tag{4}$$

the approximation of taking only purely longitudinal phonons in the normal processes is not always poor. If all the three phonon branches have almost equal frequencies we get approximately the same result whether we assume purely longitudinal phonons or take into full account the polarization properties. When there are transverse branches with frequencies differing much from the corresp-

onding longitudinal frequency the approximation does not hold and a more detailed calculation is required. This is the case in sodium.

On of the main results in ENGELSBERG's and SCHRIEFFER's [1] paper is that there exists a region where the electrons are not well-defined quasi-particles. To investigate this point we have formed the spectral function A given by

$$A(p, \omega) = \frac{1}{\pi} \frac{|\operatorname{Im} M_{\text{el-ph}}(p, \omega)|}{\left[\omega - \frac{p^2}{2m} + \mu - \operatorname{Re} M_{\text{el-ph}}(p, \omega)^2\right]^2 + [\operatorname{Im} M_{\text{el-ph}}(p, \omega)]^2}. \tag{5}$$

The spectral function obeys a sum rule

$$\int A(p, \omega) \, d\omega = 1. \tag{6}$$

A plot of A is given for three energies $\varepsilon_p = \frac{p^2}{2m} - \mu$ in the critical region where the quasi-particle approximation will not hold (Fig. 3—5). The earlier result that the quasi-particle picture is not very good in this region is confirmed. However,
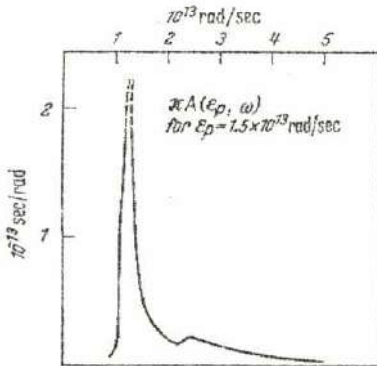
Fig. 3

Fig. 4

Fig. 3
The spectral function for $\varepsilon_p = 1.5 \times 10^{13}$ rad/sec
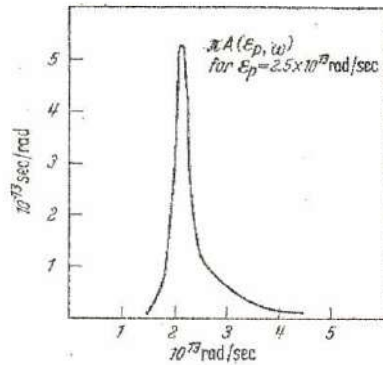
Fig. 4
The spectral function for $\varepsilon_p = 2.5 \times 10^{13}$ rad/sec
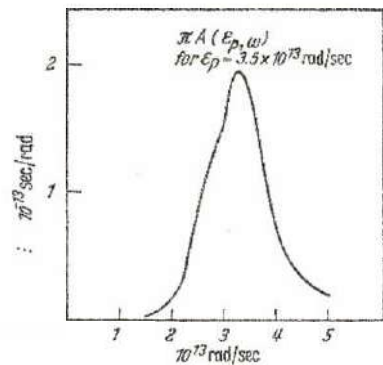
Fig. 5
The spectral function for $\varepsilon_p = 3.5 \times 10^{13}$ rad/sec

Fig. 5

the parts of the spectral wave function that can not be taken into account by using a single Lorentzian curve do not contribute more than about 20% to the sum rule (6). One should notice that the strength of the electron-phonon coupling in ENGELSBERG-SCHREFFER's paper is taken to be much larger than that of sodium. This explains why our curves are much more smooth.

G. GRIMVALL:

To evaluate the real part of the self-energy at finite temperatures is complicated and we are left with one extra integration in the expression corresponding to (2 a).
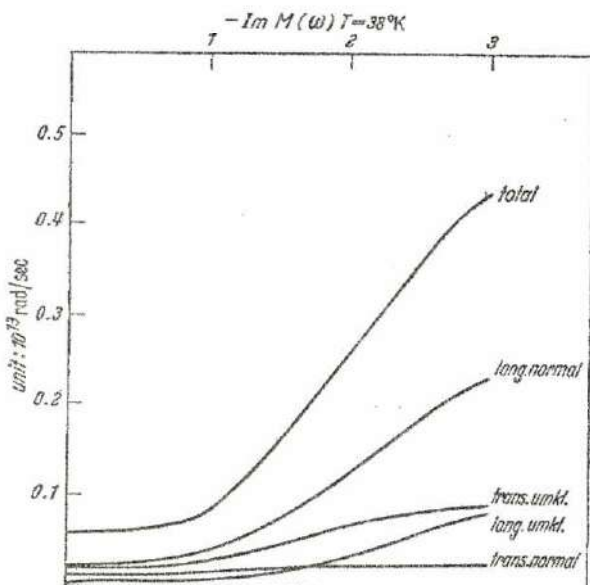
Fig. 6. Contributions to the imaginary part of the self-energy at $T = 38°K$

Fig. 7. The total value of the imaginary part of the self-energy for different temperatures

The imaginary part, however, offers no more difficulties than we have in the zero temperature case. Instead of (2b) we have the expression

$$\text{Im}\,M_{\text{el-ph}}(p,\omega) = -\frac{m}{16\,p\,\pi^2} \sum_\lambda \int_0^{2\pi} d\varphi \int_0^{2k_F} \frac{dq\,q(\hat{e}_{\lambda},q\cdot q)^2\,h^2(q)}{\omega_\lambda(q)} \times$$
$$\times \{1 - f(\omega - \omega_\lambda(q)) + f(\omega + \omega_\lambda(q)) + 2N(\omega_\lambda(q))\}, \tag{7}$$

where f is the F. D.-function and N the B. E.-function.
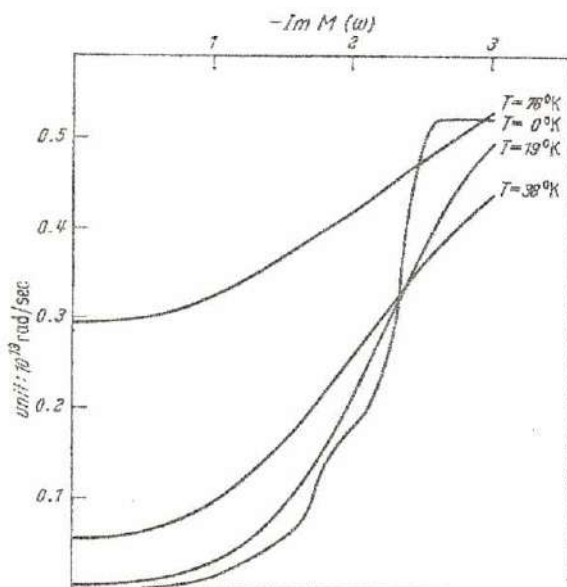
In Fig. 6 the result is given for $T = 38\,°\text{K}$. The Debye temperature of sodium is appoximately $160\,°\text{K}$. In Fig. 7 we give the total value of $\text{Im}\,M_{\text{el-ph}}(\omega)$ for the temperatures $T = 0$, 19, 38 and $76\,°\text{K}$. At finite temperatures $\text{Im}\,M_{\text{el-ph}}(0)$ is different from zero. At temperatures much lower than the Debye temperature $\text{Im}\,M_{\text{el-ph}}(\omega)$ follows a T^3-law [4, 14].

Discussion

After all these calculations a natural question is whether it is really necessary to include all details of the phonon properties. To answer this question we investigate two typical cases, the effective mass and the damping law (3) for electrons close to the Fermi surface. Let us first consider the effective mass in the [100]-direction. By taking coupling to purely longitudinal phonons the contribution from the normal processes is underestimated by about 10%. The umklapp part is more difficult to discuss since there is ambiguity in the directions of the transverse modes if the correct solution is not known. We therefore consider only the longitudinal umklapp process. Also in this case we get an underestimation of about 10%. A comparison to the calculations of ANIMALU et al. [9], where a Debye sphere is used for the Brillouin zone and the Jones' approximation for the umklapp part, shows significant deviations. Next let us consider the damping law (3). What is said here is also relevant for the low temperature limit of (7). With purely longitudinal vibrations we get in the [100]-direction for the two constants $B_l = 9.5 \cdot 10^{-3}$ and $B_t = 0$, i. e. an underestimation of the damping by about 45%. In other directions we also get deviations of about the same magnitude.

Finally we have investigated anisotropy in the damping and in the effective mass. The total contribution from phonon interactions to the effective mass of an electron in the [111]-direction is found to be about 2% less than the corresponding value in the [100]-direction. This is also approximately the estimated numerical uncertainty from interpolations and integrations, so we conclude that there is practically no anisotropy in the effective mass.

The total damping according to formula (3) is for an electron in the [111]-direction 16% lower and for an electron in the [110]-direction 35% lower than the damping in the [100]-direction. There is thus a considerable anisotropy in this quantity, and one should observe that it originates from the "transverse" part.

References

[1] ENGELSBERG, S., and J. R. SCHRIEFFER: Phys. Rev. 131, 993 (1963).

[2] SCHRIEFFER, J. R.: Theory of superconductivity. New York: Benjamin 1964.

[3] MIGDAL, A. B.: Soviet Phys. — JETP 34, (7) 996 (1958).

[4] ABRIKOSOV, A. A., L. P. GORKOV, and I. E. DZYALOSHINSKII: Methods of quantum field theory in statistical mechanics. Englewood Cliffs, N. J.: Prentice Hall 1963.
[5] FERRELL, R. A.: Bull. Amer. Phys. Soc. 3, 203 (1958).
[6] QUINN, J. J., The Fermi surface. Proceedings of the international conference at Cooperstown. Ed. by W. A. HARRISON and M. B. WEBB. New York: John Wiley, August 1960.
[7] NAKAJIMA, S., and M. WATABE: Progr. Theoret. Phys. 29, 341 (1963).
[8] DARBY, J. K.: in the paper N. ASHCROFT and J. WILKINS: Phys. Letters 14, 285 (1965).
[9] ANIMALU, A. O. E., F. BONSIGNORI, and V. BORTOLANI: Nuovo Cimento 52 B, 83 (1966).
[10] SHAM, L. J.: Proc. Roy. Soc. A 283, 33 (1965).
[11] BJÖRKMAN, G., and G. GRIMVALL: to be published.
[12] KREBS, K.: Phys. Rev. 138, A 143 (1965).
[13] WOODS, A. D. B., B. N. BROCKHOUSE, R. H. MARCH, A. T. STEWARD, and R. BOWERS: Phys. Rev. 128, 1112 (1963).
[14] ELIASHBERG, G. M.: Soviet Phys. — JETP, 12, (6) 1000 (1961).

TEMPERATURE DEPENDENT EFFECTIVE MASSES OF CONDUCTION ELECTRONS

GÖRAN GRIMVALL

Institute of Theoretical Physics, Göteborg, Sweden

Abstract—The temperature dependence of the effective electron mass which appears in the heat capacity, cyclotron resonance and amplitude of de Haas–van Alphen effect is discussed. An accurate calculation is reported for sodium at low temperatures. An Einstein model gives the temperature dependence of the thermal mass as a universal function of T/θ_E. This function is evaluated and plotted.

TEMPERATURE DEPENDENT EFFECTIVE
MASSES OF CONDUCTION ELECTRONS

GÖRAN GRIMVALL

Institute of Theoretical Physics, Göteborg, Sweden

Abstract—The temperature dependence of the effective electron mass which appears in the heat capacity, cyclotron resonance and amplitude of de Haas–van Alphen effect is discussed. An accurate calculation is reported for sodium at low temperatures. An Einstein model gives the temperature dependence of the thermal mass as a universal function of T/θ_E. This function is evaluated and plotted.

INTRODUCTION

THE INTERACTION between lattice vibrations and conduction electrons in a metal will give rise to a self energy $M_{el\text{-}ph}$ for the electrons. The self energy is energy and temperature dependent, so we will have for example a temperature dependent deviation from the linear specific heat of the electrons. Buckingham and Schafroth [1] have given a treatment with a constant electron-phonon coupling and a Debye model for the phonons. They obtain an expression for the free energy in the form of integrals which cannot be evaluated in a closed form. Krebs[2] has given a plot of a numerical calculation of these integrals. The region $T \ll \theta_D$ has also been treated by Eliashberg[3]. In this paper we give a more accurate calculation of the temperature dependence of renormalization effects, in particular for sodium.

THE SELF ENERGY AND THE EFFECTIVE MASS

We calculate the real part of the self energy $M_{el\text{-}ph}$ for sodium using Green function methods. To lowest order $M_{el\text{-}ph}$ can be written[4]

$$M_{el\text{-}ph}(p, \omega) = \sum_\lambda \int \frac{d^3 p\, g^2(\mathbf{q})}{(2\pi)^3}$$

$$\left\{ \frac{1 - f_{p'} + N_{\lambda q}}{\omega - \epsilon_{p'} + \mu - \omega_\lambda(\mathbf{q})} + \frac{f_{p'} + N_{\lambda q}}{\omega - \epsilon_{p'} + \mu + \omega_\lambda(\mathbf{q})} \right\}. \quad (1)$$

We want to have a complete knowledge about the phonons also off symmetry directions. Therefore we must rely on some model to calculate the eigenvalues $\omega_\lambda(\mathbf{q})$ and the corresponding polarization vectors (which are in general not purely longitudinal or transverse). Krebs[5] has proposed a simple model which gives good agreement with experiments in the symmetry directions. We have used his model to calculate eigenvalues and eigenvectors at 46 points in an irreducible part of the first Brillouin zone[6]. Sodium is highly anisotropic so this procedure will probably introduce some error (cf a discussion for lead in[7]). However we will see later that the precise form of the phonon spectrum is not very important. The temperature dependence of the phonon spectrum is neglected. The electron-phonon matrix element g is taken from the so called non-local model by Sham [8]. This is the only important approximation or uncertainty in our calculations. It involves the question of good pseudo-potentials and is an enormous problem in itself. Sham's calculation is one of the most detailed, and the fact that his matrix element does not give the correct limit ($2\epsilon_F/3$) for $q = 0$ is of no importance here (cf discussion below). Our final result is not at all so sensitive to the precise form of the electron-phonon coupling as can be the case when one calculates phonon frequencies[9] or electrical conductivity[10].

Using a computer program we have then performed a detailed calculation where we

have taken into full account that the lattice vibrations are in general not purely longitudinal or transverse. We have also treated properly all umklapp-processes, using a correct shape of the Brillouin-zones[11].

The increase δm of the effective mass at the Fermi level, due to electron-phonon interaction, is plotted in Fig. 1. δm is defined as
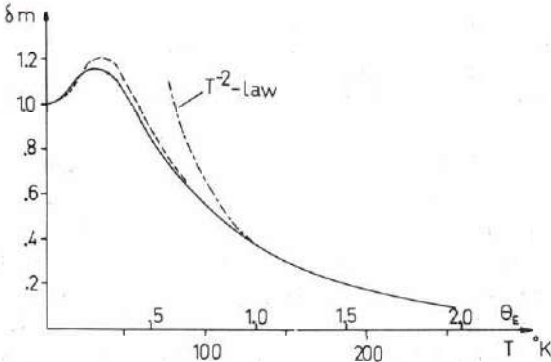
Fig. 1. The temperature dependence of the contribution $(\delta m)_{el\text{-}ph}$ to the effective electron mass at the Fermi level for Na (normalized to unity for $T = 0$). Full drawn curve = accurate calculation. Dashed line = the universal temperature dependence in an Einstein model, cf. equation (2). For sodium we have taken $\theta_E = 130°$K. Asymptotic T^{-2}-law is also shown.

$-\partial \mathrm{Re}\, M_{el\text{-}ph}(\omega)/\partial\omega$ evaluated for $\omega = 0$. The result is normalized to unity for $T = 0$. In the limit of high temperatures we get a T^{-2}-law, which is also shown in the figure. For $T \ll \Theta_D$ we have the well-known $T^2 \ln T$-law[1, 3]. If one uses an Einstein model for the phonons, the temperature dependence

factors out as a universal function F of the single variable T/Θ_E. (Θ_E = Einstein temperature).

$$F(T/\theta_E) = \frac{4}{\pi^2}\left(\frac{\theta_E}{T}\right)^2 \sum_{n=0}^{\infty}$$

$$\times \frac{2n+1}{\left[(2n+1)^2 + \frac{1}{\pi^2}\left(\frac{\theta_E}{T}\right)^2\right]^2}. \qquad (2)$$

F has been normalized to unity for $T \to 0$. We see from Fig. 1 that an Einstein model gives a good description. In Fig. 2 we give $\mathrm{Re}\, M_{el\text{-}ph}(\omega)$ for $T = 0$ in an accurate calculation[7] and also $\mathrm{Re}\, M_{el\text{-}ph}(\omega)$ in an Einstein model for $T = 0$[8] and $T = \theta_D$. At finite temperatures the singularity in $\mathrm{Re}\, M_{el\text{-}ph}$ is smeared out and the Einstein model gives a good description. In Fig. 3 we have plotted the density of states $N(\omega) = N_0[1 - (\partial M_{el\text{-}ph}(\omega)/\partial\omega)]$ obtained from the accurate calculation for sodium[11].

It is perhaps astonishing that an Einstein model gives such a good result. We can however understand it in simple terms. The origin of the effective mass is virtual processes connecting two electron states close to the Fermi surface. As in the case of real transitions (i.e. damping of electrons) the resulting effect depends primarily on the strength of the interaction and on the available phasespace for transitions. The density of states increases linearly in the momentum transfer
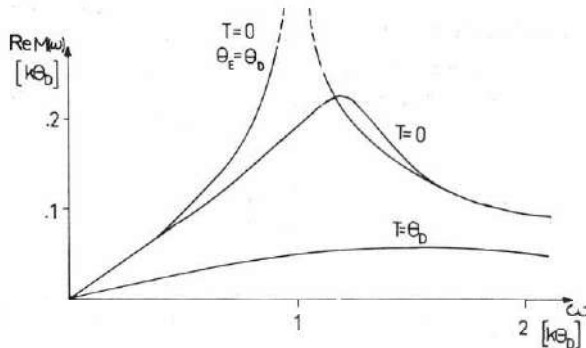
Fig. 2. $\mathrm{Re}\, M_{el\text{-}ph}$ (ω) for Na at $T = 0$ in an accurate calculation and $\mathrm{Re}\, M_{el\text{-}ph}$ (ω) for $T = 0$ and $T = \theta_D$ in an Einstein model ($\theta_E = \theta_D$).
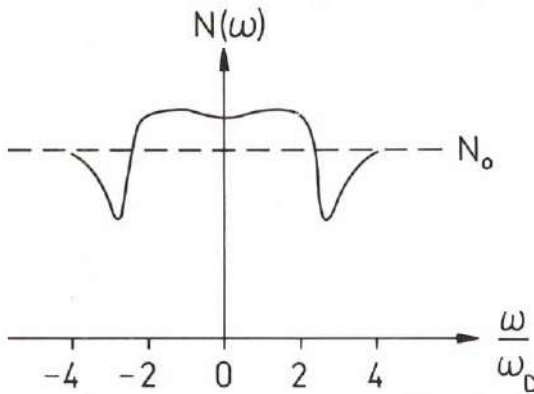
Fig. 3. Density of states $N(\omega) = N_0\left[1 - \dfrac{\partial M_{el-ph}(\omega)}{\partial\omega}\right]$ for Na in the vicinity of the Fermi level.

q. The effective electron–phonon coupling is zero for $q = 0$ and then shows an oscillatory behaviour with the first node at $q \sim 2k_f$. Thus there is no dominance of the long-wavelength phonons (as can be the case for the damping of electrons close to the Fermi surface, see [11]), but instead an average mainly over high-energy phonons. This is the reason for the success of the Einstein model.

By a mere scaling it is possible to get rough results also for other simple metals. In Table 1 we give some relevant parameters for Na, Al and Pb. T_0 is defined as that temperature at which the electronic contribution to the specific heat approximately equals that of the lattice vibrations in a non-superconducting state.

Table 1. Some parameters for the metals Na, Al *and* Pb

metal	$\left(\dfrac{\delta m}{m}\right)_{el-ph}$	θ_D (°K)	$T_0°K^{(c)}$
Na	0·19[a]	150	1·5
Al	0·49[b]	418	7
Pb	1·05[b]	94·5	1

[a] GRIMVALL G., *Physik Kondens. Materie* **6**, 15 (1967).
[b] ASHCROFT N. and WILKINS J., *Phys. Lett.* **14**, 285 (1965).
[c] T_0 is the temperature at which the electronic and lattice specific heats are approximately equal in a normal state.

EXPERIMENTAL VERIFICATION

It has been shown[13] that in many cases (e.g. spin susceptibility, electrical and thermal conductivity) there is a cancellation effect so that no renormalization effects from interaction with phonons should be included in the electron mass. However one should in principle see these effects in the specific heat, cyclotron resonance and the amplitude of de Haas–van Alphen oscillations[13, 14]. We first discuss the electronic specific heat. At zero temperature the specific heat starts linear in temperature and is directly proportional to the effective electron mass. At finite temperatures we can write

$$C_v = \gamma_0 T + \gamma_1(T)T \qquad (3)$$

where $\gamma_0 T$ is the specific heat in the absence of electron-phonon interaction. $\gamma_1(T)$ incorporates these effects and can be considered as proportional to a temperature dependent mass correction. From Fig. 2 it is clear that both the ω and T dependence of Re $M_{el\text{-}ph}$ $(\omega; T)$ is essential. We get the following expression, in the notation of Prange and Kadanoff[13], for $\gamma_1(T)$:

$$\gamma_1(T) = \frac{2}{T^2}P \int dE dE' \frac{d\Omega}{4\pi} \frac{d\Omega'}{4\pi} N_0(k)N_0(k)$$
$$\times \frac{\partial f_0(E)}{\partial E}\frac{\partial f_0(E')}{\partial E'}$$
$$\times \left\{ [\nu(q)]^2 \frac{(E-E')^2}{E-E'+\omega_q} \right\}. \qquad (4)$$

P denotes that the principle value should be taken. $d\Omega$ is solid angle integration over the Fermi surface and N_0 is a directional dependent density of electron states. $\nu(q)$ is the electron-phonon coupling and f_0 the usual F.D.-factor. An accurate calculation is very difficult to perform but again the temperature dependence factors out as a universal function of T/θ_E if we use an Einstein model for the phonon spectrum. This is the only approximation and all the details in coupling strength etc. are retained in full. For the function

giving the temperature dependence we then get from (4)

$$\gamma_1(T) \propto \frac{1}{T^2} P \int dE\, dE' \frac{\partial f_0(E)}{\partial E} \frac{\partial f_0(E')}{\partial E'}$$

$$\times \left\{ \frac{(E-E')^2}{E-E'+\omega_E} \right\}. \quad (5)$$

These integrals do not lead to an expression as simple as (2) but for completeness we give the result in an appendix. A plot of $\gamma_1(T)$, normalized to 1 for $T = 0$, is given in Fig. 4. It is evident that a true phonon spectrum will considerably decrease the sharp peak of γ_1 at low temperatures.
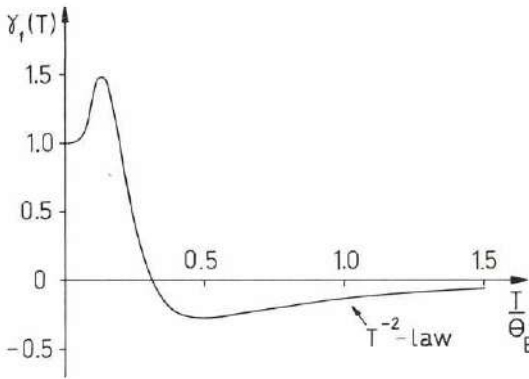
Fig. 4. The function $\gamma_1(T)$ giving the correction to the thermal effective mass. $\gamma_1(T)$ is normalized to 1 for $T = 0$.

We note that the electron-phonon interaction for $T > 0.3\, \theta_E$ leads to a specific heat which is lower than the "free" electron value. This fact can be elucidated by a simple entropy consideration. The entropy $S(T)$ is given by

$$S(T) = \int_0^T \frac{C_v}{T'}\, dT' = \int_0^T [\gamma_1 + \gamma_1(T')]\, dT' =$$

$$= S_0 + \int_0^T \gamma_1(T')\, dT'. \quad (6)$$

For high temperatures (i.e. $T \ll \theta_E$) Re $M_{el\text{-}ph}$ is negligible. As entropy is a state function we then must have the same value

for $S(T)$ as in a non-interacting electron-phonon system. Hence the last integral in (6) goes to zero as $T \to \infty$ and $\gamma_1(T)$ must be negative for some T.

Now we will consider the question of experimental verification. Because of the lattice contribution to the specific heat we can normally only measure the electronic part at very low temperatures (cf Table 1). At temperatures $T \gg \theta_E$ anharmonicity in the lattice vibrations complicates an analysis. The data of Table 1 and inspection of Figs. 1 and 4 show that for simple metals and with present experimental accuracy it is not possible to investigate the region of the maximum in $\gamma_1(T)$, and it would be very difficult to see the temperature dependence of $\gamma_1(T)$ at low temperatures. For metals with a complicated electron structure and a large effective mass (eg. vanadium,[2]) the effect seems to be noticable. One can also use the fact that the electronic specific heat in a superconducting state decreases exponentially with temperature while the lattice vibrations give the same contribution as in a normal state. The experimental accuracy is however not good enough.

In a magnetic field $M_{el\text{-}ph}$ is essentially unaffected[14], but Landau levels are formed at intervals $\omega_c(\omega_c = \text{cyclotron frequency})$. The amplitude in de Haas–van Alphen oscillations is heavily damped already at a few degrees Kelvin. If we try to compensate the decrease by the use of still higher (presently unattainable) magnetic fields we meet with new effects when $\omega_c \sim \omega_D$[14, 15]. If we in the case of cyclotron frequency measurement fulfil the requirements $\omega_c \ll \omega_D$ and $\omega_c\tau \gg 1$ by taking $\omega_c = 0.1\, \omega_D$ and $\omega_c\tau = 50$, a rough estimate gives a maximum temperature of the order 10°K. $\omega_c = 0.1\,\omega_D$ corresponds to a field of about 10^5 G. In this estimation we have supposed that at 10°K damping comes essentially from electron-phonon interaction which is cubic in T, and we have used results from [11]. In conclusion it seems to us that a quantitative experimental verification of the

temperature effect is very difficult with present experimental accuracy. An improvement in the experimental accuracy should give at least a statistically significant difference in the mass for different temperatures.

REFERENCES

1. BUCKINGHAM M. J. and SCHAFROTH M. R., *Proc. phys. Soc.* **A67**, 828 (1954).
2. KREBS K., *Phys. Lett.* **6**, 31 (1963).
3. ELIASHBERG G. M., *Soviet Phys. JETP* **12**, 1000 (1961).
4. SCHRIEFFER J. R., *Theory of superconductivity*, Chap. 7. Benjamin, New York (1964).
5. KREBS K., *Phys. Rev.* **138**, A143 (1965).
6. For details see BJÖRKMAN G. and GRIMVALL G., *Phys. Status Solidi* **19**, 863 (1967).
7. STEDMAN R. ALMQVIST L. and NILSSON G., *Phys. Rev.* **162**, 549 (1967).
8. SHAM L. J., *Proc. R. Soc.* **A283**, 33 (1965).
9. CLAESSON T. and GRIMVALL G., *J. Phys. Chem. Solids* **29**, 387 (1968).
10. WISER N., *Phys. Rev.* **143**, 393 (1966).
11. The analogous treatment of M_{el-ph} for $T = 0$ and TmM_{el-ph} for $T \neq 0$ is described in detail in GRIMVALL G., *Physik Kondens. Materie* **6**, 15 (1967).
12. ENGELSBERG S. and SCHRIEFFER J. R., *Phys. Rev.* **131**, 993 (1963).
13. PRANGE R. E. and KADANOFF L. P., *Phys. Rev.* **134**, A566 (1964).
14. FOWLER M. and PRANGE R. E., *Physics* **1**, 315 (1965).
15. SCHER H. and HOLSTEIN T., *Phys. Rev.* **148**, 598 (1966).
16. JOLLEY L. B., *Summation of Series*. Dover, New York (1961).

APPENDIX

With an Einstein model for the phonon energies, the temperature dependence of $\gamma_1(T)$ is completely contained in the expression (5). We now integrate twice using the method of residues. The last integration requires care in the handling of poles and integration path and we must impose a restriction on one of the resulting sums (equation (A2)). The final expression for $\gamma_1(T)$, normalized to unity for $T = 0$, is

$$\gamma_1(T) = \frac{3}{2\pi^2}\left\{\frac{4}{\pi^2}\left(\frac{\theta_E}{T}\right)I - 1\right\}\left(\frac{\theta_E}{T}\right)^2 \tag{A1}$$

where

$$I = \sum_{n=0}^{N \ll M} \sum_{m=0}^{M} -\frac{\pi^4}{2}\frac{(e^x - e^{-x})}{(1 - e^x)^2(1 - e^{-x})^2} + (2m+1) \times$$

$$\frac{2x}{\pi}\frac{4x^2(2m+1)^2/\pi^2 - 3[x^2/\pi^2 + (2n+1)^2 - (2m+1)^2]^2}{\{[x^2/\pi^2 + (2n+1)^2 - (2m+1)^2]^2 + 4x^2(2m+1)^2/\pi^2\}^3}$$

$$+ (2m+1) \times$$

$$\frac{4x}{\pi}\frac{x^2/^2 + (2n+1)^2 - (2m+1)^2}{\{[x^2/\pi^2 + (2n+1)^2 - (2m+1)^2]^2 + 4x^2(2m+1)^2/\pi^2\}^2} \tag{A2}$$

with $x = \theta_E/T$; $M, N \to \infty, N \ll M$.

The sum in (A2) is not divergent in spite of the constant exponential term. Starting from some known series[16]. It is possible to derive the relation

$$\frac{e^x - e^{-x}}{(1 - e^{-x})^2(1 - e^x)^2}$$
$$= \frac{16}{\pi^3}\sum_{n=0}^{\infty}\frac{y^3}{[(2n+1)^2 + y^2]^3} - \frac{12}{\pi}\sum_{n=0}^{\infty}\frac{y}{[(2n+1)^2 + y^2]^2} \tag{A3}$$

where $y\pi = x + i\pi(2m+1)$; m integer.

A straight forward but tedious calculation now gives, that the divergent terms in the sum (A2) cancel, but the complicated form of (A2) does not simplify when (A3) is inserted.
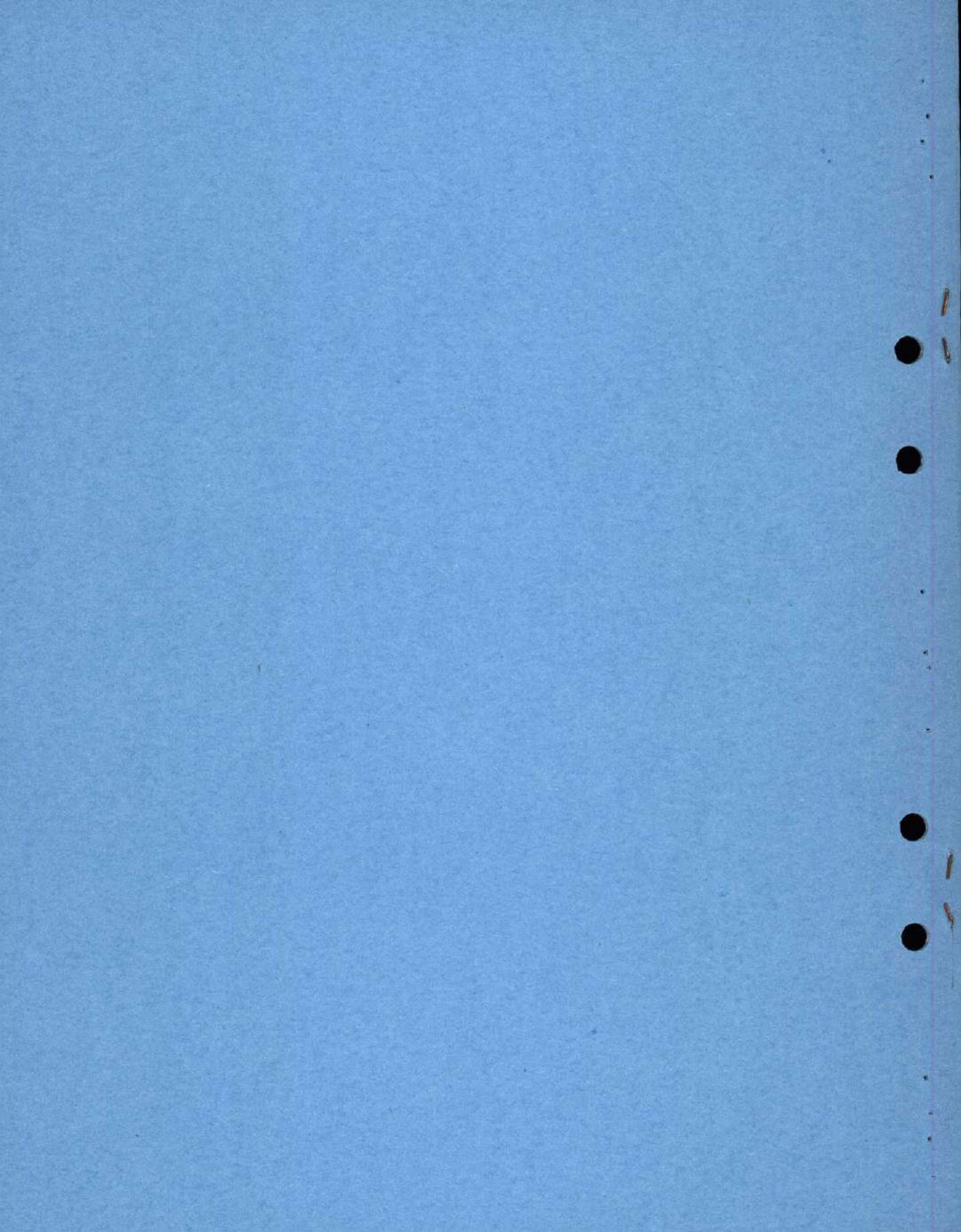
Reprinted from

SOLID STATE COMMUNICATIONS

TEMPERATURE EFFECTS IN CYCLOTRON RESONANCE AND SPECIFIC HEAT ELECTRON MASSES

Göran Grimvall

Institute of Theoretical Physics, Chalmers University of Technology, Göteborg, Sweden

The temperature dependence of the specific heat and cyclotron resonance effective masses is calculated for mercury. The effect seems to be within experimental reach.

RESULTS from cyclotron resonance experiments and measurements of the electronic specific heat are often given in the form of 'effective' electron masses. It is well known that the enhancement factor $1 + \lambda$ of the effective electron mass, coming from electron–phonon interaction, is temperature dependent. In this note we present calculations for mercury showing that it should be possible to measure the temperature dependence. General estimates have shown that such experiments on metals should not be feasible.[1] However the phonon spectrum of mercury, or rather the electron–phonon interaction strength times the phonon density of states, $\alpha^2(\omega)F(\omega)$, has such a special shape that experiments are in fact possible. The exceptional property of mercury is that the quantity $\alpha^2(\omega)F(\omega)$ has a strong peak at an energy corresponding to only 20°K. This is the temperature that should replace the Debye temperature or Einstein temperature in simple estimates. Moreover the enhancement factor $1 + \lambda \approx 2.6$ is one of the largest known. The enhancement factor $1 + \lambda$ is at very low temperatures the same for specific heat and cyclotron resonance and is obtained from $\lambda = -\partial M_{el-ph}(\omega)/\partial\omega$ taken at the Fermi level ($\omega = 0$) and at $T + 0$. M_{el-ph} is the electron self energy caused by electron–phonon interaction. The self energy is an explicit function of temperature, so λ will be temperature dependent, $\lambda = \lambda(T)$. At finite temperatures there will be thermally excited states, and M_{el-ph} must be considered also for energies $\omega \neq 0$. At finite temperatures or

energies the self energy is complex. In this note we mean by M_{el-ph} the real part of the self energy.

We start with a discussion of the effective mass determination using cyclotron resonance. If one keeps the temperature fixed at a low value and changes the frequency of the electromagnetic wave, there will be a change in the effective mass[2] because $M_{el-ph}(\omega)$ increases faster than linear in ω, i.e. faster than $\omega\lambda(T = 0)$. Calculations of the self energy in mercury have shown that this effect will be very difficult to observe and that very high frequencies are necessary. We therefore turn to the case of fixed frequency of the electromagnetic wave and a varying temperature. Let m_b be the effective mass in the absence of electron–phonon interaction. The cyclotron resonance mass is then to good accuracy (cf. the discussion at the end of this note) given by $m_b(1 + \lambda(T))$ for moderate frequencies and all temperatures of interest in this context. The damping of the electrons due to interaction with phonons puts an upper limit on T. Information concerning the electron–phonon interaction can be obtained in the form $\alpha^2(\omega)F(\omega)$ previously mentioned, from an analysis of tunneling experiments on superconductors. McMillan and Rowell[3] have performed such an analysis for some metals and we will use their results in our calculations. The result for the normalized quantity $\lambda(T)/\lambda(T = 0)$ is given in Fig. 1. Details about all calculations in this note will be published elsewhere. The experimental difficulites with mer-
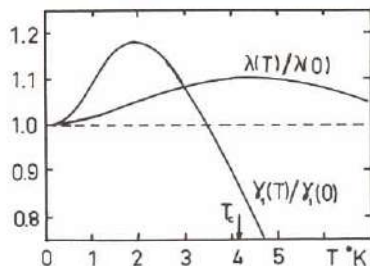
FIG. 1. The temperature dependence of the cyclotron resonance effective mass $m_c = m_b[1 + \lambda(T)]$ and the electronic specific heat $C_{e,n} = [\gamma_0 + \gamma_1(T)]T$, given in the normalized forms $\lambda(T)/\lambda(0)$ and $\gamma_1(T)/\gamma_1(0)$.

cury are considerable but nevertheless there are very good cyclotron resonance experiments[4] on this metal (at $T = 1.2°K$), so the effect seems not to be out of experimental reach. From Fig. 1 we see that for example the increase in effective mass from $T \sim 0.5°K$ to $T \sim 2°K$ is about 3 per cent. To cover this region requires a frequency higher than about 50 GHz in order to fulfil $\omega_c \tau_{el-ph} \gg 1$.

We next turn to specific heat measurements. The electronic specific heat of a metal in a normal state can be written

$$C_{e,n} = \gamma_{tot} T = (\gamma_0 + \gamma_1(T))T, \qquad (1)$$

where $\gamma_1(T)$ incorporates all effects from electron–phonon interaction. We assume the validity of an expression for the electronic specific heat at finite temperatures given by Prange and Kadanoff.[5] They find

$$C_{e,n} = (2\pi^2/3)N_0T + 2\int \frac{d\Omega}{4\pi} N_0 E$$
$$\left[\frac{\partial M_{el-ph}}{\partial T}\frac{\partial f_0}{\partial E} - \frac{\partial M_{el-ph}}{\partial E}\frac{\partial f_0}{\partial T} \right] dE \qquad (2)$$

f_0 is the usual Fermi–Dirac function and N_0 is the density of states at the Fermi level in the absence of electron–phonon interaction. The derivation of (2) is based on the equivalence between time derivatives and temperature derivatives in the Green function method. Éliashberg[6] has obtained a related expression valid at low temperatures, starting from the thermodynamic potential of the coupled electron–phonon system. It turns out to be rather easy to generalize Éliashberg's result so as to give the formula of Prange and Kadanoff. The crucial point in this

generalization is that the phonon self energy (from interaction with the electrons) is practically temperature independent. We again use $\alpha^2(\omega)F(\omega)$ to calculate $\gamma_1(T)$ from (2). The normalized result $\gamma_1(T)/\gamma_1(T = 0)$ is given in Fig. 1.

Let us now consider a measurement of the specific heat in both the normal and the superconducting state of mercury ($T_c = 4.2°K$) in the region below $\sim 0.7°K$. The lattice contribution, which will be assumed to be the same in the two states, is of the same order of magnitude as $C_{e,n}$. The specific heat $C_{e,s}$ of the electrons in the superconductor has decreased to an almost negligible value. Taking the difference ΔC between the total specific heat in the two states, we are therefore left with the term $C_{e,n} = \gamma_{tot} T = [\gamma_0 + \gamma_1(T)]T$. We could for example plot $\Delta C/T\gamma_{tot}(T = 0)$ as a function of temperature. This curve should first show a slight increase (the effect we are looking for) before it eventually decreases due to the onset of $C_{e,s}$. Experiments by van der Hoeven and Keesom[7] on mercury have an estimated uncertainty just as big as the effect considered here. As they did not take very many points in the interesting temperature region, a conclusive analysis of their data is impossible. It would be interesting with a renewed and careful investigation of the temperature interval $0.5-1°K$. It should be remarked that a direct separation in the normal state of a T^3-part for the lattice specific heat is impossible at $T \sim 0.7°K$ as the Debye temperature has already started to deviate from its limiting value at $T = 0$. The determination of the specific heat difference between the two states from a knowledge of the critical field $H_c(T)$ as a function of temperature is not accurate enough to show the increase in γ_{tot} but the method is excellent to obtain the limiting value $\gamma_{tot}(T = 0)$.[8] $H_c^2(T)$ depends on the *free* energy so the effect we are looking for will be partly cancelled.

The peaks in the two curves of $\lambda(T)$ and $\gamma_1(T)$ in Fig. 1 do not occur at the same temperature. This is because the increases of $\lambda(T)$ and $\gamma_1(T)$ have two separate reasons. In cyclotron resonance experiments we are interested in electrons within the range $\sim kT$ of thermal smearing at the Fermi level. In the heat capacity however, the main contribution comes from electrons excited

to energies larger than kT as can easily be seen from the standard derivation of the specific heat of a degenerate Fermi gas. Therefore the possibility of exciting electrons to energies where the self enegry $M_{el-ph}(\omega)$ deviates from the form $\lambda\omega$ is of importance. In fact this effect dominates the effect from a change in the slope $\lambda(T)$ with temperature.

We have here only considered mercury, which is theoretically very favourable. Another metal with similar properties is lead, for which theoretical results will be given elsewhere. The transition temperature T_c of lead (7.2°K) is somewhat too low to make specific heat measurements promising, but for the cyclotron resonance case lead would be a possible alternative.

REFERENCES

1. GRIMVALL G., *Physics Chem. Solids* 29, 1221 (1968).

2. SCHER H. and HOLSTEIN T., *Phys. Rev.* 148, 598 (1966).

3. McMILLAN W.L. and ROWELL J.M., in *A Treatise on Superconductivity* (Edited by PARKS R.D.) to be published.

4. DIXON A.E. and DATARS W.R., *Phys. Rev.* to be published.

5. PRANGE R.E. and KADANOFF L.P., *Phys. Rev.* 134, A566 (1964).

6. ÉLIASHBERG G.M., *Soviet Phys. JETP* 16, 780 (1963).

7. HOEVEN B.J.C. VAN DER, Jr., and KEESOM P.H., *Phys. Rev.* 135, A631, (1964).

8. FINNEMORE D.K. and MAPOTHER D.E. *Phys. Rev.* 140, A507 (1965).

Die Temperaturabhängigkeit der Effektivmasse in Quecksilber bei Zyklotronresonantzmessungen und Messungen der Spezifische Wärme wird berechnet. Es scheint möglich, dieser Effekt in Experiment zu bestätigen.
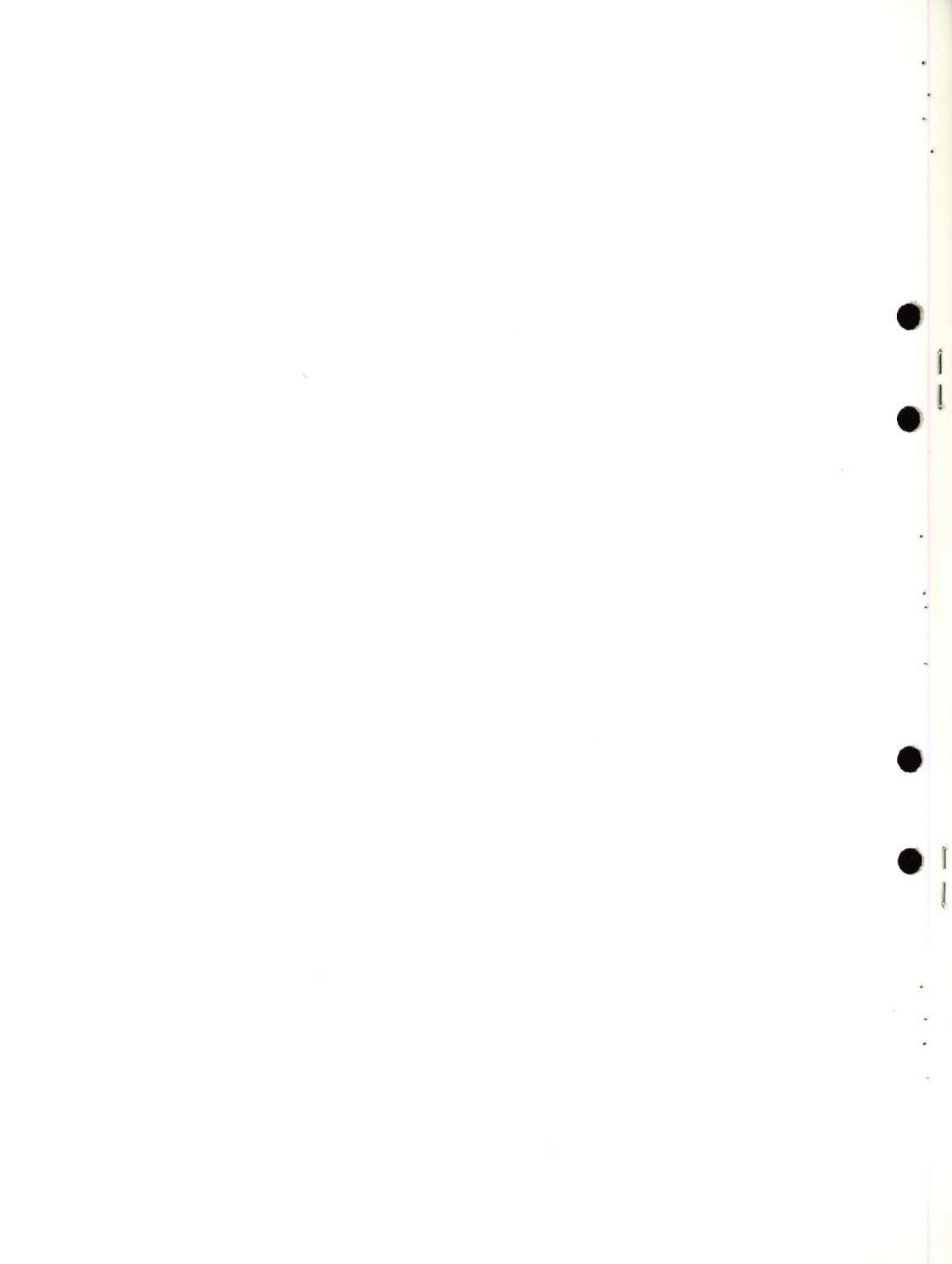
October 24, 1968

Report 69-1

New aspects on the electron-phonon

system at finite temperatures with

an application on lead and mercury

by

Göran Grimvall

Inst. of Theoretical Physics

Fack

S-402 20 Göteborg 5

Sweden

The electron-phonon system in lead and mercury

Abstract

The paper deals with the influence of the electron-phonon
interaction on the properties of the conduction electrons in
lead and mercury. The quasi-particle properties are con-
sidered in detail using Green functions. Special attention
is given to temperature effects in the effective mass as
measured in cyclotron resonance or the electronic specific
heat. It is shown that such a temperature dependence in the
effective mass for lead and mercury should be possible to
verify with the present experimental technique. The electro-
nic specific heat in the normal state is far from linear in
T at $T \sim T_c$, a fact which has some consequencies for the
interpretation of experiments on the thermodynamics of the
superconducting state.

Introduction

The purpose of this paper is to give a detailed quantitative presentation of the effects of electron-phonon interaction on the conduction electrons in lead and mercury. We start with a calculation of the electron Green function, as this function in principle contains the information on the electron proper- ties. After a discussion of the quasi-particle picture we will use many-body technique to calculate quantities that are di- rectly measurable in experiments, e.g. the electronic specific heat and the cyclotron resonance frequency. In particular we will investigate in detail concepts like the effective electron mass and the density of electron states at finite temperatures. The input data concerning the electron-phonon interaction will be taken from the results of McMillan and Rowell obtained by analysing tunneling data in superconductors.

The electron self energy

The method of Green functions in many body theory is now so well known, that we do not here repeat all the basic concepts that can be found in textbooks (1.2). Let us denote by $M_{el-ph}(\underline{p},\omega)$ the contribution from the electron-phonon inter- action to the self energy of the conduction electrons. The general first order formula for $M_{el-ph}(\underline{p},\omega)$ at finite tempe- ratures is

$$M_{el-ph}(p,\omega) = \sum_{\lambda} \int \frac{d^3 p'}{(2\pi)^3}\, g^2(q) \left\{ \frac{1 - f_{p'} + N_q}{\omega - \varepsilon_{p'} + \mu - \omega_\lambda(q)} + \frac{f_{p'} + N_q}{\omega - \varepsilon_{p'} + \mu + \omega_\lambda(q)} \right\} \qquad (1)$$

We have used f and N for the usual F.D. and B.E. factors. The phonon frequencies $\omega_\lambda(q)$ are labelled by momentum q and branch index λ, and ω is counted from the Fermi energy μ. ε_p, the energy of an electron with momentum p in the absence of electron-phonon interaction. Finally the electron-phonon interaction strength corresponding to momentum transfer $q = p - p'$ is denoted by $g^2(q)$. As has been shown by Migdal, $M_{el-ph}(p, \omega)$ is only weakly dependent on p. Sometimes therefore p will be dropped and it is understood that $|p| = P_F$, the Fermi momentum.

A direct integration in momentum space of eq. 1 is a difficult task. However if one is interested only in the result for M_{el-ph} and accepts a calculation that is not ab initio, the integrations can be carried out easily. The information about $g(q)$ is then taken from the inversion of the gap equations in an analysis of tunneling data in superconductors. Let $\alpha^2(\omega)F(\omega)$ be the product of electron-phonon

interaction $\alpha^2(\omega)$ (with transferred energy instead of momentum as variable) and the density of phonon states $F(\omega)$. More precisely the following relation holds [3]

$$\alpha^2(\omega)F(\omega) = \frac{\sum_\lambda \int \frac{dS'}{v_F'} \int \frac{dS}{v_F} \; g^2(\underline{q}) \; \delta(\omega - \omega_\lambda(\underline{q}))}{(2\pi)^3 \int \frac{dS}{v_F}} \tag{2}$$

The integrations in eq. (2) go over the Fermi surface. The average of $M_{el-ph}(\underline{p},\omega;T)$ over all directions $\underline{p}$ at the Fermi surface can then be written (in the following M_{el-ph} denotes this average)

$$M_{el-ph}(p,\omega;T) = \int dc \int d\omega' \; \alpha^2(\omega')F(\omega') \left\{ \frac{1-f(c)+N(\omega')}{\omega-c+\mu-\omega'} + \frac{f(c)+N(\omega')}{\omega-c+\mu+\omega'} \right\} \tag{3}$$

It is thus possible to circumvent all difficulties with the electron-phonon interaction strength, phonon frequencies, Umklapp processes, shape of the Fermi surface etc. and end up with more simple integrations. To see the effect of considering averaged M_{el-ph} over the Fermi surface, we can make a comparison with an earlier calculation [4] for the elastically highly anisotropic sodium, for which eq. (1) was actually solved in all detail. According to this calculation the value of $\partial \, Re \, M_{el-ph}/\partial \omega$ differs very

little for $\underline{p}$ in different symmetry directions. This is
however not the case for the imaginary part Im $M_{el-ph}(\underline{p}, \omega)$
at very low energies ω . For higher values of ω , M_{el-ph}
gets contributions from so many points in q-space all
over the Fermi surface, that it should be fairly isotropic
in $\underline{p}$. There remains the anisotropy in M_{el-ph} from aniso-
tropy in the band structure. Therefore some caution is
necessary for example in the interpretation of cyclotron
resonance experiments.

The quantity $\alpha^2(\omega)F(\omega)$ has been determined for lead and
mercury by McMillan and Rowell[3]. Its shape is not very
different from that of the phonon spectrum, indicating
that $\alpha^2(\omega)$ is not very strongly dependent on the
energy ω . In fig. 1 we give $\alpha^2(\omega)F(\omega)$ from McMillan and
Rowell and F(ω) from Stedman et. al.[5] for lead. There is
a small but clear discrepancy between the upper frequency
limits of $\alpha^2(\omega)F(\omega)$ and F(ω), which is supposed to be
due to surface effects[3]. This point will be of no importance
in our analysis. The results for Re M_{el-ph} and Im M_{el-ph}
when eq. (3) was solved with McMillans and Rowell's
$\alpha^2(\omega)F(\omega)$ are given in figs. 2 and 3 (lead) and fig. 4
(mercury). For small energues Re $M_{el-ph}(\omega;T)$ is linear in
ω, and $1 - \partial \mathrm{Re}\, M_{el-ph}(\omega)/\partial \omega = 1 + \lambda$ is what is
generally called the enhancement factor due to electron-
phonon interaction in the effective mass or density of

states. McMillan and Rowell give $\lambda = 1.5$ (Pb) and

$\lambda = 1.6$ (Hg) from their data. Of practical interest is

the life time $\tau = 1/\left[2 \, \text{Im} \, M_{el-ph} (\omega;T)\right]$ of an

electron at low temperatures. As $\alpha^2(\omega)F(\omega)$ is not known

for very low energies, the very low temperature behaviour is

uncertain, but the values of τ for an electron at the

Fermi surface given in fig. 5 could be used in estimates.

One should not forget that there is a temperature indepen-

dent impurity scattering which in pure materials can corre-

spond to a life time $\tau \sim 10^{-9} - 10^{-10}$ sec.

Knowing $M_{el-ph}(\omega)$ we can easily form the spectral weight

function $A(p,\omega)$.

$$A(p,\omega) = \frac{1}{\pi} \frac{\text{Im} \, M_{el-ph}(\omega)}{\left[\omega - \varepsilon_p + \mu - \text{Re} \, M_{el-ph}(\omega)\right]^2 + \left[\text{Im} \, M_{el-ph}(\omega)\right]^2} \tag{4}$$

There is a sum rule that $A(p,\omega)$ always obeys,

$$\int A(p,\omega) \, d\omega = 1 \tag{5}$$

It may happen that $A(p,\omega)$ has a narrow Lorentz shape of

width Γ at $\omega = \omega_0$ superposed on a more or less smooth

background. We than say that we have a well defined quasi-

particle of energy ω_0 and life time $\tau = 1/(2\Gamma)$, whose

strength is $1/(1 - \partial \, Re \, M_{el-ph}(\omega)/\partial\omega)$, the latter
quantity being the contribution to the sum rule, eq. (5),
from the peak. ω_o is the solution of the equation

$$\omega_o = \varepsilon_p - \mu + Re \, M_{el-ph}(\varepsilon_p, \omega_o) \tag{6}$$

As has been shown by Engelsberg and Schrieffer[6], one does
not expect conduction electrons with a strong coupling to
the lattice to show quasi-particle character for energies
$\varepsilon_p - \mu$ comparable to phonon energies. Fig. 6 shows $A(p,\omega)$
for lead at three values of ε_p (i.e. three values of p)
in the most interesting energy region. The interpretation of
the first of these figures can simply be stated as follows:
A ''bare'' electron with momentum p is inserted into the
ground state of the metal, and we ask for the time behaviour
of the system. If there were no interactions between the in-
serted electron and the rest of the system, we would have a
time dependence given by the frequency $(\varepsilon_p - \mu)/h$ and this
excitation would have an infinite life time. The sharp peak
in fig. 6 reflects the fact that the electron-phonon interaction
causes the system to partly behave as if we had an electron
with momentum p but with a new excitation energy $(\varepsilon_p - \mu)/(1 + \lambda)$
(cf. eq. 6). The peak is not infinitely sharp so this ex-
citation will have a finite life time. The broad wing of
$A(p,\omega)$ on the upper side of the Fermi level is a consequence
of the fact that a phonon can be emitted when the ''bare''
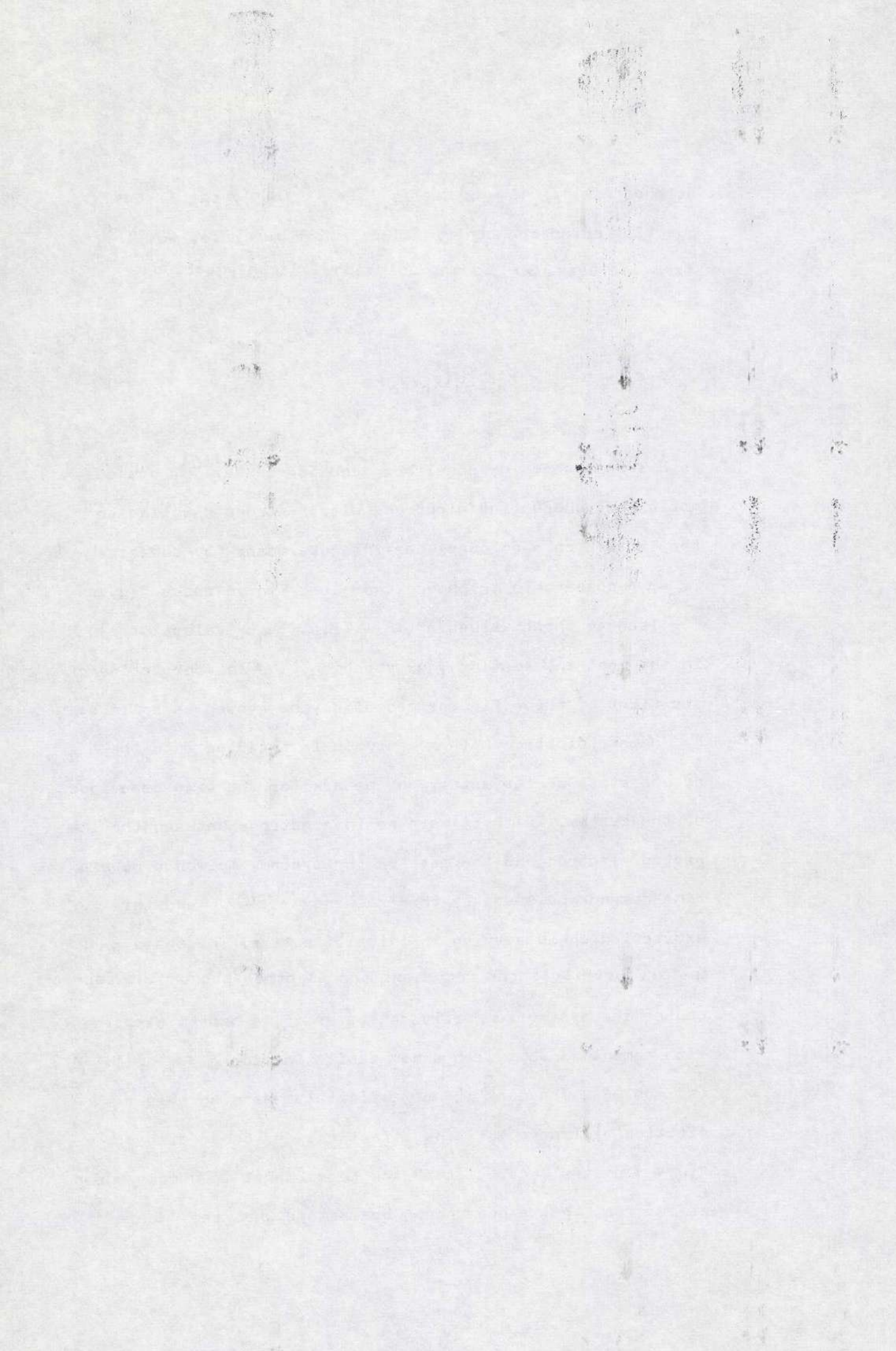
electron is inserted. The part of $A(p, \omega)$ for $\omega < 0$
gives information about the "extraction" of an electron
from the ground state. Also in this case can a phonon be
excited. The sharp peak in fig. 6a contributes $1/(1 + \lambda) = 0.40$ to the sum rule, eq. (5). The system can thus be de-
scribed as having a well defined quasi-particle whose
strength is only 0.40. At higher energies ϵ_p, fig. 6b,
the electron peak has moved into the upper phonon peak and
the system shows no quasi-particle behaviour at all. Finally
for still higher energies ϵ_p, fig. 6c, a large portion of
the sum rule is filled by the Lorentz shaped curved cen-
tered at an energy roughly that of the inserted "bare" electron.
However the damping is now so large that it is not much mean-
ing in adopting a quasi-particle picture. At finite tempera-
tures there is no longer a clear distinction between holes
($\omega < 0$) and particles ($\omega > 0$) in the interpretation of
$A(p, \omega)$, but with our definition of M_{el-ph} the sum rule,
eq. (5), still holds. In fig. 6 we show (dotted curve) how
the sharp quasi-particle peak is considerably broadened al-
ready when $T = 11$ ^{o}K. The spectral function for mercury would
be qualitatively the same as that of lead. In conclusion it
seems that we can use the quasi-particle concept only at very
low energies $\epsilon_p - \mu$. In all other cases, when higher
energies are important, the full shape of $A(p, \omega)$ must be re-
tained when electron properties are calculated. This limita-
tion is after all not serious as in many experiments (e.g.
low temperature specific heat, cyclotron resonance) only low

energy excitations are involved. Moreover Prange and Kada-
noff [7] have argued that for example the electronic specific
heat at all temperatures can be written in a form that is
mathematically the same as the standard Landau quasi-particle
formulation. Therefore, as Prange and Kadanoff have pointed
out, the break down of the quasi-particle concept in an
electron-phonon system is partly a semantic matter. We refer
to their paper for further details. See also an excellent re-
view by Schrieffer [8].

The density of states

After having obtained the spectral function $A(p, \omega)$, we can
sum over all momenta p, to get the density of states at an
energy ω close to the Fermi level. The important contri-
bution comes from the region $p \sim p_F$. We find a relation
similar to the sum rule,

$$\int A(p,\omega) \ d\varepsilon_p = 1 \tag{7}$$

and thus this concept of density of states does not contain
any electron-phonon many-body corrections. This is the den-
sity of states that is measured in a tunneling experiment [8].
It is because of the weak momentum dependence of

$M_{el-ph}(\underline{p}, \omega)$ that electron-phonon effects do not enter.
For the case of electron-electron interaction there is no
corresponding property of the self energy and the density
of states does contain many body corrections.[9] However
it is well known that for example the electronic specific
heat and the cyclotron resonance frequency are affected by
the electron-phonon interaction. The result is often stated
in the form that the effective mass or the density of states
at the Fermi level are enhanced by a factor
$1 + \lambda = 1 - \partial \, \mathrm{Re} \, M_{el-ph}(\omega=0; T=0) / \partial \omega$. To distinguish
this concept of density of states from that first introduced
we shall call it a level density for quasi-particles. Let us
consider the electrons close to the Fermi level in a metal,
but with no electron-phonon interaction. The electron states
can be labeled by the momentum $\underline{p}$ and have an energy ϵ_p.
$A(p, \omega)$ is a delta function at $\omega = \epsilon_p$. As the electron-
phonon interaction is switched on, the peak in $A(p, \omega)$ de-
creases in strength and shifts towards lower energies, but
still we can label the excitation by the momentum $\underline{p}$. When the
interaction is fully turned on we have a system where the
quasi-particle spectrum has a level density increased by a
factor $1 + \lambda$, and with a decrease in strength $1/(1 + \lambda)$
for each level. It is really non-trivial how many-body correc-
tions enter different electronic properties. A theoretical
treatment of some important cases, e.g. the specific heat, and
references to other works in the field, can be found in the
paper by Prange and Kadanoff[7]. It turns out that most

electronic properties are unaffected by electron-phonon many body corrections, because not only the level density byt also the wave function will be modified, and these two effects often cancel. Quantities that do contain many-body corrections are the specific heat, the cyclotron resonance frequency and the amplitude in the de Haas- van Alphen effect. They all show the same increase by a factor $1 + \lambda$ in the effective mass (or the density of levels) at low temperatures. When the temperature is increased, high energy excitations become important, and the complete form of the spectral function $A(p, \omega)$ must be considered. This means that our concept of density of levels is no longer well defined. However for the case of the specific heat it turns out that $1 - \partial \operatorname{Re} M_{el-ph}(\omega; T)/\partial \omega$ can be given an interpretation, although a formal one, also for finite temperatures. Prange and Kadanoff[7] have argued that the electronic specific heat can be calculated from the usual expression (first integral of eq. 16) in Landau's quasiparticle theory provided that the energy $E(\underline{k})$ is the solution of the equation

$$E(\underline{k}) = \varepsilon_{\underline{k}} - \mu + \operatorname{Re} M_{el-ph}(\underline{k}, E(\underline{k}); T) \tag{8}$$

This holds irrespectively of the magnitude of $\operatorname{Im} M_{el-ph}$. Again it is the weak momentum dependence of M_{el-ph} that leads to this remarkable result. Eq. (8) formally gives a density of states in energy space which is enhanced by a factor $1 - \partial \operatorname{Re} M_{el-ph}(\omega; T)/\partial \omega$ compared to the

non-interacting case. If fig. 7 we plot $1 - \partial \text{Re } M_{el-ph}(\omega; T=0)/\partial\omega$
as this is a convenient quantity in our subsequent discussion
on the electronic specific heat. Because our "density of states"
is of a formal nature, we should not be surprised to find
that it can become negative for some energies. The total spe-
cific heat is obtained by an integration over all energies,
and the final result is of course always positive.

Cyclotron resonance

In cyclotron resonance experiments results are often given
in the form of "effective" masses. The electron-phonon mass
enhancement is for low temperatures and frequencies (i.e.
frequency of the applied electromagnetic field) given by the
factor $1 - \partial \text{Re } M_{el-ph}(\omega=0; T=0)/\partial\omega = 1 + \lambda(T=0)$. Be-
cause of the temperature and energy dependence of M_{el-ph}
there will be deviations from this simple result if we raise
the temperature[10] or frequency[11] (the case of high mag-
netic fields[12] will not be considered here). High frequency
cyclotron resonance has been treated theoretically by Scher
and Holstein[11]. They find for the surface independence Z
at T=0

$$Z = R + iX = 2R_o \, e^{-i\pi/3}\left[\sigma(\omega)\right]^{-1/3} \tag{9}$$

where

$$R_o = 8/9(\omega^2 \pi m v_F \sqrt{3}/ne^2 c^4)^{1/3} \tag{10}$$

and

$$\sigma'(\omega) = \int_{\mu-\hbar\omega}^{\mu} \frac{d\epsilon}{\hbar\omega} \coth\left[\pi\left\{-i\ \frac{\omega + \mathrm{Re}\ M_{el-ph}(\epsilon) - \mathrm{Re}\ M_{el-ph}(\epsilon + \hbar\omega)}{\hbar\omega_c}\right.\right.$$

$$\left.\left. + \frac{\mathrm{Im}\ M_{el-ph}(\epsilon) + \mathrm{Im}\ M_{el-ph}(\epsilon + \hbar\omega)}{\hbar\omega_c}\right\}\right] \tag{11}$$

ω_c is the frequency $eH/m_b c$, where no electron-phonon effects are included in the electron effective mass m_b. When the frequency is not too high, it is a good approximation to take

$$\sigma'(\omega) \approx \coth\left[\pi\left\{-i\ \frac{\omega}{\omega_c}\left[1 - \partial\, \mathrm{Re}\ M_{el-ph}(\omega=0)/\partial\,\omega\right] + 2\ \frac{\mathrm{Im}\ M_{el-ph}(\omega=0)}{\hbar\omega_c}\right\}\right] \tag{12}$$

and we arrive at the standard result with resonance ocuring at frequencies ω,

$$\omega = n\left(\frac{eH}{m_{eff}c}\right) \quad , \text{ n integer} \tag{13}$$

where

$$m_{eff} = m_b \left[1 + \lambda (T=0) \right]$$ (14)

As long as $\mathrm{Re}\ M_{el-ph}(\omega + \omega_c)$ is linear in $\omega + \omega_c$, eq. (12) is a good approximation to eq. (11) and the same effective mass will be seen. Now compare with figs. 2 and 4 of $\mathrm{Re}\ M_{el-ph}(\omega)$. For high enough frequencies we have $\mathrm{Re}\ M_{el-ph}(\omega + \omega_c) - \mathrm{Re}\ M_{el-ph}(\omega) \neq \lambda \omega_c$ and this will lead to a shift in the resonance frequency. It is evident from figs. 2 and 4 that very high frequencies are required to see this shift (1 meV corresponds to a frequency $\sim$ 240GHz). At the same time the damping factor in eq. (12) becomes large. Consequently this type of experiment will be very difficult. We refer to the paper by Scher and Holstein [11] for a detailed model calculation.

The possibility of seeing a temperature effect in the effective mass is more promising. At finite temperatures Fermi-Dirac factors must be inserted in the in the integrand of eq.(11) and the integration then goes over all ϵ , i.e. we effectively get a thermal smearing of the integration limits. This will be of only minor importance for the form of the resonance condition if kT is so small that only the region where $\mathrm{Re}\ M_{el-ph}(\omega)$ is linear in contributes to the integral. It then follows that the effective mass measured in a cyclotron resonance experiment at

not too high frequencies is given by

$$m_{eff} = m_b \left[1 + \lambda(T) \right] \tag{15}$$

It remains to calculate the temperature dependence of $\lambda(T) = - \partial \, Re \, M_{el-ph}(\, \omega=0;T)/\partial\omega$. This problem has been considered in an earlier paper [8] both in an accurate calculation for sodium and in an Einstein model. The result of the Einstein model is, that (T) first increases with T to a maximum $\sim 1.2 \, \lambda(0)$ at T $\sim 0.3 \, \theta_E$. $\lambda(T)$ then gradually decreases to zero. In figs 8 and 9 we show $\lambda(T)$ for lead in an accurate calculation based on $\alpha^2(\omega)F(\omega)$ from McMillan and Rowell. A corresponding curve for mercury is given in fig 10. Experiments are always restricted to low temperatures, where the well known condition $\omega_c \tau \gg 1$ can be fulfilled. The results for $\lambda(T)$ (figs. 8 and 10) and τ_{el-ph} (fig. 5) show that if the frequency of the electromagnetic field is higher than about 50 GHz it is possible to cover a temperature range where m_{eff} shifts by about 3% both for lead and mercury. With present experimental technique this is however a very high frequency. If very high magnetic fields are used, one can easily cover a larger temperature range but then our theory is not valid.

The electronic specific heat

The electron-phonon interaction causes the low temperature
specific heat of the conduction electrons to be enhanced by
the same factor $1 + \lambda$ as the low temperature cyclotron
resonance effective mass. In this section we investigate the
deviations from this result as the temperature is increased.
An expression for the electronic specific heat valid at arbi-
trary temperatures has been given by Prange and Kadanoff[7].
They base their deraivation on the equivalence between tempera-
ture derivaties and time derivaties. A related expression
valid at low temperatures has been given by Eliashberg[14],
who started from the thermodynamic potential for the coupled
electron-phonon system. In appendix 1 we show how Eliashberg's
result can be generalized to give the formula of Prange and
Kadanoff (eq. 16)

$$C_v = 2 \int \frac{d^3k}{(2\pi)^3} E(\underline{k}) \frac{\partial f}{\partial T}_o(E(\underline{k})) = 2 \int \frac{d\Omega}{4\pi} N_o \int dE \, E \, \times$$

$$\times \left\{ \left[1 - \frac{\partial}{\partial E} \text{Re} \, M_{el-ph}(E;T) \right] \frac{\partial f}{\partial T}_o(E) + \frac{\partial}{\partial T} \text{Re} \, M_{el-ph}(E;T) \frac{\partial f}{\partial E}_o(E) \right\} \tag{16}$$

This expression can be rewritten in a form that is more
suitable for us.

$$C_v = \frac{2\pi^2}{3} T N_o + \frac{2}{T} P \int dE \, dE' \, d\omega \, N_o \frac{\partial f}{\partial E}_o(E) \frac{\partial f}{\partial E}_o(E') \frac{(E-E')^2}{E-E'+\omega} \alpha^2(\omega) F(\omega) \tag{17}$$

Finally we can write the specific heat as

$$C_v = \left[\gamma_0 + \gamma_1(T)\right] T \qquad\qquad (18)$$

where γ_0 is the value in the absence of electron-phonon interaction and $\gamma_1(T)$ incorporates all these effects.

$\gamma_1(T)$ can be calculated from one integral in eq. 17. As $T \to 0$, $\gamma_1(T) \to \lambda(0) \gamma_0$. It is a well know fact [1,14] that $\gamma_1(T)$ first increases with T and that this increase goes as $T^2 \ln T$. It is also known that renormalization effects disappear as $T \to \infty$, and consequently $\gamma_1(T) \to 0$ in this limit. The behaviour of $\gamma_1(T)$ can be characterized by two temperatures, that at which $\gamma_1(T)$ has its maximum and that above which $\gamma_1(T)$ is essentially zero. To get some insight in the general behaviour of $\gamma_1(T)$ we have in a previous paper [10] investigated an Einstein model, i.e. $\alpha^2(\omega)F(\omega)$ is a delta function at $\omega = k\theta_E$. In this model $\gamma_1(T)$ has a maximum ($\sim 3/2$ of $\gamma_1(0)$) at $T \sim \theta_E/8$ and $\gamma_1(T)$ is zero for $T \sim \theta_E/4$. $\gamma_1(T)$ then has a smaller minimum and approaches zero from below. From the form of eq. 17 it follows that θ_E should be a characteristic temperature not for the phonon spectrum but for $\alpha^2(\omega)F(\omega)/\omega$. For a monovalent metal like sodium, $\alpha^2(\omega)F(\omega)/\omega$ is dominated by the coupling to the high energy longitudinal phonon modes and the usual Debye temperature θ_D should be a good value for θ_E. For polyvalent metals, however, there is a strong coupling via Umklapp processes to the transverse modes. The characteritic Einstein temperature θ_E to be used in calculations of

$\gamma_1(T)$ (and also $\lambda(T)$) can therefore be considerably
lower than θ_D. For lead one finds $\theta_E \sim 45$ $^\circ$K and for mer-
cury $\theta_E \sim 20$ $^\circ$K. This causes the peak in $\gamma_1(T)$ to appear
at temperatures that are much lower than seems in general
to be realized. The effect is very pronounced in mercury, whose
properties have been reported in a previous letter[13]. In
figs. 8 and 9 we show $\gamma_1(T)/\gamma_1(0)$ for lead calculated
from eq. 17 with McMillan's and Rowell's[3] $\alpha^2(\omega)F(\omega)$.
The result for mercury is given in fig. 10. The peak in $\gamma_1(T)$
at $T \sim 6$ $^\circ$K lies <u>below</u> the transition temperature to the
superconducting state ($T_c = 7.2$ $^\circ$K). Already at $T \sim 20$ $^\circ$K
there are practically no renormalization effects left. For
mercury the peak appears at a still lower temperature (2 $^\circ$K)
to be compared with $T_c = 4.2$ $^\circ$K.

A brief argument will be given why the peak in $\gamma_1(T)$
appears at such a low temperature compared to the Debye
temperature and why it is enough to consider the change in
slope $\lambda(T)$ in the case of cyclotron resonance but not for
the specific heat. Let us first discuss the specific heat.
Consider the term in eq. 16 containing $\partial f/\partial T = -(E/T)\partial f/\partial E$.
The function $\partial f/\partial E$ has a rather narrow peak "of width kT",
but after multiplication with E^2 we get a function that has
a broad maximum at $E \sim 2.4$ kT, i.e. already at temperatures
much lower than the Debye temperature do we begin to pick up
contributions to the specific heat from regions where
Re M'_{el-ph} changes non-linearly with energy (cf. figs. 2, 4

and 7. This is why the peak in $\gamma_1(T)$ can occur at such a
low temperature as $T \sim 0.1 \; \Theta_D$. The remaining term in the inte-
grand of eq. 16 containing the temperature derivative of the
self energy is of little importance and does not invalidate
our discussion above. For the case of cyclotron resonance
we are really restricted to energies within a narrow range
around the Fermi level. There is no factor in the integrand
of eq. 11 that makes high energy excitations important, on the
contrary they have a large damping factor. Therefore we always
stay within the region where $\mathrm{Re} \; M_{el-ph}(\omega;T)$ is linear in
and it is enough to find the temperature dependence of the
effective mass from a knowledge of $\lambda(T)$.

An interesting question is, whether it is really possible to
see the temperature dependence of $\gamma_1(T)$ in specific heat
measurements. Let us here consider a measurement of the
specific heat of lead in a normal state (i.e. in a magnetic
field). Measurements on the superconducting state will be dealt
with in the next section. The lattice contribution goes as
T^3 and the electronic part is linear in T. Let us define a
temperature T_0 at which the lattice and electronic parts
are approximately equal. For lead, $T_0 = 1.3 \; ^{\circ}K$ and for mercury
$T_0 = 0.6 \; ^{\circ}K$. At the temperature where $\gamma_1(T)$ has its maximum,
the interesting quantity $[\gamma_1(T) - \gamma_1(0)]$ T makes only 0.5%
of the total specific heat for lead[15] (0.4% for mercury).
An additional important point is that the lattice part does
not follow a T^3-law at these temperatures (i.e. Θ_D can no

longer be considered as temperature independent). The high
high temperature specific heat shows a linear increase coming
from the electronic term and also from anharmonic effects. If we
could find some estimate of the anharmonic term (e.g. from
measurements of phonon frequency shifts by neutron scattering)
it should be possible to verify qualitatively that the linear
electronic term changes slope from the region of very low
temperatures to the region $T \gtrsim \theta_D$.

Specific heat in superconductors

The results just obtained have some important consequencies
for an analysis of the thermodynamic properties of super-
conductors. Of experimental importance is the difference
ΔC in the total specific heat between the normal and the
superconducting state of a metal.

$$\Delta C = C_{n,tot} - C_{s,tot} \tag{19}$$

The quantity ΔC can either be obtained directly by
calorimetric methods or calculated from measurements of the
critical field H_c as a function of temperature. In the latter
case, thermodynamics gives

$$\Delta C = \frac{T H_c}{4\pi} \frac{d^2 H_c}{dT^2} + \frac{T}{4\pi}\left(\frac{dH_c}{dT}\right)^2 \tag{20}$$

It is generally assumed[15] that the lattice part can be taken
to be the same in the normal and in the superconducting
state, and thus one arrives at an experimentally determined

difference

$$C_{n,e} - C_{s,e} = \Delta C \qquad (21)$$

between the electronic specific heat of the two states. To a fairly good approximation $C_{s,e}$ has an exponential behaviour

$$C_{s,e} = const.e^{-(const. \; T/T_c)} \qquad (22)$$

where T_c is the transition temperature when no magnetic fields are present. As $\Delta C - [\gamma_0 + \gamma_1(T)] T = -C_{s,e}$ goes exponentially to zero with T_c/T, the experimental uncertainties in ΔC and $\gamma_0 + \gamma_1(0)$ makes it meaningless to consider $C_{s,e}$ at temperatures below say $T_c/T=5$. But the exponential decrease of $C_{s,e}$ with temperature opens up a new possibility to see the temperature dependence of $\gamma_1(T)$. We can for example plot $\Delta C/[(\gamma_0 + \gamma_1(0))T]$ as a function of T. This ratio will start with the value 1 at T=0 and then increase slightly (in mercury a few percent) before the eventual decrease due to the onset of $C_{s,e}$. The possibilities to experimentally verify this effect in mercury has previously been considered [13].

We next consider what modifications the temperature dependence of $\gamma_1(T)$ will give to earlier experimental determination of $C_{s,e}$ [16]. The relative change in $\gamma_1(T)$ for lead

When $T_c/T = 1$ is large but at the same time $C_{n,e}$ is only
about 1/3 of ▲C and $C_{s,e}$ is only increased by 3%. At
lower temperatures the relative influence on $C_{s,e}$ is larger,
for $T_c/T = 1.7$ one finds that the earlier values of $C_{s,e}$
should be increased by about 10%. Thus the changes in
$C_{s,e}$ are not unimportant, and the correction is larger
than the given experimental uncertainty. However the devi-
ation of $C_{s,e}$ in lead from the BCS result is still large.
For mercury the situation is qualitively the same as for
lead. We end this section with two remarks. The first con-
cerns the ration $(C_{s,e}/C_{n,e})_{T=T_c}$. In a BCS-model this ratio
is 2.43. Standard analysis of experiments on superconductors
gives $(C_{s,e}/C_{n,e})_{T=T_c} = 3.7$ for lead[16], and the difference
between this value and the BCS result is some times taken as
a crude measure of the strong coupling character of lead. A
proper analysis along the lines of this paper decreases the
experimental value from 3.7 to 3.3. For mercury[17] the
corresponding change is an increase from 2.9 to 3.2. Therefore
there is not much meaning in a comparison of ratios
$(C_{s,e}/C_{n,e})_{T=T_c}$ for strong coupling superconductors. The
second remark concerns the possible experimental verification
of a difference in the lattice specific heat between a normal
and a superconducting state. Such attempts should contain a
careful analysis of the effects dealt with here in order to
avoid spurious results.

Conclusions

The electron-phonon system of polyvalent metals differ from
that of for exampls the alkali metals in several respects.
It is not only that the polyvalent metals have a stronger
coupling, but also the characteristic phonon energy is very
low due to the strong coupling to transverse modes via Um-
klapp processes. We have investigated the consequencies of
these facts on the electronic properties of lead and mer-
cury.

The electronic excitations can conveniently be described by
spectral functions. We have calculated the spectral function
for several energies and temperatures and as expected we do
in general not have the structure of single particle like
excitations. The effective electron mass as measured by
cyclotron resonance has a temperature dependence which can
in general be neglected, but for lead and mercury this
effect is large enough to be seen with the present experi-
mental technique. The normal electronic specific heat shows
a strong deviation from the usual linear increase with
temperature. It is difficult to measure this effect directly
but a study of the metal both in the superconducting state
and in the normal state (i.e. with and without an applied
magnetic field) can make it is possible to verify the non-
linear increase.

Acknowledgement

Appendix

It is well known that the specific heat of a non-magnetic
metal in the limit of low temperatures can be divided up
into two terms, one proportional to T^3 coming from the
phonons and one linear in T from the electrons. The
effect of electron-phonon interaction can easliy be
absorbed in the electronic part by the introduction of an
enhanced effective electron mass. In the literature there
are at least two attempts to go beyond the limit of low
temperatures. Eliashberg [14] started from an expression
for the thermodynamic potential in order to find the first
correction to the linear behaviour of the electronic speci-
fic heat. Prange and Kadanoff [7] made quite a different
approach and from the similarity between time derivatives
and temperature derivatives they obtained a formula for the
specific heat which they claim is valid at all temperatures.
We will here show that Eliashberg's formula can be general-
ized so as to give the result of Prange and Kadanoff.

Using a method developed by Luttinger and Ward

Eliashberg [14] finds the following expression for the

thermodynamic potential Ω of the coupled electron-

phonon system:

$$\Omega = -2T \sum_P \left\{ \ln\left[-G^{-1}(P)\right] + M(P)G(P) \right\}$$

$$+ \frac{T}{2} \sum_Q \left\{ \ln\left[-D^{-1}(Q)\right] + \Pi(Q)D(Q) \right\}$$

$$-T^2 \sum_P \sum_{P'} g^2_{P-P'} \; G(P')D(P-P')G(P') \tag{A 1}$$

with

$$M(P) = -T \sum_{P'} G(P')D(P-P')g^2_{P-P'} \tag{A 2}$$

and

$$\Pi(Q) = 2g^2_q \, T \sum_P G(P)G(P-Q) \tag{A 3}$$

The summation over P means

$$\sum_P = \sum_{\varepsilon_n} \int \frac{dp}{(2\pi)^3} \tag{A 4}$$

with $\varepsilon_n = (2n+1)i\pi T$ and n integer. The summation over Q

is analogous with $\omega_m = 2mi\pi T$ and m integer. g^2_q is

the electron-phonon coupling. To avoid cumbersome notation

we shall not include coupling via umklapp processes or

transverse phonons. The electron-electron interaction and

phonon-phonon interaction is for the moment neglected. It

is easy to show that Ω is stationery with respect to

variations in M and Π. Therefore when we calculate the

entropy $S = -(\partial\Omega/\partial T)$ we only have to differentiate

with respect to the explicit temperature dependence of Ω

The electronic term

We start with what will eventually be interpreted as
the electronic contribution S_{el}

$$S_{el} = -(\partial \Omega_{el}/\partial T) \qquad \text{(A 5)}$$

with

$$\Omega_{el} = -2T \sum_{P} \ln\left[-G^{-1}(P)\right] \qquad \text{(A 6)}$$

To find S_{el} we make a contour integration and make use
of the analytic properties of G_R and G_A as described
by Abriskosov, Gorkov and Dzyaloshinskii[1] p. 171 and
we have

$$S_{el} = 2\int \frac{dp}{(2\pi)^3} \frac{1}{2\pi iT}\int_{-\infty}^{\infty} \varepsilon\left[-\frac{\partial f_0(\varepsilon)}{\partial \varepsilon}\right]\left[\ln G_R(p,\varepsilon;T) - \ln G_A(p,\varepsilon;T)\right] d\varepsilon \qquad \text{(A7)}$$

$f_0(\varepsilon)$ is the Fermi-Dirac equilibrium distribution function.
G_R and G_A denote the retarded and advanced electron Green
functions. They obey the relation $G_R = G_A^{*}$. Note that we
have only differentiated with respect to the explicit
temperature dependence but after this derivative has been
taken we have included the full temperature dependence in
the Green functions, i.e. in their self energy parts. We
now depart from the method of Abrikosov et.al. and first
integrate with respect to dp. We change the integration
limits for the energy in eq. A 7 to be from 0 to ∞. One
part of the integrand can then be written

$$\int d\underline{p} \left[\ln G_R(\underline{p}, c; T) - \ln G_R(\underline{p}, -c; T) \right] \qquad (A\ 8)$$

We have (Abriskosov et. al.)

$$G_R^{-1}(\underline{p}, c; T) = c - c_p - \text{Re}\, M(c; T) - i\,\text{Im}\, M(c; T) \qquad (A\ 9)$$

and

$$G_R^{-1}(\underline{p}, -c; T) = -c - c_p + \text{Re}\, M(c; T) - i\,\text{Im}\, M(c; T) \qquad (A\ 10)$$

We have then made use of the well known fact that

$M(\underline{p}, c)$ is independent of $\underline{p}$ to the order $(m/m)^{1/2}$

(electron mass to ion mass). The expression A 8 now becomes

$$p_F m_b \int dc_p \left[\ln(c - c_p - \text{Re}\, M(c; T) - i\,\text{Im}\, M(c; T) \right. -$$
$$\left. \ln(-c - c_p + \text{Re}\, M(c; T) - i\,\text{Im}\, M(c; T) \right] \qquad (A\ 11)$$

Where m_b is an effective band mass and p_F the Fermi momentum.
The contribution to the integral comes form the imaginary
part of the logarithm, i.e. from its angular argument.
The immediately finds that the integral A 11 equals

$$2i\pi m_b p_F \left[c - \text{Re}\, M(c; T) \right] \qquad (A\ 12)$$

Note that this reslut does not require that $\text{Im}\, M$ is
small. After an analogous treatment of $\ln G_A$ in eq. A 7
we end up with

$$S_{el} = \frac{m p_F}{2\pi^2 T^2} \int_0^\infty \frac{c}{\cosh^2(c/2T)} \left[c - \text{Re}\, M(c; T) \right] dc \qquad (A\ 13)$$

This is the same as Eliashberg's result with the exception
that he only wanted the lowest correction to the linear
temperature dependence of C_{el} and therefore took $Re M$
to be temperature independent. It now only remains to
compare with the result of Prange and Kadanoff. After
another derivation with respect to T, which should now also
include $Re M$, some partial integrations lead to

$$C_{el} = 2 \int \frac{d\Omega}{4\pi} N_0 \int dE \; E \left\{ \left[1 - \frac{\partial Re \; M(E)}{\partial E} \right] \frac{\partial f_0(E)}{\partial T} + \frac{\partial Re \; M(E)}{\partial T} \frac{\partial f_0(E)}{\partial E} \right\} \qquad (A \; 14)$$

where N_0 is the band density of electron states at the
Fermi level. This is exactly the reslut of Prange and
Kadanoff.

The phonon term

We next turn to the specific heat of the phonons and
consider Ω_{ph}

$$\Omega_{ph} = \frac{T}{2} \sum_Q \ln \left[-D^{-1}(Q) \right] \qquad (A \; 15)$$

The evaluation of this term is analogous to that of the
electron part.

We go from a sum over $2mi \, \pi T$ to an integration in an
imaginary ω-plane and deform the integration contour to
be partly along the real axes. The imaginary part of D is

very small and the logarithm will therefore have dis-
continuities in its angular argument when we pass the
singularity points $\omega = \pm \ \omega_q$. One finds

$$S_{ph} = \frac{1}{4} \ \sum_q \ \int_{-\infty}^{-\omega_q} - \ \int_{\omega_q}^{\infty} \frac{\partial}{\partial T} \coth(\omega/2T) \ d\omega \qquad (A \ 16)$$

After a partial integration and a change of variables
S_{ph} can be rewritten in the form

$$S_{ph} = \sum_q \ \omega_q \frac{\partial}{\partial T} \left[\frac{1}{e^{\omega_q/T} - 1} \right] - T \ \sum_q \int_0^T \frac{\omega_q}{T} \frac{\partial}{\partial T} \left[\frac{1}{e^{\omega_q/T} - 1} \right] dT \qquad (A \ 17)$$

which is just the free energy for a system of independent
harmonic oscillators. It is also the result that Prange
and Kadanoff give for the contribution from the lattice
vibrations. It should be remarked that Ω_{ph} of course is the
same as the standard textbook result for bosons using a grand
canonical ensemble, $\Omega = -kT \ \ln Z = kT \ \sum_k \ln \left[1 + \exp((\epsilon - \mu/kT) \right]$. A
methematical transformation [18] leads to the form Ω_{ph} above.
An analogous statement holds for Ω_{el} id damping is neglected.

Remaining terms in Ω

There remain several terms in Ω . When we used the nota-
tion Ω_{el} and Ω_{ph} we anticipated the fact that the
remaining terms either cancel or give a negligible con-
tribution to the entropy and the specific heat. This is
certainly true in the limit of low temperatures where
our results for C_{el} and C_{ph} are known to hold. We now
set out to prove it also for elevated temperatures.
We use the notation

$$\Omega' = \Omega_a + \Omega_b + \Omega_c = \tag{A 18}$$

$$-2T \sum_P M(P)G(P) + \frac{T}{2} \sum_Q (Q)D(Q) - T^2 \sum_P \sum_{P'} G(P)G(P')D(P-P')$$

In the usual way we can go over from a summation to an integration.

$$\Omega_a = -\frac{1}{2\pi i} \int \frac{dp}{(2\pi)^3} \int_{-\infty}^{\infty} dc \ \operatorname{tgh}(c/2T) \Big[M_R(p,c)G_R(p,c) - M_A(p,c)G_A(p,c) \Big] \tag{A19}$$

$M_R(p,c)$ can be expressed as[19]

$$M_R(p,c) = \int \frac{dp'}{(2\pi)^3} g_{p-p'}^2 \Bigg\{ i \int_{-\infty}^{\infty} \frac{dc'}{4\pi} \operatorname{tgh}(c'/2T) \Big[G_R(p',c') - G_A(p',c') \Big] D(p-p',c-c')$$

$$+ \frac{1}{2} \Big[G_R(c+\omega_{p-p'},p') + G_R(c-\omega_{p-p'},p') \operatorname{coth}(\omega_{p-p'}/2T) \Big] \Bigg\}$$
$$\tag{A 20}$$

$M_A(p,\varepsilon)$ has an analogous expression with G_A instead of G_R in the last bracket of eq. 20. Taking into account that $G_R = G_A^*$, we can write

$$\Omega_a = -\frac{1}{2\pi i} \int \frac{dp}{(2\pi)^3} \int_{-\infty}^{\infty} dc \ \operatorname{tgh}(c/2T) \int \frac{dp'}{(2\pi)^3} g_{p-p'}^2 \int_{-\infty}^{\infty} dc' \ \operatorname{tgh}(c'/2T) \times$$

$$\times \operatorname{Im} G_R(p,c) \operatorname{Im} G_R(p',c') D(p-p',c-c')$$

$$- \frac{1}{2} \int \frac{dp'}{(2\pi)^3} g_{p-p'}^2 \Big[G_R(p,c) \Big(G_R(p',c+\omega_{p-p'}) + G_R(p',c-\omega_{p-p'}) \Big)$$

$$- c.c. \Big] \operatorname{coth}(\omega_{p-p'}/2T) \tag{A 21}$$

Because of the stationarity of Ω with respect to M we shall only take the temperature derivative of $\tanh(\varepsilon/2T)$ when we form $S_a = (\partial\Omega_a/\partial T)$. It is easy to see that $\Omega_c = -\Omega_a/2$, but in Ω_c the temperature derivatives are to be taken both for the coth and the two tgh factors. The temperature derivatives of tgh will lead to exactly cancellning terms in S_a and S_c. In S_a there remain terms containing integrals of the type (note that $G_R = G_A^*$)

$$\int dp' g_{p-p'}^2 \int_{-\infty}^{\infty} \left[\frac{\partial}{\partial T} \tanh(\varepsilon/2T)\right] \left[\text{Re } G_R(\underline{p},\varepsilon) \text{ Im } G_R(\underline{p}',\varepsilon+\omega_{\underline{p}-\underline{p}'}) + \right.$$

$$\left. + \text{ Re } G_R(p,\varepsilon) \text{ Im } G_R(\underline{p}',\varepsilon-\omega_{\underline{p}-\underline{p}'})\right] \tag{A 22}$$

Compare this with an expression for $\text{Re}\,\Pi(k, \omega_0)$ (Abrikosov et.al. p 179)

$$\text{Re}\,\Pi(\underline{k}, \omega_0) = \frac{2}{(2\pi)^4} g_{\underline{k}}^2 \int dp \int_{-\infty}^{\infty} d\varepsilon \quad \tanh(\varepsilon/2T) \times \tag{A 23}$$

$$\times \left[\text{Re } G_R(\underline{p}-\underline{k},\varepsilon-\omega_0) \text{ Im } G_R(\underline{p},\varepsilon) + \text{Re } G_R(\underline{p},\varepsilon+\omega_0) \text{ Im } G_R(\underline{p}-\underline{k},\varepsilon)\right]$$

$\text{Re}\,\Pi(\underline{k}, \omega_0)$ is practically independent of the frequency ω_0 when $\omega_0 \ll \mu_F$ and we can put it equal to zero in eq. A 23. Eq. A 22 is of the same structure and we can also here put $\omega_{\underline{p}-\underline{p}'} = 0$. From the solution of eq. A 23 (Abrikosov et.al. p 179) it follows that the self energy parts of the electron Green function are not important and that $\text{Re}\,\Pi(\underline{k})$ is practically temperature independent. It follows that the remaining term in S_a and the corresponding terms in S_c can be rewritten in a form containing $\partial\Pi/\partial T$ and can thus be neglected. We are finally left with S_b and the term in S_c that originates from the temperature derivative of coth $(\omega_{\underline{p}-\underline{p}'}/2T)$. S_b is as usual evaluated with a complex contour integration. Using that (cf Abrikosov et.al.) $D_R = D_A^*$, $\text{Im}\,\Pi$ is small of order $(m/\tilde{m})^{1/2}$ and $\text{Im } D(\underline{q},\omega)$ is sharply peaked at $\omega = \pm \omega_{\underline{q}}$ we get

$$S_b = -\frac{1}{2} \sum_{\underline{q}} \text{Re}\,\Pi(\underline{q}) \cdot \frac{\partial}{\partial T}\coth(\omega_{\underline{q}}/2T) \tag{A 24}$$

Recalling that Re $\prod(k, \omega_o)$ as given by eq. A 23 is in-
dependent of ω_o we find cancellation between S_b and the
remaining term in S_c. In summing up, Eliashberg's thermo-
dynamic potential leads to the result of Prange and
Kadanoff for the specific heat of the coupled electron-
phonon system

Explicit electron-electron interactions have been neglected
as well as band effects. We include then afterwards as
a correction to the effective density of states at the
Fermi level. The neglect of phonon-phonon interactions
is more serious. With increased temperature, the phonon
frequencies will shift and also eventually be less well
defined. However the presentation here is valuable, as it
enables a separation of anharmonic effects from the measured
high temperature specific heat.

References

1. Abrikosov,A.A., L.P.Gorkov, and I.E.Dzyaloshinskii:
   Methods of quantum field theory in statistical mechanics.
   Englewood Cliffs, N.J.: Prentice Hall 1963.

2. Schrieffer,J.R.: Theory of superconductivity. New York: Benjamin 1964.

3. McMillan,W.L., and J.M.Rowell: A chapter in Superconductivity
   edited by R.Parks: to be published.

4. Grimvall,G.: Phys.kondens.Materie 6, 15 (1967).

5. Stedman,R., L.Almqvist, and G.Nilsson: Phys.Rev. 162, 549 (1967).

6. Engelsberg,S., and J.R.Schrieffer: Phys.Rev. 131, 993 (1963).

7. Prange,R.E., and L.P.Kadanoff: Phys.Rev. 134, A566 (1964).

8. Schrieffer,J.R.: In: Many-body Theory I, edited by R.Kubo.
   Tokyo: Syokabo 1966.

9. Lundqvist,B.L.: Phys.kondens.Materie 7, 117 (1967).

10. Grimvall,G.: J.Phys.Chem.Solids 29, 1221 (1968).

11. Scher,H., and T.Holstein: Phys.Rev. 148, 598 (1966).

12. Fowler,M., and R.E.Prange: Physics, 1, 315 (1965).

13. Grimvall,G.: Solid State Comm. (in press).

14. Eliashberg,G.M.: Soviet Phys.-JETP, 16, 780 (1963).

15. van der Hoeven Jr,B.J.C.,and P.H.Keesom:Phys.Rev.137,A103(1965).

16. Neighbour,J.E.,J.F.Cochran,and C.A.Schiffman:Phys.Rev.
    155, 384 (1967).

17. van der Hoeven Jr,B.J.C.,and P.H.Keesom:Phys.Rev. 135,A631 (1964).

18. Luttinger,J.M.,and J.C.Ward: Phys.Rev. 118,1417 (1960).

19. Eliashberg,G.M.:Soviet Phys.-JETP 12, 1000 (1961).

Figure captions

Fig. 1   The phonon density of states $F(\omega)$ and the effective
electron-phonon interaction $\alpha^2(\omega)F(\omega)$ for lead.

Fig. 2   The real part of the self energy, $\text{Re } M_{el-ph}(\omega;T)$ for
lead at different temperatures.

Fig. 3   The imaginary part of the self energy $M_{el-ph}(\omega;T)$,
for lead at different temperatures.

Fig. 4   The real and imaginary parts of the self energy M_{el-ph}
for mercury at $T=0$.

Fig. 5   The average life time of an electron at the Fermi level
as a function of temperature. The dashed part of the
curve is somewhat uncertain.

Fig. 6   The spectral function $A(p,\omega)$ for lead at $T=0$ and for
different energies ε_p. (a: $\varepsilon_p = 2$ meV, b: $\varepsilon_p = 8$ meV,
c: $\varepsilon_p = 18$ meV), In curve a, there is a sharp delta
function at $\omega=0.8$ meV. This peak is considerably
broadened at finite temperatures. The dashed curve is
for $T=11\ ^oK$.

Fig. 7   The density of states in the vicinity of the Fermi level
for lead at $T=0$. The density of states is defined form-
ally as $1 - \partial \text{Re } M_{el-ph}(\omega)/\partial\omega$.

Fig. 8   The temperature dependence in lead for the slope $\lambda(T)$
of the self energy at $\omega=0$, and for the electron-phonon
enhancement $\gamma_1(T)$ of the electronic specific heat.
The curves are normalized to 1 for $T=0$. T_c is the trans-
ition temperature to the superconducting state.

Fig. 9   The temperature dependence in lead of the slope $\lambda(T)$
of the self energy at $\omega=0$ and of the electron-phonon
enhancement $\gamma_1(T)$ of the electronic specific heat.

Fig. 10 The temperature dependence in mercury of the slope λ (T)
of the self energy at $\omega=0$ and of the electron-phonon
enhancement γ_1(T) of the electronic specific heat. The
curves are normalized to 1 for T=0.

Figure captions

Fig. 1   The phonon density of states $F(\omega)$ and the effective
         electron-phonon interaction $\alpha^2(\omega)F(\omega)$ for lead.

Fig. 2   The real part of the self energy, Re $M_{el-ph}(\omega;T)$ for
         lead at different temperatures.

Fig. 3   The imaginary part of the self energy $M_{el-ph}(\omega;T)$,
         for lead at different temperatures.

Fig. 4   The real and imaginary parts of the self energy M_{el-ph}
         for mercury at $T=0$.

Fig. 5   The average life time of an electron at the Fermi level
         as a function of temperature. The dashed part of the
         curve is somewhat uncertain.

Fig. 6   The spectral function $A(p,\omega)$ for lead at $T=0$ and for
         different energies ε_p. (a: $\varepsilon_p = 2$ meV, b: $\varepsilon_p = 8$ meV,
         c: $\varepsilon_p = 18$ meV). In curve a, there is a sharp delta
         function at $\omega = 0.6$ meV. This peak is considerably
         broadened at finite temperatures. The dashed curve is
         for $T=11$ ^oK.

Fig. 7   The density of states in the vicinity of the Fermi level
         for lead at $T=0$. The density of states is defined form-
         ally as $1 - \partial$ Re $M_{el-ph}(\omega)/\partial\omega$.

Fig. 8   The temperature dependence in lead for the slope $\lambda(T)$
         of the self energy at $\omega = 0$, and for the electron-phonon
         enhancement $\gamma_1(T)$ of the electronic specific heat.
         The curves are normalized to 1 for $T=0$. T_c is the trans-
         ition temperature to the superconducting state.

Fig. 9   The temperature dependence in lead of the slope $\lambda(T)$
         of the self energy at $\omega = 0$ and of the electron-phonon
         enhancement $\gamma_1(T)$ of the electronic specific heat.

Fig. 10   The temperature dependence in mercury of the slope λ (T)
           of the self energy at ω=0 and of the electron-phonon
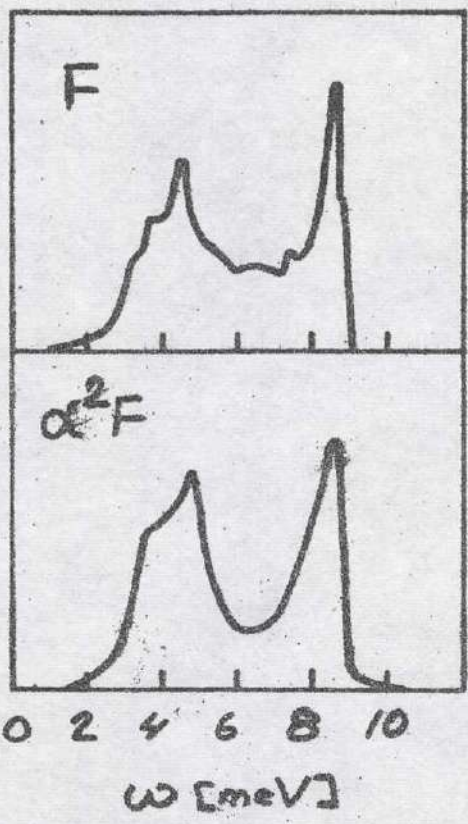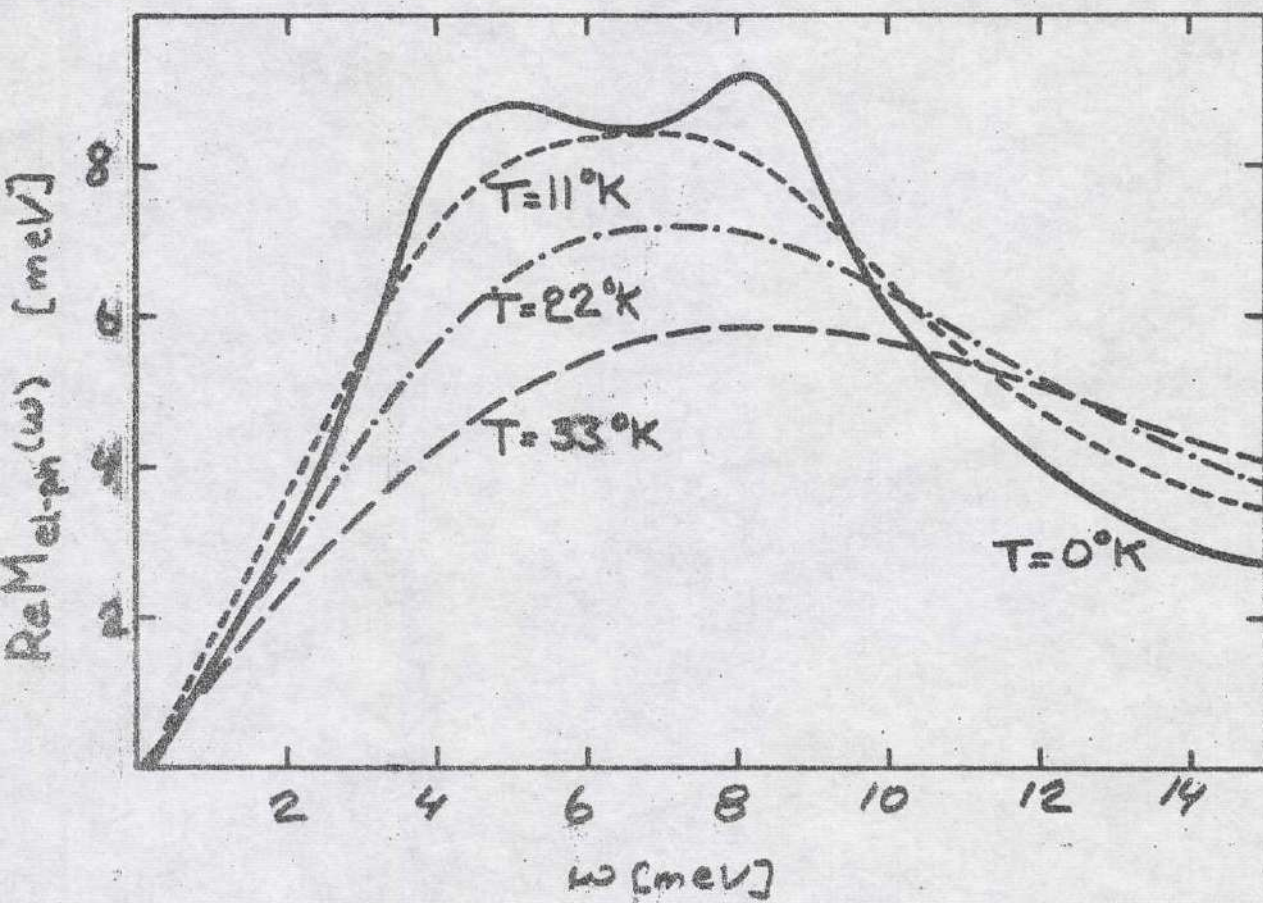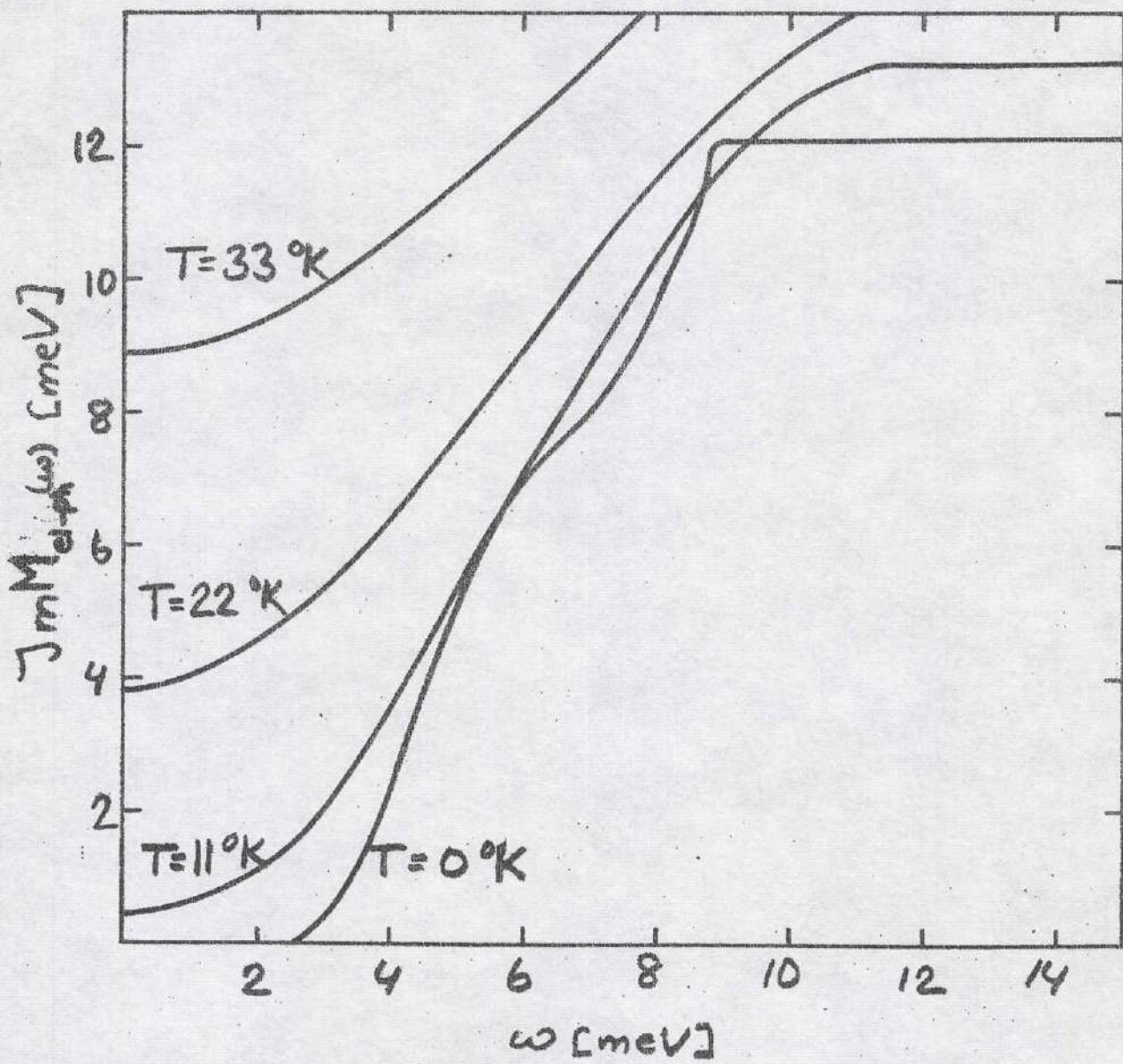   enhancement γ_1(T) of the electronic specific heat. The
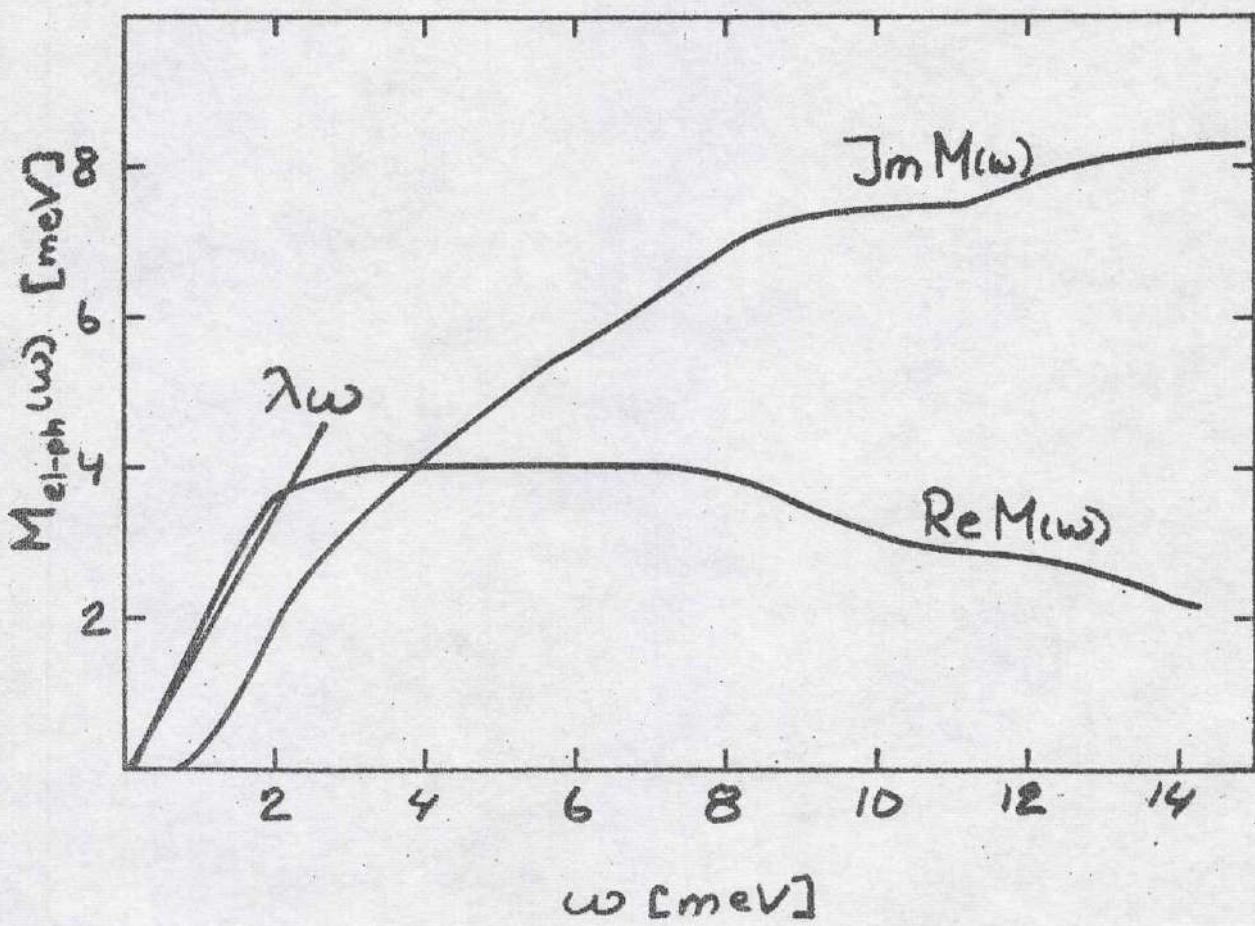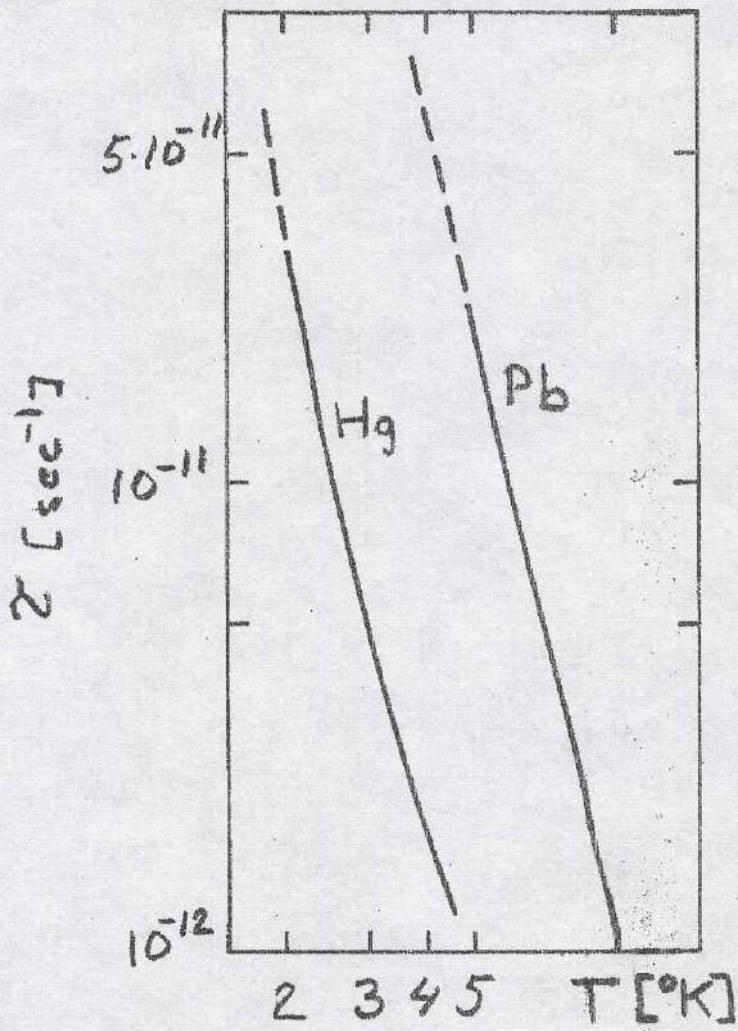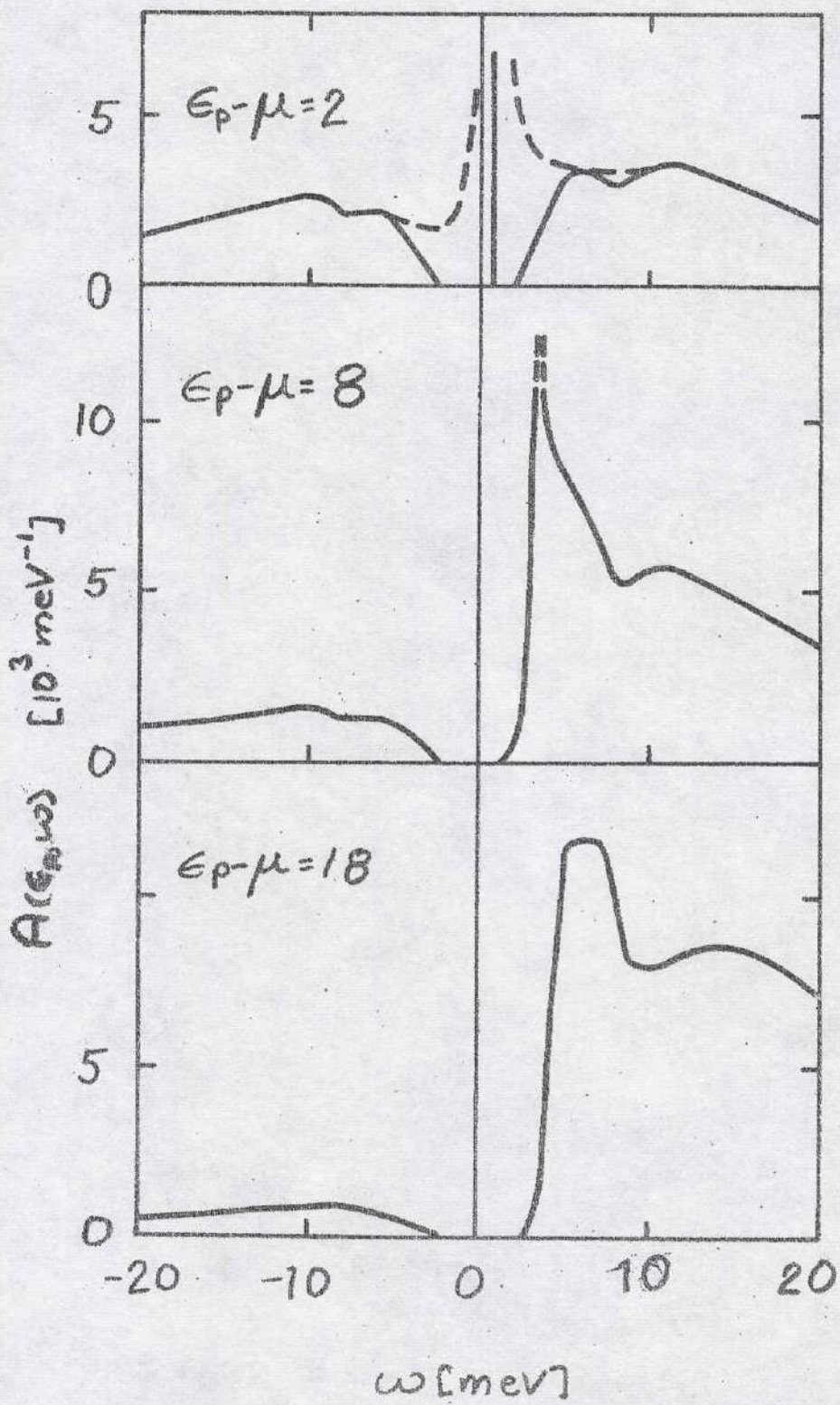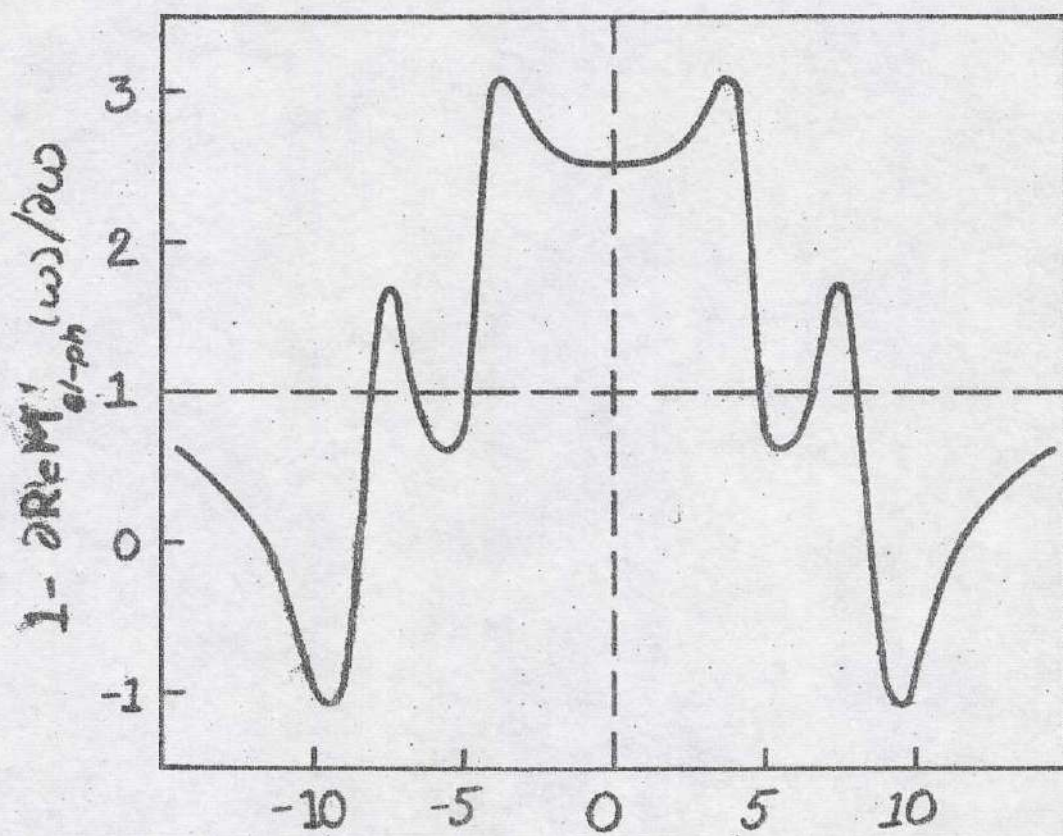   curves are normalized to 1 for T=0.

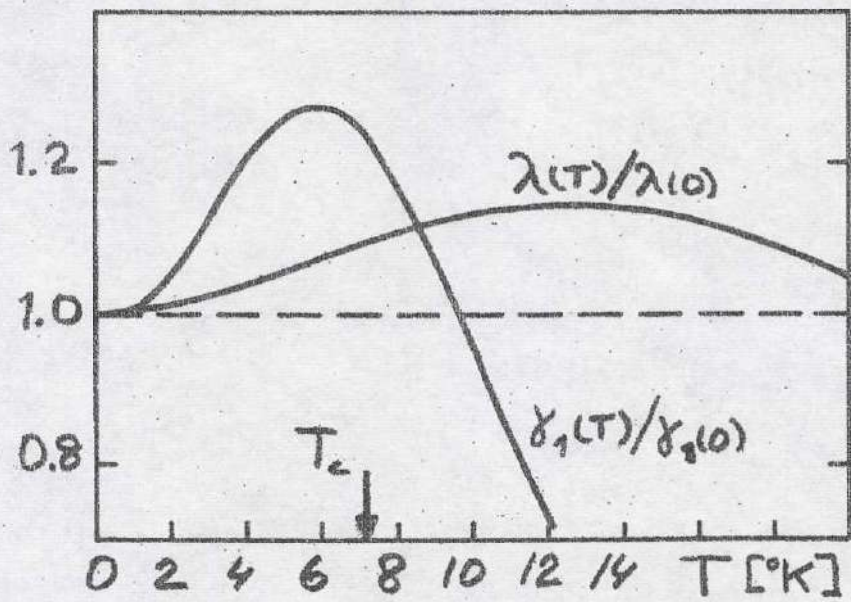Fig. 1
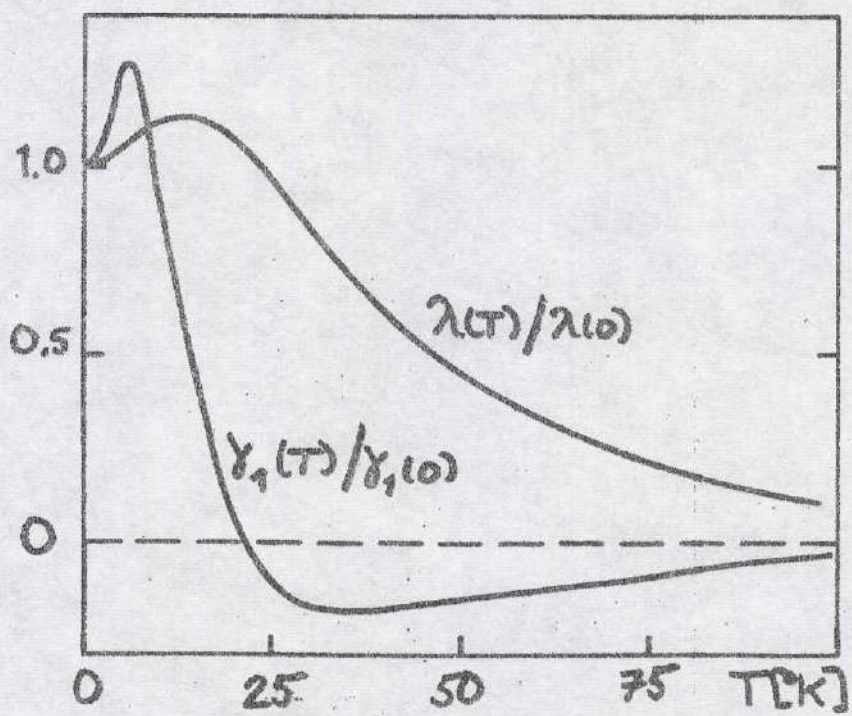
Fig. 2
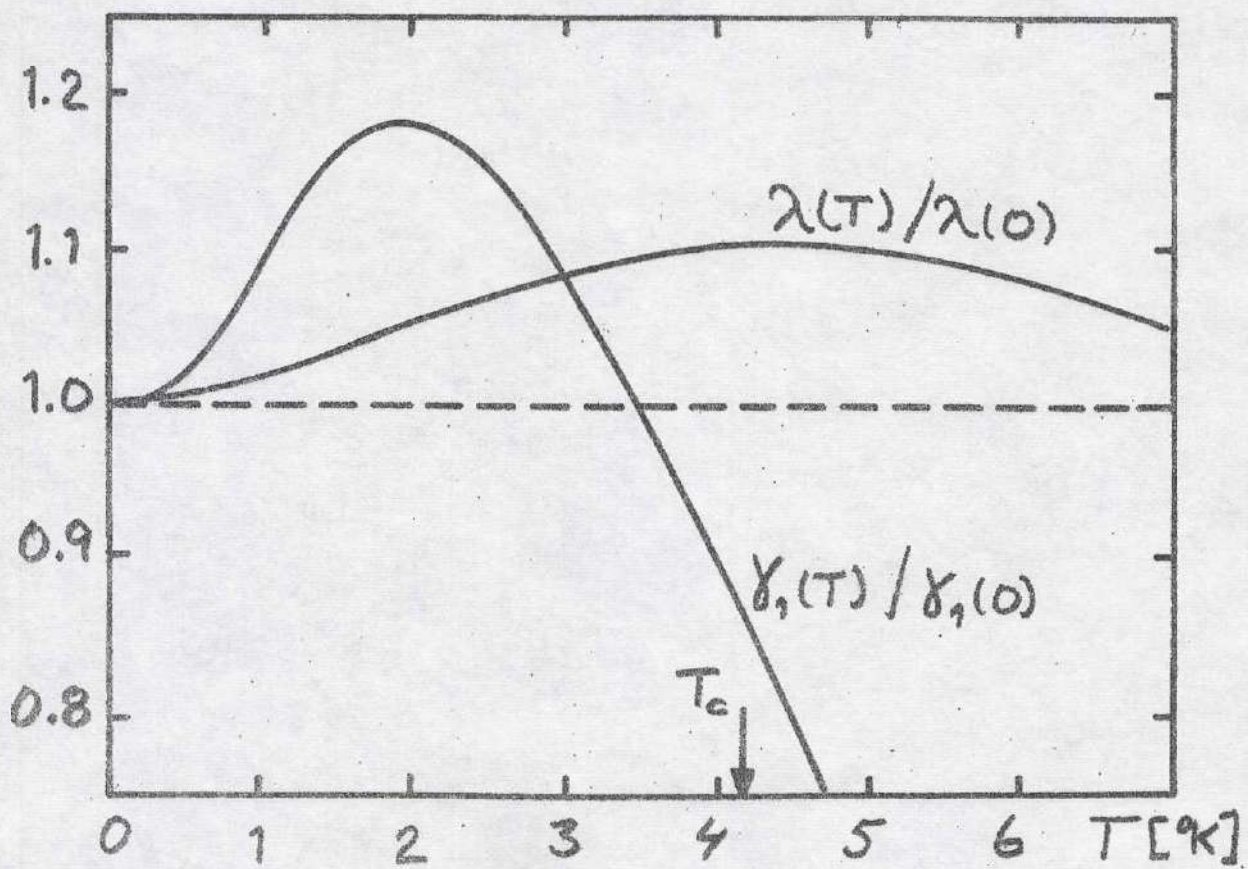
Fig. 3

Fig. 4

Fig. 5

Fig. 6

Fig. 7

Fig. 8

Fig. 9

Fig. 10

Conductivities in Normal Metals from Measurements on Superconductors

Göran Grimvall

Institute of Theoretical Physics, Göteborg, Sweden

A calculation of the high temperature electrical resistivity for lead, indium and tin is performed starting from data obtained when the gap equation for tunneling in superconductors is inverted. A main result is the average $\overline{1 - \cos\Theta}$ where Θ is the scattering angle. The result is discussed in detail.

On a calculé la résistivité électrique à haute température du plomb, de l'indium et de l'étain en partant de l'équation du gap pour l'effet tunnel dans les supraconducteurs. Le résultat principal se révèle dans l'expression moyenne $\overline{1 - \cos\Theta}$ où Θ est l'angle de dispersion. Une discussion détaillée de ce résultat termine ce travail.

Wir berechnen die elektrische Leitfähigkeit bei hohen Temperaturen in Blei, Indium und Zinn, ausgehend von Experimenten im supraleitenden Zustand (Inversion der „gap equation"). Ein Hauptresultat ist der Mittelwert $\overline{1 - \cos\Theta}$, wo Θ der Streuwinkel bedeutet. Das Ergebnis wird im einzelnen diskutiert.

Introduction

Electrical conductivity is one of the most fundamental properties of solid metals. Although the physics is well understood, calculations are consistently in poor quantitative agreement with experiments. The first serious attempt to calculate theoretically the conductivity was made some thirty years ago by BARDEEN [1]. Since then many authors have tried to improve the calculations, especially for the alkali metals. These attempts have been very disappointing. WISER [2] has given a discussion of the origin of some of the difficulties met with. Calculations for polyvalent metals are less frequent. Lately PYTTE [3] has tried two different pseudopotentials for the electron-phonon coupling in aluminum, and he got results differing by almost a factor two (at $T = 300\ °K$), the experimental value lying in between. CARBOTTE and DYNES [4] have obtained a somewhat better agreement, the significance of their results is however doubtful in view of PYTTE's results.

Among all more or less uncertain points in a theoretical calculation are: The phonon spectrum including its temperature dependence, the electron-phonon coupling, the shape of the Fermi surface, the density of electron states on the Fermi surface, the thermal expansion of the lattice, and of course approximations made in the formal expressions for the resistivity (cf. the discussion below). In this paper we show that many of these uncertainties can be overcome, if one uses information from the inversion of the gap equation that describes the superconducting state. This is of course not a "first principles" calculation, but nevertheless it is a challenging task to find high temperature resistivity from measure-

ments on a superconducting state. The result demonstrates nicely the consistency of the data and provides a check on the key theoretical assumptions.

General formalism

We closely follow the approach given by ZIMAN [5]. Using a variational method, the resistivity can be written

$$\varrho = \frac{9\pi\hbar}{6\,M\,e^2\,N\,k\,T\,I} \sum_\lambda \int\!\!\int \frac{q^2\,(\hat{e}_{\lambda q}\cdot q)^2\,v^2(q)}{[e^{\hbar\omega_\lambda(q)/kT} - 1]\,[1 - e^{-\hbar\omega_\lambda(q)/kT}]}\,\frac{dS}{v}\,\frac{dS'}{v'},\tag{1}$$

where

$$I = (12\,\pi^3 h)^2 \left| \int v_q\,(\hat{u}\cdot q)\,\frac{\partial f_q^0}{\partial\varepsilon_q}\,dq \right|^2 = \overline{K_{\mathrm{F}}^2}\,S^2.$$

A phonon with wavevector q (always to be reduced to the first Brillouin zone) and polarization index λ has the frequency $\omega_\lambda(q)$ and polarization vector $\hat{e}_{\lambda,q}$. The equilibrium Fermi-Dirac distribution is denoted by f^0. The quantities v and v' are velocities of an electron on the Fermi surface and n the number of conduction electrons per unit volume. K_{F} is a directional dependent Fermi wavenumber. We take k_{F} as the Fermi wavenumber for a spherical Fermi surface (i. e. a free electron model) and S_0 the area of the Fermi surface in this model. S is the true free area of the Fermi surface. Further $\hat{u}$ denotes a unit vector along the applied electric field. The Boltzmann constant is denoted by k and m is the mass of a free electron. The electron-phonon coupling is given by $v(q)$.

The choice of trial functions in the variational procedure that leads to Eq. (1) has been investigated by KOHLER [6] and SONDHEIMER [7]. The error introduced in Eq. (1) by our specific choice is of no importance for our calculation. Phonon drag is also completely neglected, i.e. the phonon system is assumed to be in thermal equilibrium. This is probably a very good approximation in the temperature range we will consider ($T \gtrsim \Theta_{\mathrm{D}}/3$). Except for these limitations, Eq. (1) is a very general expression that contains in full all details about the electron and phonon systems.

From a numerical inversion [8] of the gap equations for a superconductor it is possible to find very accurate ($\sim 1\%$) values of the quantity $\alpha^2(\omega)\,F(\omega)$ [9]

Fig. 1. $\alpha^2(\omega)\,F(\omega)$ much resembles the density of states $F(\omega)$. The curve shown is typical in shape for lead and indium

$$\alpha^2(\omega)\,F(\omega) = \frac{\sum_\lambda \int\!\!\int \frac{(\hat{e}_{\lambda,q}\cdot q)^2\,v^2(q)\,\delta(\omega - \omega_\lambda(q))}{(2\,\pi)^3\,2\,M\,N\,\hbar\,\omega_\lambda(q)}\,\frac{dS}{v}\,\frac{dS'}{v'}}{\int \frac{dS}{v}}.\tag{3}$$

The denominator in Eq. (3) is related to the total density of electron states $N_{\mathrm{bs}}(0)$ on the Fermi surface (including bandstructure but not electron-phonon interaction).

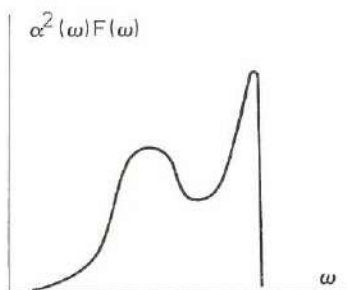$$N_{\mathrm{bs}}(0) = \frac{1}{4\,\pi^3} \int \frac{dS}{\hbar\,v}.\tag{4}$$

$\alpha^2(\omega)$ is the energy dependent electron-phonon coupling and $F(\omega)$ is the density of phonon states. $\alpha^2(\omega) F(\omega)$ has been obtained by McMILLAN and ROWELL [8] for some superconductors, e.g. lead, indium and tin. We give a typical form of $\alpha^2(\omega) F(\omega)$ in Fig. 1. Comparing Eqs. (1) and (3) we find, that apart from the factor q^2 in the integrand of Eq. (1) the two expressions are very similar. If we had a spherical Fermi surface, then

$$q^2 = 2 k_F^2 (1 - \cos \Theta),$$ (5)

where Θ is the angle between the initial and final state of a scattered electron. For a non-spherical Fermi surface we get a slight difference that we neglect. We will also take $\overline{K_F} = k_F$ in Eq. (2). As $S_0 = 4 \pi k_F^2$ and the density of electron states at the Fermi level in a free electron model $N_{fe}(0) = 3 mn/\hbar^2 k_F^2$ we find when combining Eqs. (1), (2), (3), (4) and (5) and using $k_F^3 = 3 \pi^2 n$

$$\varrho = \overline{(1 - \cos \Theta)} \left(\frac{S_0}{S} \right)^2 \frac{N_{bs}(0)}{N_{fe}(0)} \frac{4 \pi m \hbar}{n k T e^2} \int \frac{\alpha^2(\omega) F(\omega) \omega \, d\omega}{[e^{\hbar \omega/kT} - 1][1 - e^{-\hbar \omega/kT}]},$$ (6)

where $\overline{(1 - \cos \Theta)}$ is an average value for the scattering processes in Eq. (1). The quantity $\alpha^2(\omega) F(\omega)$ was measured at very low temperatures $(T < T_c)$. Before we can proceed to a numerical evaluation of Eq. (6) we must analyse that further temperature dependence, which does not explicitly lie in the exponential terms. One consequence of raising the temperature is, that the phonon frequencies change. Also there will be a thermal expansion of the lattice.

As the complete temperature dependence of $\alpha^2(\omega) F(\omega)$ is very difficult to discuss we instead consider the so called Bloch model (cf. ZIMAN [5] Eq. 9.7.1) for electrical resistivity. At high temperatures $(T \gg \Theta_D)$ it can be written

$$\varrho = \frac{\pi^3 \hbar^3 k_F T}{4 m e^2 k n_a \Theta_R^2}.$$ (7a)

The general form is

$$\varrho = \frac{\pi^3 \hbar^3 k_F}{m e^2 k n_a \Theta_R} \left(\frac{T}{\Theta_R} \right)^5 \int_0^{\Theta_R/T} \frac{z^5 dz}{[e^z - 1][1 - e^{-z}]}.$$ (7b)

Here n_a is the number of conduction electrons per atom and Θ_R a Debye temperature to be used in resistivity calculations. Θ_R is of the same order of magnitude as Θ_D used in heat capacity formulae. In this model we see, that apart from the explicit dependence on Θ_R, ϱ is proportional to k_F, i.e. the inverse of the lattice parameter. The thermal expansion is in our case alway less than 1%, so the change in k_F can be neglected. On the other hand Θ_R will change appreciably. This term can easily be taken into account if we use temperature dependent phonon frequencies in Eqs. (1), (3) and (6). The average shift in $\omega_\lambda(q)$ amounts to 10% or even more in the range of temperatures we consider and can thus not be neglected.

The temperature dependence of the phonon frequencies $\omega_\lambda(q)$ is treated in an approximation where we assume that we always have a system of harmonic oscillators but with a frequency changing with the temperature. We make the crude approximation that all phonon frequencies change in the same way, i.e.

$$\omega_\lambda(q; T) = \omega_\lambda(q; T = 0) \cdot A(T),$$ (8)

where $A(T)$ is a function of temperature. (We note that this approximation does

not refer to any special shape of the dispersion curves.) Let us consider some region in the wave vector space in Eq. (3). Let us also assume all quantities in Eq. (3) except $\omega_\lambda(q)$ as independent of temperature. At $T = 0$ the considered set of q-values for a specific branch λ will give contributions to $\alpha^2(\omega)F(\omega)$ in an interval $\Delta\omega$ around $\omega_\lambda(q)$. For finite temperatures the same scattering processes contribute to $\alpha^2(\omega)F(\omega)$ in a frequency interval whose width and position have both been shifted by $A(T)$. The strength of the interaction is only changed by $1/A(T)$ coming from the term $1/\omega_\lambda(q)$ in the double integral in Eq. (3). It is thus not difficult to take into account the temperature dependence due to shifts in the phonon frequencies.

For $A(T)$ we must find a proper average over all phonons. We assume that

$$A(T) = 1 - \gamma T \qquad (9)$$

where γ is a constant. The shift at low temperatures ($T \ll \Theta_D$) is then probably overestimated, but these temperatures lie outside the region we treat.

Results

We have used data from the inverted gap equations for lead, indium and tin [8] to integrate Eq. (6). The constant γ in Eq. (9) was determined so as give the experimentally measured value of $(d\varrho/dT)/\varrho$ at $T = 273\,°$K. For lead we can compare the value of γ with a measurement of frequency shifts between 80 °K and 300 °K made by STEDMAN et al. [10] using neutron scattering technique. Their measurements show that the shift differs very much for different phonons. The shift is largest in the sound wave limit and can even be positive near the boundaries of the first Brillouin zone. Thus it can be very misleading to use e.g. ultrasonic data to find γ. Also the average $A(T)$ is not the same for different properties such as heat capacity, Debye-Waller factors or resistivity because of different weighting factors. We have estimated γ from STEDMAN's curves and found agreement with that obtained from $(d\varrho/dT)/\varrho$ at $T = 273\,°$K.

For $T \ll \Theta_D$ the low energy part of $\alpha^2(\omega)F(\omega)$ becomes important. In this region the relative uncertainty in $\alpha^2(\omega)F(\omega)$ is large, and also the behaviour of $1 - \cos\Theta$ is not known so we have not found it justified to go to lower temperatures than $T \approx \Theta_D/3$. This is of course regrettable, as it leaves out an interesting temperature region.

To get an absolute value for ϱ we must know S_0/S, $N_{bs}(0)/N_{fe}(0)$ and $\overline{1 - \cos\Theta}$. If we however consider $\varrho(T)/\varrho(T = 273\,°K)$, then the first two terms related to the Fermi surface have no influence. Moreover $\overline{1 - \cos\Theta}$ is not expected to vary much in the temperature region we are interested in ($T \gtrsim \Theta_D/3$). The reason for this is that the metals we investigate are polyvalent metals where umklapp processes are very important. As the temperature is lowered the exponential terms will decrease the relative importance of the high frequency phonons. This will however affect so many regions over the Fermi surface, that the average $\overline{1 - \cos\Theta}$ should stay practically constant. With these assumptions $\varrho(T)/\varrho$ ($T = 273\,°$K$)$ is readily evaluated from Eqs. (6), (8) and (9). We give the results for lead and indium in Figs. 2 and 3 together with experimental values. The agreement is very good, but not a very significant check on the accuracy of the theory. In fact the temperature

variation depends so strongly on the exponential terms that even a crude model for the phonons (e.g. a Debye model) will give a good description irrespective of the form of the electron-phonon interaction and other details. This has been known for a long time; indeed the famous Bloch formula (Eq. (7) for electrical resistivity is surprisingly good for interpolation between high and low temperatures. In Fig. 2 we also plot $\varrho(T)/\varrho(T = 273\,°\mathrm{K})$ from Bloch's formula, using $\Theta_R = 86\,°\mathrm{K}$. MAC DONALD [11] found this value of Θ_R to give a good fit with experiments. Actually we have used $\Theta_R = 86\,°\mathrm{K}$ at $T = 273\,°\mathrm{K}$ and then made the same correction as above, i.e. $\Theta_R = 86\,[1 - \gamma(T - 273)]$.
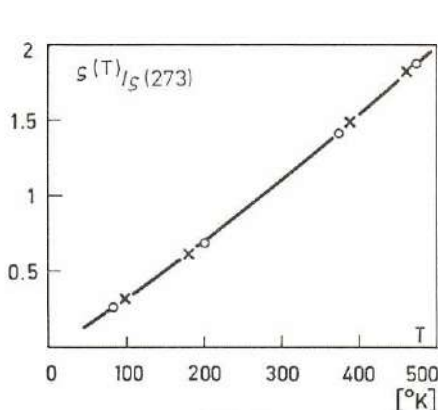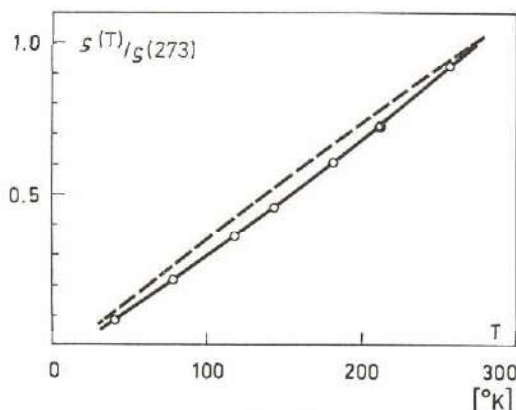
Fig. 2. $\varrho(T)/\varrho(T = 273\,°\mathrm{K})$ for lead. —— this work. $+$ Bloch's formula. Experimental values (o) from HOLBORN [21]

Fig. 3. $\varrho(T)/\varrho(T = 273\,°\mathrm{K})$ for indium. —— this work with $\omega_\lambda(q)$ shifted with temperature. ---- no shift in $\omega_\lambda(q)$. Experimental values (o) from SWENSON [23]

An absolute value of $\varrho(T)$ could be obtained only if we knew S/S_0, $N_{bs}(0)/N_{fe}(0)$ and $\overline{1 - \cos\Theta}$. From experiments on anomalous skin effect CHAMBERS [12] has determined S/S_0 for several metals. He gives $S/S_0 = 0.46$ for lead and $S/S_0 = 0.43$ for tin. These values are not very accurate and CHAMBERS estimates the value for lead to be too low. AUBREY [13] also measured the anomalous skin effect and found $S/S_0 = 0.55 \pm 0.05$ for lead. ANDERSSON and GOLD [14] made de Haas-van Alphen experiments and OPW calculations for lead. Their result is $S/S_0 = 0.59$. ASHCROFT [15] has discovered an error in the calculations of ANDERSSON and GOLD. A corrected value is $S/S_0 = 0.69 \pm 0.05$. STEDMAN et al. [16] have made accurate studies of the Fermi surface of lead based on the observation of Kohn anomalies in the phonon dispersion curves. From the results of these measurements they built a model of the Fermi surface. The measured [17] free area is 0.70 ± 0.01. MINA and KHAIKIN [18] studied the Fermi surface of indium in cyclotron resonance experiments and OPW calculations. Their result is $S/S_0 = 0.85$ while DHEER [19] found $S/S_0 = 0.93$ from measurements of the anomalous skin effect. ASHCROFT and LAWRENCE [20] got $S/S_0 = 0.81$ in a calculation for indium. The quantity $N_{bs}(0)/N_{fe}(0)$ has been estimated by McMILLAN [9] from a knowledge of Debye temperatures, superconducting transition temperatures and the

electron effective mass enhancement due to electron-phonon interaction. The values of S/S_0 and $N_{bs}(0)/N_{fe}(0)$ used in this paper are given in the Table.

We have compared Eq. (6) with experimental values for the resistivity at $T = 273\,°K$ to find a value for $\overline{1 - \cos\Theta}$. The result is given in the Table. Experimental values are taken from HOLBORN [21] (Pb), GOLOVASHKIN and MOTULEVICH [22] (Pb), SWENSON [23] (In) and GUETHS et al. [24] (Sn). For indium and tin the values used here are averages, as these metals are anisotropic. CHAMBERS considered his value of S/S_0 for lead to be too low. We suspect that the value for tin is also too low, so we give an alternative value of $\overline{1 - \cos\Theta}$ based on $S/S_0 = 0.5$. It is very satisfying that $\overline{1 - \cos\Theta}$ then comes out with a reasonable value for all three metals. We recall that other calculations of ϱ often are in error by a factor two or more.

Table

element	valence	$N_{bs}(0)/N_{fe}(0)$	S/S_0	$\gamma \cdot 10^4$ $°K^{-1}$	$\varrho\,(T=273\,°K)_{exp.}$ $\mu\Omega cm$	$\overline{1 - \cos\Theta}$
Pb	4	0.87	0.7	2	20.4	1.1
In	3	0.89	0.85	5	8.0	0.8
Sn	4	0.82	0.43	2	10.7	0.5
			(0.5)			(0.7)

From the Table we see, that $\overline{1 - \cos\Theta}$ is approximately the same for the three metals Pb, In and Sn. (The uncertainty in $\overline{1 - \cos\Theta}$ is rather large, say $10-20\%$, mainly because of the uncertainty in S/S_0). That the average scattering angle is almost the same is also to be expected, for $\overline{1 - \cos\Theta}$ is the same as an average of $q^2/2k_F^2$, ($q^2 = 2k_F^2 \cdot (1 - \cos\Theta)$, see Eq. (5)). Let us assume an Einstein model for the phonon frequencies. As all three branches then are degenerate, we can choose the polarization vector $\hat{e}_{\lambda,q}$ so that $q \cdot \hat{e}_{\lambda,q} = |q|$ for one branch and zero for the other branches (also for umklapp processes). The weighting function for $q^2/2k_F^2$ then is $(q/2k_F)^3\,v^2(q/2k_F)$ (cf. Eq. (1) after the surface integrations have been transformed to a volume integration). The electron-phonon interaction $v(q/2k_F)$ has approximately the same shape for all metals [25]. It goes to a constant for small q and has a node just below $q/2k_F = 1$. As an average is taken, it is of course only the shape of $v^2(q/2k_F)$ that is important and not the magnitude. For comparison we used this approximate method to find $\overline{1 - \cos\Theta}$ for lead. The pseudopotential was taken from ASHCROFT and WILKINS [26] and the result was $\overline{1 - \cos\Theta} = 0.61$. This is expected to be too low as the Einstein model gives too much weight to the region $q/2k_F \geq 0.5$ where high energy transverse phonons are most important. It is also interesting to make a comparison with the value of $\overline{1 - \cos\Theta}$ corresponding to the onset of umklapp processes. For lead this happens when $\overline{1 - \cos\Theta} = 0.4$.

The thermal conductivity K could also be calculated in a similar manner. At high temperatures, however, the electron-phonon scattering process is essentially elastic so we have the Wiedemann-Franz law [5, 27] and there is no need for a separate calculation of K. The region of low temperatures is out of our reach for the same reason as in the case of electrical conductivity.

Conclusion

Starting with results from tunneling in superconductors (i.e. inverted gap equations) we have followed the usual variational approach to calculate the electrical resistivity for three polyvalent metals, lead, indium and tin. The results are in very good agreement with experiments, contrary to the general findings in resistivity calculations. The standard theory therefore seems to be sufficiently accurate, at least at not too low temperatures ($T \gtrsim \Theta_D/3$).

References

1. BARDEEN, J.: Phys. Rev. **52**, 688 (1937).
2. WISER, N.: Phys. Rev. **143**, 393 (1966).
3. PYTTE, E.: J. Phys. Chem. Solids **28**, 93 (1967).
4. CARBOTTE, J. P., and R. C. DYNES: Phys. Letters **25 A**, 532 (1967).
5. ZIMAN, J. M.: Electrons and Phonons. Oxford: Clarendon Press 1960.
6. KOHLER, M.: Z. Phys. **125**, 679 (1949).
7. SONDHEIMER, E. H.: Proc. Roy. Soc. A **203**, 75 (1950).
8. MCMILLAN, W. L., and J. M. ROWELL: A chapter in a treatise on superconductivity edited by R. D. PARKS. To be published.
9. MCMILLAN, W. L.: Phys. Rev. **167**, 331 (1968).
10. STEDMAN, R., L. ALMQVIST, G. NILSSON, and G. RAUNIO: Phys. Rev. **162**, 545 (1967).
11. MACDONALD, D. K. C.: Handbuch der Physik, Bd. 14, S. 137. Berlin-Göttingen-Heidelberg: Springer 1956.
12. CHAMBERS, R. G.: Proc. Roy. Soc. A 215, 481 (1952).
13. AUBREY, L. E.: Phil. Mag. 8, 1001 (1960).
14. ANDERSSON, J. R., and A. V. GOLD: Phys. Rev. **139**, A 1459 (1965).
15. ASHCROFT, N. W.: Thesis, University of Cambridge (1964).
16. STEDMAN, R., L. ALMQVIST, G. NILSSON, and G. RAUNIO: Phys. Rev. **163**, 567 (1967).
17. ALMQVIST, L.: Private communication.
18. MINA, R. T., and M. S. KHAIKIN: Soviet Physics JETP **24**, 42 (1966).
19. DHEER, P. N.: Proc. Roy. Soc. A **260**, 333 (1961).
20. ASHCROFT, N. W., and W. E. LAWRENCE: To be published.
21. HOLBORN, L.: Ann. Phys. **59**, 145 (1919).
22. GOLOVASHKIN, A. I., and G. P. MOTULEVICH: Soviet Physics JETP **17**, 271 (1963).
23. SWENSON, C. A.: Phys. Rev. **100**, 1607 (1955).
24. GUETHS, J. E., C. A. REYNOLDS, and M. A. MITCHELL: Phys. Rev. **150**, 346 (1966).
25. HARRISON, W. A.: Pseudopotentials in the Theory of Metals. New York: Benjamin 1966.
26. ASHCROFT, N. W., and J. WILKINS: Private communication.
27. CHESTER, G. V., and A. THELLUNG: Proc. Phys. Soc. **77**, 1005 (1961).

GÖRAN GRIMVALL
Institute of Theoretical Physics
Fack
S-402 20, Göteborg 5

An analysis of the temperature

and pressure dependence of the

electrical resistivity in lead.

by

G. Grimvall and C. Lydén

Institute of Theoretical Physics

Fack

S-402 20   Göteborg 5

Sweden

Abstract

    The volume dependence of the high temperature electrical resistivity has been treated in detail for lead. Volume changes caused by external pressure as well as thermal expansion have been considered. Experiments on the volume dependence of the effective electron mass have been reanalysed with an inclusion of electron-phonon interaction. Finally, we have found no experimental support for a net effect from a Debye-Waller factor and multi-phonon processes.

Introduction.

The purpose of this paper is threefold. We will try to account for the volume (i.e. pressure) dependence of the electrical resistivity in a detailed calculation based not on models but on data from experiments on other metallic properties. Secondly, it has been conjectured that the Debye-Waller factor and multiphonon processes might cancel in the electrical resistivity and we will therefore analyse this question with the help of available experimental data. Finally we reanalyse experiments on the volume dependence of the effective electron mass and take into account the variation in the electron-phonon enhancement factor. We will consider lead, because of lack of relevant data for other elements.

Theory

There are numerous calculations in the literature[1] of the volume dependence of the electrical resistivity in metals. Although some of them are very elaborate, they make use of models and assumptions that we now know are much too crude. We will base our analysis on Ziman's[2] well known solution of the transport problem obtained with a variational method:

$$\rho = \frac{3\pi\hbar}{2e^2 MNkTS^2 k_F^2} \sum_\lambda \iint \frac{q^2(\hat{\underline{e}}_{\lambda,\underline{q}} \cdot \underline{q})^2 \mathcal{U}^2(|\underline{q}|)}{\left[e^{\hbar\omega_{\lambda,\underline{q}}/kT} - 1\right]\left[1-e^{-\hbar\omega_{\lambda,\underline{q}}/kT}\right]} \frac{dS}{v} \frac{dS'}{v'} \tag{1}$$

$\underline{q} = \underline{k} - \underline{k}'$. The integration dS extends over the Fermi surface, whose free area is S. Phonons of branch λ and wavevector $\underline{q}$ have frequencies $\omega_\lambda(\underline{q})$ and polarization vectors $\underline{\hat{e}}_\lambda$. The electron-phonon interaction has been approximated by the form factor $\mathcal{U}(|\underline{q}|)$ that only depends on the magnitude of the momentum transfer $\underline{q} = \underline{k} - \underline{k}''$. M is the ion mass, N the number of unit cells per unit volume and v and v' the velocities

of an electron at the Fermi surface. The rest of the quantities have
their usual meaning. An earlier calculation of resistivities for some
polyvalent metals[3] with the use of eq. 1 was in good agreement with
experiments and the results obtained in this paper are also reasonable,
so we beleive that eq. (1) is accurate enough in this context. It is
interesting to note that we could in principle make a self consistent
treatment, if we knew how the pseudopotential changed with pressure.
Once we had this information we could calculate changes in the phonon
frequencies, the shape of the Fermi surface and the density of states
of the conduction electrons, but such a procedure would not only be
very difficult but also in practise give inaccurate results. Instead
we will use all available information to see how different parts in
eq. 1 contribute to a change in ρ. For a discussion of the volume de-
pendence it is very convenient to consider $(d \ln \rho / d \ln V)$ and we write

$$\frac{d \ln \rho}{d \ln V} = \frac{2 \, d \ln m_b}{d \ln V} - \frac{2 \, d \ln \Theta_R}{d \ln V} + \frac{d \ln I_R}{d \ln V} + 1 \qquad (2)$$

The first term on the right hand side of eq. 2 comes from the volume
dependence of the band density of states at the Fermi level, i.e.
essentially from dS/v, and we have taken an average over the Fermi
surface in the form of an effective mass. We will always consider
the resistivity at high temperatures (i.e. $T \gg \Theta_D$) and then the pho-
non frequencies come in as $1/\omega_\lambda^2(\underline{q})$ in the integrand of eq. 1. This
leads to the term $-2(d \ln \Theta_R / d \ln V)$. The phonon spectrum is different-
ly weighted in different properties like e.g. the electrical resistivi-
ty and the vibrational specific heat. The relative frequency shift is
not the same for all phonons and we must therefore be careful to spe-
cify which experiment we are considering. This is why we use the nota-
tion Θ_R and it does not imply the use of a Debye model or any other
model. $(d \ln I_R / d \ln V)$ contains the effect of a variation in the form
factor $\mathcal{U}(q)$. Finally there remain some terms that we assume to vary

linearly with the lattice dimension and this gives +1 in the right hand side of eq. 2. We will later consider volume changes caused by external pressure and by the thermal expansion so we do not yet specify whether the temperature or the pressure is to be kept constant in the derivatives in eq. 2.

The thermal expansion coefficient β can be written

$$\beta/K_T = (\frac{\partial S}{\partial V})_T \tag{3}$$

where K_T is the isothermal compressibility and S the entropy. At low temperatures the thermal expansion of a non-magnetic metal consists of one contribution from the conduction electrons, which is linear in T, and one phonon contribution which goes like T^3. The entropy of the electrons is proportional to the total effective electron mass and it is evident from eq. 3 that a measurement of the low temperature thermal expansion can give information about the volume dependence of the effective mass. A review of this method has been given by Collins and White[4]. A measurement of the pressure dependence of the critical field of a superconductor can in principle give the same information about the effective mass. At present this latter type of experiment seems to be less accurate than the first method[5]. In both cases the change in the total effective mass m_{eff} is obtained. If we neglect the influence of electron-electron interaction, we can write

$$m_{eff} = m_b (1 + \lambda) \tag{4}$$

where $1 + \lambda$ is the factor by which the band mass m_b is increased due to electron-phonon interaction. For λ we can write[6]

$$\lambda = \frac{1}{(2\pi)^3 MN\hbar} \sum_\lambda \iint \frac{(\hat{e}_{\lambda,q} \cdot q)^2}{\omega_\lambda^2(q)} \, \nu(|q|) \, \frac{dS}{v} \, \frac{dS'}{v'} / \int \frac{dS}{v} \tag{5}$$

Therefore, in analogy with eq. 2

$$\frac{d \ln m_{eff}}{d \ln V} = \frac{d \ln m_b}{d \ln V} + \frac{\lambda}{1 + \lambda} \frac{d \ln \lambda}{d \ln V} \tag{6}$$

where

$$\frac{d \ln \lambda}{d \ln V} = \frac{d \ln m_b}{d \ln V} - \frac{2d \ln \Theta_\lambda}{d \ln V} + \frac{d \ln I_\lambda}{d \ln V} \qquad (7)$$

Like in eq. 2 the term $-2(d \ln \Theta_\lambda/d \ln V)$ is the effect of shifts in the phonon frequencies but now they are averaged according to eq. 5. The last term, $(d \ln I_\lambda/d \ln V)$, is the result of a change in $\mho(q)$ in eq. 5. The derivatives in eq. 6 are to be taken at constant temperature (cf. eq. 3). There is no à priori reason why the various band masses we have introduced should have the same volume dependence, as they correspond to different averages over the Fermi surface. However, we do not expect them to behave in a very different way, and moreover this point is not crucial for any of the conclusions in this paper.

Pressure dependence of the resistivity.

The resistance of various metals under pressure has been measured by Bridgman[7]. After taking into account that we want resistivity instead of resistance, we have at room temperature and in the limit of small volume changes $(d \ln \rho/d \ln V)_T = 6.9$. Fisher[8] obtained the value 6.5, but Bridgman considers his experimental method to be somewhat uncertain. Throughout this paper we will use the compressibility and thermal expansion coefficient of Gschneider[9] to convert from experimentally determined pressure or temperature derivatives to corresponding volume derivatives.

The phonon term $(d \ln \Theta_R/d \ln V)_T$ could in principle be obtained from measurements of phonon frequencies in lead under pressure. The experimental uncertainties are, however, very large, and we defer a closer discussion of this experiment to the later comparison between effects of an external pressure and of thermal expansion. The standard approach in the literature has been to take $(d \ln \Theta_R/d \ln V)_T$ equal to the well known Grüneisen constant γ_G, without any further justification. In appen-

dices 1 and 2 we show that the use of γ_G is a reasonable approximation for lead.

The term $(d \ln I_R/d \ln V)$ is very difficult to discuss accurately. In order to make any further progress possible, we already in eq. 1 made the approximation with a formfactor $U(q)$ which only depends on the magnitude of the momentum transfer. In a polyvalent metal this leads to erroneous results for those scattering processes where $\underline{k}$ and $\underline{k}'$ differ by a reciprocal wave vector[10]. On the other hand recent calculations by Carbotte and Dynes[11], using the form factor for all scattering processes, has given quite good results for both lead and aluminium, indicating that this approximation could give a good over all description. There are recent measurements of the deHaas-van Alphen effect in lead under pressure[14]. From this experiment, the two derivatives dV_{111}/dp and dV_{200}/dp of the form factor can be deduced. It turns out that a simple model, like Harrison's pseudopotential, gives a value for these derivatives which is correct in sign but too small by a factor five. The Fermi level shifts in opposite direction to what is expected from the free electron case. One must therefore be very careful to draw conclusions from simple models. There are several complications in a calculation of $(d \ln I_R/d \ln V)$ from the de Haas-van Alphen data. The volume dependence of the resistivity is even more sensitive than the resistivity itself to the location of the node of the form factor, for there is a cancellation effect from the contributions from either side of the node. The Fermi surface is not spherical so we are not strictly limited to scattering processes with $(q/2k_F) \leq 1$. Experimental errors in the de Haas-van Alphen data and the breakdown of the form factor description at reciprocal wavevectors add to the difficulties. Therefore we do not find a detailed numerical calculation very significant. Instead we use the deHaas-van Alphen data for V_{111} and V_{200} and their pressure derivatives to estimate $(d \ln I_R/d \ln V)$, as it comes from eq. 1.

With allowance for the uncertainties mentioned we find $0.5 \lesssim$
$\lesssim (d \ln I_R/d \ln V) \lesssim 3$.

Some quantities (the number of unit cells per unit volume, the
free Fermi surface area and the length of q-vectors) were assumed to scale
with the lattice spacing. One can have some doubt about this point, for
the de Haas-van Alphen measurements mentioned gave a net change in the
cross sectional area for some orbits that was twice that which would re-
sult from a pure scaling. However, we do not believe that the considered
orbits are typical for the average behaviour of the Fermi surface. Remem-
ber that the number of electrons per unit cell is constant, so the Fermi
surface encloses a constant volume in the reciprocal space.

For the remaining term $(d \ln m_b/d \ln V)$ we have no reliable in-
formation. We will therefore assign to it a value which makes eq. 2 hold.
The result is summarized in the table. The errors given are somewhat ar-
bitrary. They only serve the purpose of indicating which terms are best
known, and the order of magnitude of the uncertainties. We will comment
on the results in the next section.

Pressure dependence of the effective mass.

The value of $(d \ln m_{eff}/d \ln V)_T$ obtained from measurements of
the low temperature thermal expansion ofr lead[4] is 1.0 ± 0.5. The va-
lue of λ for lead has been obtained by McMillan and Rowell[6] from tun-
neling experiments in superconductors. They find $\lambda = 1.5$. The term
$(d \ln \theta_\lambda/d \ln V)_T$ will be set equal to γ_G. See the appendices for a jus-
tification. Finally we make an estimate of $(d \ln I_\lambda/d \ln V)$ analogous to
that used for the resistivity. In fact the only difference is an addi-
tional factor q^2 in the integral for ρ as compared to the integral for λ.
Proceeding in the same way as for the resistivity we have estimated
$1 \lesssim (d \ln I_\lambda/d \ln V) \lesssim 3$.

Several interesting conclusions can now be drawn. Although

(d ln I/d ln V) is very uncertain, it is no doubt that it is positive
and can be quite large. The experimental results for (d ln ρ/d ln V)$_T$
and (d ln m_{eff}/d ln V) then both require that (d ln m_b/d ln V) is ne-
gative and not very small in magnitude. The band mass is closely rela-
ted to the form factor so it is natural that a strong volume dependen-
ce in one of them also leads to a strong volume dependence in the other.
For a long time it has been thought that shifts in the phonon frequen-
cies give the essential contribution to (d ln ρ/d ln V) in simple me-
tals. Our analysis shows that there are other important contributions
in lead but that they come in with opposite signs and almost cancel.

Nonlinear temperature dependence of the resistivity.

As the temperature is increased, the resistivity will increase
due to the explicit temperature dependence as it appears in eq. 1, but
there will also be an additional effect coming from changes in the other
quantities in the same relation. This additional variation will be very
similar to the volume effect at constant temperature discussed above.
At high temperatures the explicit temperature dependence gives a linear
increase in the resistivity. For lead at room temperature there still
remains a small correction to this linear behaviour from the exponen-
tial terms, but this correction can easily be estimated if the phonon
spectrum is approximated by two Einstein peaks that are given the weights
found in appendix 2. The so evaluated explicit temperature dependence is
subtracted from the measured temperature coefficient for the resistivi-
ty. The rest can conveniantly be expressed in the same form as eq. 2 if
we only remember that the experiment is performed under constant pressure
instead of constant temperature, i.e. we consider (d lnρ/d ln V)$_P$ and
therefore (d ln Θ_R/d ln V)$_P$ should contain both a volume effect and an
additional purely anharmonic effect (cf appendix 1). The rest of the
terms in eq. 2 come only from the thermal expansion of the lattice. There

are, however, some other differences as compared to the pressure effect at constant temperature. In our starting formula, eq. 1, we have not included any Debye-Waller factor or multiphonon scattering processes. These two effects come in with opposite signs and it is still an open question whether they cancel exactly or not[13]. If they do not cancel, we can tentatively include them with an additional multiplicative factor $\exp(-\alpha T)$ in eq. 1, leading to a term $-\alpha T(d \ln T/d \ln V)_P$ in eq. 2. Simple estimates show[13] that any of the two effects considered separately gives a contribution to $(d \ln \rho/d \ln V)_P$ which can be even larger than that coming from the thermal expansion, so it is not a small correction we are discussing. As the temperature is raised, there will also be an increase in the resistivity due to thermally created lattice imperfections. It has been shown experimentally[14] for lead that such effects are negligible at room temperature.

From resistivity measurements we have calculated $(d \ln \rho/d \ln V)_P$ at room temperature and find 4.5 (Holborn[15]), 4.7 (Leadbetter, Newsham and Picton[14]) and 5.0 Pochapsky[16]). As an average we take $(d \ln \rho/d \ln V)_P = 4.7 \pm 0.3$. It should be remarked that this value stays constant within 10 % up to about 500°K. There is a significant difference $(d \ln \rho/d \ln V)_T - (d \ln \rho/d \ln V)_P = 2.2 \pm 0.6$ which can come from the fact that $(d \ln \Theta_R/d \ln V)_T$ and $(d \ln \Theta_R/d \ln V)_P$ are not equal, but also from a Debye-Waller factor and multiphonon processes. We first consider phonon shifts. The electrical resistivity is a scattering phenomenon. Therefore data from inelastic neutron scattering at different temperatures could give us the correct shifts to be used in $(d \ln \Theta_R/d \ln V)_P$. Such experiments have been performed by Stedman, Almqvist and Nilsson[17], and also by Brockhouse et. al.[18]. The two sets of data agree within experimental uncertainties. There is also a general agreement with specific heat measurements on lead by Leadbetter[19].

In fig. 1 we summarize som experimentally determined

$\gamma_q = (d \ln \omega_q/d \ln V)_P$ for the longitudinal and transverse branches in the [100]-direction. Other branches and directions show a similar behaviour. In the same figure we include the corresponding values $\gamma_q = (d \ln \omega_q/d \ln V)_T$ obtained by Quittner and Lechner[20] from neutron scattering experiments under pressure. We also give points from tunneling experiments in superconductors under pressure by Zavaritskii, Istkevich and Voronovskii[21] and Frank and Keeler[22]. In tunneling experiments one can measure the location in energy of the van Hove singularities in the phonon spectrum. The resolution in the tunneling experiments is not very good, and the points in fig. 1 represent some average of the shifts in the van Hove singularities for the longitudinal branch. Therefore this method is not useful for our purposes, although it is an experiment that is much easier to perform than inelastic neutron scattering under pressure. Even though the experimental uncertainties are large, it is evident that the relative frequency shift varies considerably with the wave vector $\underline{q}$, and it would be very misleading to base an analysis on shifts in the elastic constants. The shifts in the pressure experiments (i.e. a pure volume effect) are in general larger than the shifts obtained when the lattice expands under constant pressure. Theoretical calculations confirm these conclusions[22]. From Stedman et al.[17] we estimate $(d \ln \theta_R/d \ln V)_P =$ = 1.4 ± 0.5. We have then given all modes equal weight just as for the high temperature γ_G. This leads to a difference $2(d \ln \theta_R/d \ln V)_T -$ $2(d \ln \theta_R/d \ln V)_P = 2.7 \pm 1$ while $(d \ln \rho/d \ln V)_T - (d \ln \rho/d \ln V)_P =$ = 2.2 ± 0.6. The non-linear temperature dependence of the high temperature resistivity in lead can thus be naturally explained as the effect of thermal expansion and a shift in the phonon frequencies of purely anharmonic origin without any net effect from a Debye-Waller factor and multiphonon processes.

Conclusions.

We have treated the temperature and volume (pressure) dependence of the high temperature electrical resistivity of a simple metal (lead) in considerably more detail than has been done before. We have been forced to make a lot of approximations, and the quantitative results should not be taken too seriously. However, the following qualitative results hold.

(i) It is well known that the volume dependence of the resistivity, $(d \ln \rho / d \ln V)_T$ is in quantitative agreement with $2\gamma_G$, γ_G being the standard Grüneisen parameter which describes the volume dependence of the phonon frequencies. This approximate agreement holds also for lead, and it has therefore been thought that the volume dependence of the resistivity in this metal is essentially due to shifts in the phonon frequencies. We have found that there might be considerable contributions from shifts in the electron density of states at the Fermi surface and in the electron-phonon interaction described by the form factor, but these two effects come in with opposite signs and happen to almost cancel.

(ii) Sham and Ziman[12] have suggested that one should look for a non-linearity in the high temperature electrical resistivity to see if there is any net effect from a Debye-Waller factor and the opposing multiphonon processes. In addition to the effect of thermal expansion we find a non-linearity which, however, agrees both in sign and magnitude with the effect of purely anharmonic shifts in the phonon frequencies.

(iii) Finally we have reanalysed experiments on the volume dependence of the effective electron mass. In the literature on this subject it has not been recognized how large the electron-phonon enhancement of the mass is for lead. When we take this fact into account, we find that the band mass decreases when the lattice expands, instead of a supposed increase.

Appendix 1.

We follow Cowley and Cowley[24] and write for the phonon frequency $\omega(\underline{q},\lambda)$ as measured e.g. with inelastic neutron scattering

$$\omega(\underline{q},\lambda) = \omega_o(\underline{q},\lambda) + \Delta_1(\underline{q},\lambda) + \Delta_2(\underline{q},\lambda) + \Delta_3(\underline{q},\lambda) \quad . \tag{A1}$$

The three last terms represent anharmonic corrections. Δ_1 takes into account the effect of thermal expansion. Δ_2 and Δ_3 represent purely anharmonic effects, they originate from the third and fourth order derivatives of the effective interatomic potential. At high temperatures Δ_2 and Δ_3 are linear in T and they are also volume dependent. The standard Grüneisen γ_G can be expressed in the isothermal compressibility K_T and the thermal expansion coefficient β, but also as a derivative of the entropy

$$\gamma_G = \frac{\beta V}{C_V K_T} = \frac{V}{C_V} \left(\frac{\partial S}{\partial V}\right)_T \quad . \tag{A2}$$

Cowley and Cowley find for the volume dependent part ΔS of the entropy

$$\Delta S = - \hbar \sum_{\underline{q},\lambda} \frac{\partial}{\partial T} \left[\frac{1}{e^{\hbar\omega_\lambda(\underline{q})/kT} - 1} \right] \left[\Delta_1(\underline{q},\lambda) + \Delta_2(\underline{q},\lambda) + \Delta_3(\underline{q},\lambda) \right] \tag{A3}$$

Therefore the high temperature γ_G measures the average of the relative volume dependence of the phonon frequencies

$$\gamma_G = \frac{1}{3N} \sum_{i=1}^{3N} (d \ln \omega_i / d \ln V)_T \tag{A4}$$

The result above is valid when $T \gtrsim \theta_D$, but it only represents the lowest correction and must not be used at higher temperatures where the frequency shifts are more complicated and the frequencies less well defined because of damping effects. Experiments on lead by Leadbetter[19] suggest that the range of validity for lead is $\theta_D \lesssim T \lesssim 3\theta_D$ ($\theta_D \approx 90^\circ K$). From the measurements of Leadbetter we find $\gamma_G(270^\circ K) = 2.7$ and we use this value for $(d \ln \theta_R / d \ln V)_T$. (cf. appendix 2) $(d \ln \theta_\lambda / d \ln V)_T$ refers to very low temperatures but the weighting of different modes is the same as for the high temperature γ_G. At low temperatures Δ_2 and Δ_3 are small (although not zero). This fact leads us to consider γ_G calculated without the terms

Δ_2 and Δ_3, and at crystal volume $V_o = V(T = 0)$. Leadbetter gives the value 2.7 for this quantity and we thus have $(d \ln \theta_\lambda / d \ln V) = 2.7$ (cf appendix 2).

Appendix 2.

From tunneling experiments in superconductors one can obtain a quantity $\alpha^2(\omega)F(\omega)$[6], giving the product of the strength of electron-phonon interaction $\alpha^2(\omega)$ as a function of energy, and the phonon density of states $F(\omega)$. Using this function, it is possible to rewrite eq. 1 for the electrical resistivity in the form[3]

$$\rho = (\frac{S}{S_o})^2 \frac{N_{bs}(0)}{N_{fe}(0)} \frac{4\pi m \hbar \overline{(1-\cos\Theta)}}{ne^2 kT} \int \frac{\alpha^2(\omega) F(\omega) \omega d\omega}{\left[e^{\hbar\omega/kT}-1\right]\left[1-e^{-\hbar\omega/kT}\right]} \tag{A6}$$

where S/S_o is the ratio between the true free area of the Fermi surface and the area in the free electron case. $N_{bs}(0)/N_{fe}(0)$ is the corresponding ratio for the density of electron states at the Fermi level. $\overline{1-\cos\Theta}$ denotes the average of the usual factor $1-\cos\Theta$ that enters expressions for the resistivity. This factor has been rewritten in eq. 1, using $q^2 = 2k_F^2(1-\cos\Theta)$. Let us now make the assumption that $\overline{1-\cos\Theta}$ is approximately the same if it is considered separately for transverse phonons and for longitudinal phonons. In a polyvalent metal, where the resistivity is totally dominated by Umklapp scattering, this should be a reasonable approximation. We then take the high temperature limit of eq. A1 and find that the relative importance of phonons of energy ω in the resistivity is given by $\alpha^2(\omega)F(\omega)/\omega$.

In the high temperature Grüneisen γ_G, all individual $\gamma(\underline{q},\lambda)$ are equally weighted

$$\gamma_G = \int F(\omega) \bar{\gamma}(\omega) d\omega = \frac{2}{3} \bar{\gamma}_T + \frac{1}{3} \bar{\gamma}_L \tag{A7}$$

where $\bar{\gamma}(\omega)$ is an average over all individual phonon modes with energy in $[\omega, \omega+d\omega]$. $\bar{\gamma}_T$ and $\bar{\gamma}_L$ are averages for the transverse and longitudinal branches. For $\gamma_R = (d \ln \Theta_R/d \ln V)$ we could write

$$\gamma_R \approx \int \frac{\alpha^2(\omega)F(\omega)}{\omega} \bar{\gamma}(\omega) d\omega \tag{A8}$$

The function $\alpha^2(\omega)F(\omega)$ has been obtained by McMillan and Rowell[6]. It turns out that $\alpha^2(\omega)/\omega$ does not vary very much with ω in the region of

typical phonon energies. From a study of the experimentally determined $\alpha^2(\omega)F(\omega)/\omega$ we have found it reasonable to take

$$\gamma_R = \frac{3}{4} \, \bar{\gamma}_T + \frac{1}{4} \, \bar{\gamma}_L \tag{A9}$$

The individual $\gamma(\underline{q},\lambda)$ can vary very much with $\underline{q}$, but the general behaviour is the same for the transverse and the longitudinal branches (fig. 1). Therefore γ_G should not be too bad as an approximation for γ_R.

If we make a series expansion in the denominator of eq. 1, the first non-vanishing term gives a linear temperature dependence for the resistivity at high temperatures. The small correction for lead at room temperature from higher order terms can easily be estimated if we approximate $\alpha^2(\omega)F(\omega)/\omega$ by two sharp peaks at characteristic transverse and longitudinal frequencies and give them weights in the ratio 3:1 (cf eq. A9). We finally turn to $(d \ln \Theta_\lambda / d \ln V)_P$. One has rigorously[6]

$$\lambda = 2 \int \frac{\alpha^2(\omega)F(\omega)}{\omega} \, d\omega \tag{A10}$$

We therefore have approximately the same weighting of different frequencies as in the high temperature electrical resistivity.

References.

1. Grüneisen, E.: Verhandl. Deut. Phys. Ges. 15, 186 (1913).

2. Kroll, W: Z. Phys. 85, 398 (1933).

   Mott, N.F.: Proc. Phys. Soc. 46 680 (1934).

   Lenssen, M.H., and A. Michels: Physica 2, 1091 (1935).

   Frank, M.H.: Phys. Rev. 47 282 (1935).

   Grüneisen, E.: Ann. Physik 40, 543 (1941).

   Lawson, A.W.: Progr. Metal Phys. 6, 1 (1956).

   Dugdale, J.S.: Science 134, 77 (1961).

   Dugdale, J.S., and D. Gugan: Proc. Roy. Soc. 270, 186 (1962).

   Paul, W: High Pressure Physics and Chemistry, edited by R.S. Bradley,

   Vol. 1, Chap. 5. Academic Press N.Y. (1963).

   Hasegawa, A.: J. Phys. Soc. Japan 19, 504 (1964).

2. Ziman, J.M.: Electrons and Phonons. Clarendon Press, Oxford (1960).

3. Grimvall, G.: Phys. Kondens. Materie 8, 202 (1968).

4. Collins, J.G.,and G.K. White, Progress in low temperature physics 4,
   450 (1964).

5. Munn, R.W.: Phys. Rev. (1969), in press.

6. McMillan, W.L., and J.M. Rowell: A chapter in Superconductivity,
   edited by R.D. Parks, to be published.

7. Bridgman, P.W.: Proc. Amer. Acad. 72, 157 (1938).

8. Fischer, U.: Z. Physik Chem. 8, 207 (1930).

9. Gschneider, K.A.: Solid state physics 16, 275 (1964).

10. Sham, L.J.,and J.M. Ziman: Solid state physics, 15, 221 (1963).

    Pytte, E.: J. Phys. Chem. Solids 28, 93 (1967).

    Bross, H., and G. Bohn: phys. stat. sol. 20, 277 (1967).

11. Dynes, R.C., and J.P. Carbotte: Phys. Rev. 175, 913 (1968).

12. Anderson, J.R., W.J. O'Sullivan and J.E. Schirber: Phys. Rev. 153,
    721 (1967).

13. Sham, L.J., and J.M. Ziman: Solid state physics 15, 221 (1963).

14. Leadbetter, A.J., D.M.T. Newsham, and N.H. Picton: Phil. Mag. 13, 371 (1966).

15. Holborn, L.: Ann. Phys. 59, 145 (1919).

16. Pochapsky, T.E.: Acta Met. 1, 747 (1953).

17. Stedman, R., L. Almqvist, G. Nilsson, and G. Raunio: Phys. Rev. 162, 545 (1967).

18. Brockhouse, B.N.: in Phonons in perfect lattices, edited by R.W.H. Stevenson, Oliver and Boyd, Edinburg (1966).

19. Leadbetter, A.J.: J.Phys. C (Proc. Phys. Soc.) 1, 1489 (1968).

20. Quittner, G., and R. Lechner: Phys. Rev. Letters 17, 1259 (1966).

21. Zavaritskii, N.V., E.S. Itskevich, and A.N. Voronovskii: JETP letters 7, 211 (1968).

22. Frank. J.P., and W.J. Keeler: Phys. Letters 25A, 624 (1967).

23. Sandström, R., T. Högberg and U. Bohlin: Private communication.

24. Cowley, E.R., and R.A. Cowley: Proc. Roy. Soc. A292, 209 (1966).

16. Dellinger, J.A., T.D.B. Davidson and R.A. Bishop, Radio Tech. Rev. 370 (1962).

    Davidson, T.D.B., Rev. Sci. Inst. 40 (1977).

17. Stinson, G.H., Langmuir, G. Wilson, Rev., Nuclear Inst. Rev. 103 (1977).

18. Anderson, R.A., Low Temperature Nuclear Orientation, ed. E.W.
    Governor, Grenn and Hartly (1984).

19. Bauchhenss, A.L., Philips J. Phys. Rev. Lett. 1, 300 (1968).

20. Stumborg, G., van E. Ludinger, Phys. Rev. Letters B 12 x (1964).

21. Bauchhenss, R.J., Nib. Inglaterra, and E.W. Governor, Phys. Rev.
    E 31 (1969).

22. Brown, J.L., and J.E. Wolf, J. Phys. Letters 25AB 4 (1969).

23. Davidson, R.J., Hoffenn, and D. Robert, Phys. Phys. Communication.

24. Counts, J.W., and J. Philips, Proc. Phys. Soc. 82d, 301 (1966).

Table

$$(d \ln \rho/d \ln V)_{Tl} = 2(d \ln m_b/d \ln V) - 2(d \ln \theta_R/d \ln V)_{Tl} + (d \ln I_R/d \ln V) + 1$$

$$6.9 \pm 0.3 = 2(-2 \leq ... \leq 0) + 2(2.7 \pm 0.3) + (0.5 \leq ... \lesssim 3) + 1$$

$$(d \ln m_{eff}/d \ln V)_{Tl} = \frac{1+2\lambda}{1+\lambda}(d \ln m_b/d \ln V) - \frac{2\lambda}{1+\lambda}(d \ln \theta_\lambda/d \ln V)_{Tl} + \frac{\lambda}{1+\lambda}(d \ln I_\lambda/d \ln V)$$

$$1.0 \pm 0.5 = \frac{8}{5}(-2.5 \leq ... \leq -1.5) + \frac{6}{5}(2.7 \pm 0.3) + \frac{3}{5}(1 \leq ... \lesssim 3)$$

Figure caption.

Experimentally determined microscopic Grüneisen parameters $\gamma(\underline{q},\lambda)$ for the longitudinal and transverse branch in the $[\overline{1}00]$-direction. Unfillled symbols are from inelastic neutron scattering measurements by Stedman et al.[17] (○) and Brockhouse[18] (□) at different temperatures and constant pressure.

Inelastic neutron scattering under hydrostatic pressure by Lechner and Quittner[20] (●) and tunneling experiments on superconductors under pressure by Zavaritskii (■) et al.[21] and Frank and Keeler[22] (▲) give shifts that do not contain any explicit anharmonic effects. Typical experimental errors are indicated by the error bars.

Table.

Calculated contributions to the measured values of $(d \ln \rho / d \ln V)_T$ and $(d \ln m_{eff} / d \ln V)_T$. The value of $(d \ln I / d \ln V)$ is very uncertain but it is positive and large. $(d \ln m_b / d \ln V)$ has not been calculated but has instead been given a value to make the relations above hold. The errors given for the rest of the quantities are somewhat arbitrary and serve the purpose of indicating which terms are best known.